

**Physical Interpretation of Radiative Corrections: Electron $g - 2$, Lamb Shift,
and the D-term**

by

Syed Navid Reza

A thesis submitted in partial fulfillment of the requirements for the degree of

Master of Science

Department of Physics

University of Alberta

©Syed Navid Reza, 2023

Abstract

Gravitational interaction of particles is understood in terms of energy-momentum tensor (EMT) which gives information regarding the fundamental properties of a particle like mass and spin. When the matrix element of the energy-momentum tensor is written in terms of EMT form factors, we get an additional fundamental property, the D-term. The D-term is related to the spatial components of the EMT and refers to pressure, shear force distribution, and how strong forces inside the nucleon balance to form a bound state. However, the proper interpretation of the D-term is still being disputed. The D-term started gaining a lot of attention recently and experiments are ongoing in JLab and are planned in the Electron-Ion Collider in Brookhaven to measure the D-term through the deeply-virtual Compton scattering process.

In this thesis, we will present an intuitive explanation of radiative corrections in quantum electrodynamics with examples of electron $g - 2$ and Lamb shift. We will determine the D-term for a bound system like hydrogen and calculate the leading order and next-to-leading order logarithmic correction to the D-term of hydrogen atom. The goal is to verify the claim of [1] that the next-to-leading order logarithmic correction to the D-term of hydrogen follows the same physics as the Lamb shift. As a main result of this thesis, using our discussion of the radiative corrections, we will show that although the D-term has a logarithmically enhanced term like the Lamb shift, the physics is quite different from the Lamb shift.

Preface

The idea of working on all these problems belongs to my supervisor Prof. Andrzej Czarnecki. In chapter 2, I used the reasoning of [2, 3] to calculate the non-relativistic contribution to the electron $g - 2$ as in literatures it is not calculated explicitly. I found an article [4] to calculate the full electron $g - 2$ and have reproduced this calculation in 3. Prof. A. Czarnecki suggested me to work on [5] as a term paper for PHYS 512 (Advance Quantum Mechanics) course to have a better understanding of radiative corrections which is presented in 4. Chapter 5 helped to gain physical intuition on the Lamb shift which is essential to obtain the main result of this thesis. Prof. A. Czarnecki suggested me to read the Ph.D. thesis [6] to understand the NRQED Feynman rules which are derived in 6. Prof. A. Czarnecki introduced me to the topic of the D-term and I did extensive literature searching to understand the background of the D-term and energy-momentum tensors. I calculated the leading order D-term for hydrogen as a term paper for PHYS 595 (Introduction to Quantum Field theory) following the reference [7]. Prof. A. Czarnecki taught and helped me in performing loop integrals and arriving at the main result of this thesis which is discussed in chapter 7.

Acknowledgement

First and foremost, I would like to convey my gratitude towards my supervisor Prof. Andrzej Czarnecki for his guidance throughout my master's. I am thankful to him for his effort in developing my scientific mind. I learned a lot about work and research ethics from him. I am grateful to Prof. Saeed Rastgoo and Prof. Igor Boettcher for agreeing to be on my thesis defense committee. I am also thankful to my respected teachers especially Prof. Doug Gingrich for teaching me computational methods and Prof. Roger Moore for his excellent and interesting course about introductory particle physics.

I am greatly thankful to Muhammad Mubasher, Rishap Lamichhane, Elsad Cukali, Ap-sana Kafe, and Hitesh Chopra for making my university life fun and exciting. I especially like to thank Nuzhat Anjum and Md. Rashid Taher. I don't know how would I be able to survive in Edmonton without them. I am greatly thankful to all my friends from Bangladesh especially Refat Amin, Shusmoy Pandit Abir, Jaki Arefin Shoikat, Mash-Huda Rehman Shipra, M.K. Munim, Sadman Sakib, and Utsha Chowdhury for their constant communication with me and for never letting me feel that I am so far away from my homeland.

I am really thankful to my elder sister who has been always by my side. Finally, I would like to dedicate my thesis to my parents for not only raising me but for their unconditional emotional and financial support. I am especially thankful to them for teaching me right from wrong, establishing my moral ground, and making me the person I am today.

Contents

1	Introduction	1
2	Non-relativistic contribution to electron $g - 2$	5
2.1	Introduction	5
2.2	Derivation of the quantum form of the Abraham-Lorentz equation	6
2.2.1	Derivation of the quantum form of Abraham-Lorentz equation	6
2.2.2	Introducing approximations	7
2.2.2.1	Introduction of a cut-off	7
2.2.2.2	Electric Dipole approximation	8
2.2.3	The Electromagnetic field in presence of the particle	9
2.2.4	The Quantum Abraham-Lorentz equation	10
2.3	Spin dependence of the effective Hamiltonian	10
2.4	Effective Hamiltonian and electron $g - 2$	13
2.5	Conclusion	15
3	Relativistic effective Hamiltonian approach to electron $g - 2$	17
3.1	Introduction	17
3.2	Calculation of electron $g - 2$	17
3.2.1	Matrix element of the effective Hamiltonian	18
3.2.2	Calculation of the matrix element of V_{Coul}	21
3.2.2.1	Contribution of term 1	21
3.2.2.2	Contribution of term 2 and 3	22
3.2.2.3	Contribution of term 4	23
3.2.2.4	Contribution of term 5	24
3.2.2.5	Contribution of term 6	24
3.2.3	Calculation of the matrix element of the transverse Photon (U_{\perp})	26
3.2.3.1	Contribution of term 1	26
3.2.3.2	Contribution of terms 2 and 3	27

3.2.3.3	Contribution of term 4	27
3.2.3.4	Contribution of term 5	27
3.2.3.5	Contribution of term 6	27
3.2.4	Total effective Hamiltonian	29
3.2.5	Calculation of anomalous magnetic moment of electron	30
3.3	Justification of the obtained non-relativistic contribution of electron $g - 2$	31
3.4	Conclusion	31
4	Luttinger's approach to the electron $g - 2$	33
4.1	Introduction	33
4.2	Defining terms for the calculation	34
4.3	Calculation of ΔE_{static} and $\Delta E_{\text{dynamic}}$	35
4.4	Conclusion	40
5	Calculation of the Lamb Shift	41
5.1	Introduction	41
5.2	Bethe's calculation of the Lamb Shift	41
5.3	Welton's heuristic approach to the Lamb shift	44
5.4	Conclusion	46
6	Feynman rules for NRQED	48
6.1	Introduction	48
6.2	NRQED vertices	48
6.3	Virtual Fermions	51
6.4	Annihilation diagram	53
6.5	Photon propagator	54
6.6	Conclusion	55
7	The D-term for hydrogen atom	56
7.1	Introduction	56
7.2	EMT form factors and the interpretation of the D-term	57
7.2.1	Remarks about symmetric stress-energy tensor	58
7.2.2	EMT form factors	59
7.2.3	Interpretation of the D-term	60
7.2.3.1	D-term of a nuclei in the context of the liquid drop model	62
7.2.4	Experimental procedure of measuring the D-term	63
7.3	Relevant terms in the EMT in the context of QED	66

7.4	Leading order calculation of the D-term for hydrogen atom	68
7.5	Logarithmic correction to the D-term for hydrogen atom	71
7.5.1	Photonic contribution and matching to QED	72
7.5.2	Bound state calculation for $\mathcal{O}(\alpha)$ correction to the D-term	75
7.6	Discussion	78
7.7	Conclusion	79
8	Conclusion	80
A	Calculation of the source fields	86
B	The Foldy-Wouthuysen Transformation	88
C	Calculation of the matrix elements	92
C.1	Calculation of $\mathcal{V}_{\text{Coul}}$	92
C.2	Calculation of $\mathcal{H}_{\text{eff}}^\perp$	93
D	Dirac equation in magnetic field	95
E	Calculation of the loop integrals	98

List of Figures

3.2.1 Unperturbed energy levels for different combinations of number of electron and positron.	19
3.2.2 Transition diagram of electron for virtual energy levels of $\mathcal{H}_D = \beta mc^2$	20
3.2.3 Various combinations of the creation and annihilation operators of electrons and positrons.	21
3.2.4 Diagram for term (1) considering interaction with Coulomb photon.	22
3.2.5 Diagram for term (2) and (3) considering interaction with Coulomb photon.	23
3.2.6 Diagram for term (4) considering interaction with Coulomb photon.	24
3.2.7 Diagram for term (6) considering interaction with Coulomb photon.	25
3.2.8 Diagram for term (1) considering interaction with transverse photon.	26
3.2.9 Diagrams for terms (2) and (3) considering interaction with transverse photon.	27
3.2.10 Diagram for term (4) considering interaction with transverse photon.	27
3.2.11 Diagram for term (6) considering interaction with transverse photon.	28
5.2.1 Self-energy Feynman diagram for free particle.	42
6.2.1 Graphical representation of Coulomb interaction.	49
6.2.2 Graphical representation of the Darwin and spin-orbit interactions.	50
6.2.3 Graphical representation of the dipole and magnetic interactions.	50
6.3.1 Representative diagrams for fermion (positron) as an internal line.	51
6.3.2 Seagull interaction.	53
6.4.1 Annihilation contact interaction diagram.	53
7.2.1 The leading order handbag diagram for the Deeply Virtual Compton Scattering ($\gamma^* N(p) \rightarrow \gamma N(p')$).	64
7.2.2 Fits to the unpolarized DVCS cross-sections and gravitational form factor $d_1(t)$	65
7.2.3 Radial pressure distribution in the proton.	66
7.5.1 The photonic contribution of T_γ^{ij}	72

7.5.2 Bound state contribution to $T_{\gamma}^{ij} + T_{\gamma P}^{ij}$ to calculate order $\mathcal{O}(\alpha)$ correction to the D-term.	75
--	----

Chapter 1

Introduction

The goal of this thesis is to provide an intuitive explanation of radiative corrections in quantum electrodynamics (QED) processes. Radiative corrections in QED involve two kinds of interactions: vacuum fluctuation and radiative reactions (self-interaction) [2]. Vacuum fluctuation is a pure quantum mechanical effect corresponding to modifying an electron's dynamical properties due to its interaction with the vacuum. An example closely related to vacuum fluctuation is the Lamb shift which discusses how the fluctuating vacuum affects the motion of a bound electron. In Lamb shift, one averages the Coulomb potential of the nucleus and the electron's vibrational motion in the vacuum [8, 9]. In a bound system (i.e. Hydrogen atom), the fluctuating vacuum creates fluctuating electric field due to the atomic nucleus which causes fluctuation in the position of the electron which gives rise to the Lamb shift. Radiative reaction means the interaction of the electron with its own fields which includes interaction with the Coulomb and radiation field. This effect can be conceptualized using a semi-classical point of view by considering an electron surrounded by its Coulomb field and when one pushes the electron, one has to push the Coulomb field also. Basically, it represents the inertia of the self-field that the electron carries [8, 2]. An example employing the concept of self-interaction is the anomalous magnetic moment of the electron where an electron interacting with its self-field obtains a modification to its mass and magnetic moment. In this thesis, we will try to understand the concept of radiative corrections with several examples. In this regard, the thesis can be divided into two parts. In the first part, as examples of vacuum fluctuation and radiative reactions in QED processes, we will provide an intuitive calculation of the anomalous magnetic moment of the electron and Lamb shift. The second part will involve the main discussion of the thesis, a comparatively new concept, the so-called D-term. The D-term is also a fundamental property like mass and spin and it arises when we take the matrix element of the energy-momentum tensor (EMT) and write them in terms of gravitational form factors [10]. The D-term usually refers to the pressure distribution, struc-

ture, and how forces balance to form a bound state [11]. The D-term obtained very little attention in the past as to measure the gravitational or EMT form factors, we need to probe the experiment by the weakest of the fundamental forces, gravity or consider a scattering experiment with the till unknown mediating particle of gravitational interactions, graviton [10, 11]. In recent years, the D-term started receiving a lot of attention in the scientific arena as now it is possible to measure the EMT form factors through an indirect process namely deeply virtual Compton scattering or hard exclusive meson production [12, 13, 14]. In this thesis, we will consider the D-term in the context of QED for a bound state like hydrogen. We will follow the calculation of [7, 1] and work out the leading and next-to-leading order corrections to the D-term. In [1], the authors have claimed that the next-to-leading order correction to the D-term has the same physics as the Lamb shift. As our main result of this thesis, we will refute this statement and the intuition gained from our discussion of the physical interpretation of the radiative corrections will serve in this purpose. The outline of the thesis is as follows.

In Chapter 2, we will study the anomalous magnetic moment of the electron or electron $g - 2$. We will work out the non-relativistic contribution to the total one-loop anomaly of the Schwinger factor $\frac{\alpha}{2\pi}$ [15]. This chapter is motivated by the papers [2, 3]. This approach of calculating the electron $g - 2$ is directly related to the experimental measurement of the g factor. Experimentally the g factor is measured from the ratio of Larmor and cyclotron frequency. The main theme of this chapter is to obtain the effective Hamiltonian containing the effects of vacuum fluctuation and radiation reaction. From the effective Hamiltonian we will get the modified Larmor and cyclotron frequency and the ratio of them to the first order will provide us the non-relativistic contribution to the electron $g - 2$. We will see that most of the contribution to the electron $g - 2$ comes from the non-relativistic domain and the modification to the cyclotron frequency provides most of the contribution to this anomaly.

In Chapter 3, we will work out the total one-loop contribution to the electron $g - 2$ and obtain the Schwinger factor using relativistic formalism. This chapter is motivated by the work submitted by Jacques Dupont-Roc and Claude Cohen-Tannoudji to the Les Houches summer school in the 1982 session [4]. In this chapter, we will identify the Feynman diagrams that are relevant to the electron $g - 2$ from which we will then obtain the total effective Hamiltonian. From the effective Hamiltonian, we will get the modified Larmor and cyclotron frequency which will give us the electron $g - 2$. We will then take the non-relativistic limit to justify our result obtained in chapter 2. We will see that the relativistic calculation does not require a cut-off like the non-relativistic calculation which indicates a lack of covariance in the non-relativistic formalism.

In Chapter 4, we will discuss Luttinger's approach to the calculation of the anomalous

magnetic moment of the electron [5]. This approach is intuitive and does not depend on any renormalization schemes or cut-offs. The main motivation of Luttinger for his calculation was to avoid the artificial renormalization scheme introduced by Schwinger for his calculation of electron $g - 2$ [15]. He thought of this problem in the context of an electron in a homogenous magnetic field. The lowest energy state of the Dirac operator in a homogenous magnetic field that does not depend on any applied field and it corresponds to the state where $g = 2$. So the true contribution to the anomaly should come from the higher order terms upon employing perturbation in powers of the external field. The self-energy terms or the 0th order terms will contain all the divergences and by isolating the terms dependent on the magnetic field, we will get the true change in energy corresponding to the anomaly of electron magnetic moment.

In Chapter 5, we will study the first well-known example of radiative corrections, the Lamb shift. Interaction between the vacuum energy fluctuation and the electron in the hydrogen atom is the primary cause of the Lamb shift. In this chapter, we will start by discussing Bethe's approach to the Lamb shift [16]. Bethe considered the bound electron's self-energy in an intermediate quantum state and subtracted the free electron's self-energy. Although the self-energy of the bound and free electron are linearly divergent the result is divergent logarithmically. This logarithmic divergence is the primary feature of the Lamb shift. Next, we will discuss Welton's heuristic approach to the Lamb shift [9]. This approach is more intuitive and we can see a clear physical picture of the Lamb shift from this approach. In a bound system, the fluctuating vacuum creates fluctuating electric fields which push the electron causing position fluctuation in the motion of the electron. This position fluctuation modifies the Coulomb potential energy between the electron and nucleus. The average of the Coulomb potential energy and the electron's vibrational motion in the vacuum give rise to the famous Lamb shift.

Before discussing the D-term, in Chapter 6, we will derive the Feynman rules for non-relativistic quantum electrodynamics (NRQED). We will follow the calculation scheme of a Ph.D. thesis by Patrick Labelle presented at Cornell University in 1994 [6]. This way of deriving the NRQED Feynman rules is far simpler than the proper way where one starts with the derivation of QED Feynman rules and rederive them in the non-relativistic limit. Here we will simply write down the QED Feynman rules and expand them in powers of $\frac{p}{m}$ [6]. This way of deriving the NRQED rules might introduce some sign ambiguity in the overall phase but as most of the calculation in particle physics relies on taking the square of the matrix element of scattering amplitude, we can ignore this drawback [6]. With the help of these NRQED Feynman rules, we will calculate the logarithmic corrections to the D-term.

In chapter 7, we will discuss the D-term and present our main finding of this thesis.

The mechanical properties of a particle are encoded in the gravitational form factors and these form factors arise by taking the matrix element of the energy-momentum tensor. In this chapter, we will see that when we take the matrix element of the energy-momentum tensor, alongside mass and spin, one more fundamental property of a particle emerges, the D-term. We will discuss several interpretations of the D-term namely pressure, shear force distribution, charge radius, and mechanical stability. For gaining better intuition of the D-term, we will calculate the D-term for a nucleus in the context of the liquid drop model. We will also provide an experimental procedure for measuring the D-term by looking at deeply virtual Compton scattering. Until this point, the D-term had been considered in the context of quantum chromodynamics. To understand the D-term better, instead of considering the bound system of quarks and gluons, we will look at a bound system like hydrogen and calculate the leading and next-to-leading order correction to the D-term in the context of quantum electrodynamics. The motivation is to verify the claim of [1] that the next-to-leading order correction to the D-term follows the same physics as the Lamb shift. This will help us to gain a better understanding of the Lamb shift as well as the D-term. We will follow the paper [7] to calculate the leading order D-term and [1] to calculate the logarithmic divergent term. From our understanding of the Lamb shift and radiative corrections described in the earlier chapters, we will see that although the D-term has logarithmic divergence as the Lamb shift, it is not the Lamb shift as advertised in [1]. This is the main result of this thesis.

Finally in chapter 8, we will present our concluding remarks for this thesis and discuss future goals.

Chapter 2

Non-relativistic contribution to electron $g - 2$

2.1 Introduction

The g factor is a dimensionless quantity that characterizes the magnetic moment of a particle. To be more specific, it is the proportionality coefficient between the angular momentum \vec{J} and the magnetic moment $\vec{\mu}$ expressed in the units of the so-called magneton $q/(2m)$, where q is the charge and m is the mass of the particle,

$$\vec{\mu} = g \frac{q}{2m} \vec{J}. \quad (2.1.1)$$

For a point scalar particle orbiting a static nucleus, the angular momentum arises from the orbital motion. In this case g equals 1, which is the reason of the particular form of the magneton.

For a spinning particle in its rest frame, the angular momentum is the spin. Clearly, the magnetic moment depends on the distribution of the charge in the particle. For example, if all the charge is concentrated on the axis of rotation, the charge remains at rest and no magnetic moment arises, so that $g = 0$. For a proton, which contains charged quarks, the measured value of g is about 5.6 [17].

For an electron, the Dirac equation predicts that the g factor is 2. But in 1948, experiments found that the electron g factor is slightly larger than 2 [18]. This discrepancy is known as the anomalous magnetic moment of the electron or electron's $g - 2$. Experimentally the g factor of the electron can be measured from the ratio of Larmor and cyclotron frequencies.

In this chapter, we will see how the interaction of the electron with its own field and vacuum modifies the Larmor and cyclotron frequency and thus the g factor. To get an

understanding of how these effects play a role in modifying the g factor, we will work on the non-relativistic domain and find the non-relativistic contribution to the total one-loop anomaly in the magnetic moment of the electron. First, we will find the quantum version of the Abraham-Lorentz equation for an atom-field system using the Heisenberg equation of motion. Heisenberg equation of motion for field and atomic variables derived from the combined atom-field system is analogous to the equation of motion of a forced harmonic oscillator [2, 3]. The homogenous part of the solution describes the vacuum field where no photon is present and it corresponds to spontaneous emission; the forced part describes the source field produced by the electron itself (radiation reaction), corresponding to stimulated emission of radiation [3]. From the quantum Abraham-Lorentz equation, we will see that the mass of the electron has been changed. Then we will calculate the spin-dependent part of the effective Hamiltonian which will give us the anisotropic Lande g factor. Finally from the effective Hamiltonian containing the renormalized mass and anisotropic Lande g factor, we will then obtain the modified Larmor and cyclotron frequency which will give us the electron $g - 2$ in the non-relativistic domain. In this chapter, we will work with standard S.I. units.

2.2 Derivation of the quantum form of the Abraham-Lorentz equation

2.2.1 Derivation of the quantum form of Abraham-Lorentz equation

In this section, we will derive the Heisenberg equation of motion for the combined atom-field system and obtain the analogous quantum form of the Abraham-Lorentz equation. We consider an electron subjected by some field (electric or magnetic) and the radiation field exerted by the electron itself when moving. The radiation field of the electron has both electric and magnetic components. The electric field is divided into two parts: the longitudinal field $\mathbf{E}_{||}$ which is the instantaneous Coulomb field created by the electron and the transverse field \mathbf{E}_{\perp} . The transverse field \mathbf{E}_{\perp} , vector field \mathbf{A} and the magnetic field \mathbf{B} expanded as a set of plane waves normalized in a cube of volume L^3 are given by [2]

$$\mathbf{E}_{\perp}(\mathbf{R}) = \sum_{\mathbf{k}, \epsilon} (\mathcal{E}_k \epsilon e^{i\mathbf{k} \cdot \mathbf{R}}) a_{\mathbf{k}\epsilon} + \text{hc}, \quad (2.2.1)$$

$$\mathbf{A}(\mathbf{R}) = \sum_{\mathbf{k}, \epsilon} (\mathcal{A}_k \epsilon e^{i\mathbf{k} \cdot \mathbf{R}}) a_{\mathbf{k}\epsilon} + \text{hc}, \quad (2.2.2)$$

$$\mathbf{B}(\mathbf{R}) = \sum_{\mathbf{k}, \epsilon} (\mathcal{B}_k \boldsymbol{\kappa} \times \epsilon e^{i\mathbf{k} \cdot \mathbf{R}}) a_{\mathbf{k}\epsilon} + \text{hc}, \quad (2.2.3)$$

where $\mathcal{A}_k = \sqrt{\frac{\hbar}{2\varepsilon_0 L^3 \omega}}$, $\mathcal{E}_k = i\omega \mathcal{A}_k$, $\mathcal{B}_k = i\frac{\omega \mathcal{A}_k}{c}$, $\boldsymbol{\kappa} = \frac{\mathbf{k}}{|\mathbf{k}|}$ and $a_{\mathbf{k}\epsilon}$, $a_{\mathbf{k}\epsilon}^\dagger$ are the annihilation and creation operators for a photon. hc denotes Hermitian conjugate. The fields described in Eqs. (2.2.1) to (2.2.3) are characterized by frequency ω , polarization ϵ and wave vector \mathbf{k} . The Coulomb field created by the electron is [2]

$$\mathbf{E}_{\parallel}(\mathbf{R}) = -\nabla_{\mathbf{R}} \frac{e}{4\pi\varepsilon_0 |\mathbf{R} - \mathbf{r}|}, \quad (2.2.4)$$

It is convenient to take the Fourier transform of the longitudinal field [2]

$$\mathbf{E}_{\parallel}(\mathbf{R}) = \sum_{\mathbf{k}} -i \frac{e}{2\varepsilon_0 L^3 k} \boldsymbol{\kappa} e^{i\mathbf{k}\cdot(\mathbf{R}-\mathbf{r})} + \text{hc}. \quad (2.2.5)$$

Considering non-relativistic approximation, the Hamiltonian is given by [2]¹

$$H = mc^2 + \frac{(\mathbf{p} - e\mathbf{A}(\mathbf{r}))^2}{2m} + \frac{\varepsilon_0}{2} \int d^3R \mathbf{E}_{\parallel}^2(\mathbf{R}) + \sum_{\mathbf{k}, \epsilon} \frac{\hbar\omega}{2} \left(a_{\mathbf{k}\epsilon}^\dagger a_{\mathbf{k}\epsilon} + a_{\mathbf{k}\epsilon} a_{\mathbf{k}\epsilon}^\dagger \right). \quad (2.2.6)$$

This Hamiltonian does not contain any spin-dependent terms which we will include in the next section. The energy of the longitudinal field adds a correction to the mass of the electron

$$\delta m_1 c^2 = \frac{\varepsilon_0}{2} \int d^3R \mathbf{E}_{\parallel}^2(\mathbf{R}). \quad (2.2.7)$$

2.2.2 Introducing approximations

In this section, we introduce necessary approximations: a cut-off to avoid divergences and the electric dipole approximation.

2.2.2.1 Introduction of a cut-off

To avoid the divergences in the theory it is necessary to introduce cut-offs. The divergences arise because of the contribution of the modes with large wave vectors. So, we are choosing a cut-off k_M so that

$$|\mathbf{k}| < k_M = \frac{\omega_M}{c}. \quad (2.2.8)$$

The bound for k_M is

$$\frac{\omega_0}{c} \ll k_M \ll \frac{mc}{\hbar}. \quad (2.2.9)$$

¹We are considering non-relativistic approximation as the main contribution of QED corrections come from the non-relativistic domain [8].

The upper bound is to restrict k_M to the non-relativistic domain ($\hbar\omega_M \ll mc^2$) and the reason behind the lower bound is that ω_M must be larger than the characteristic resonance frequency of the bound electron, ω_0 [2]. The drawback of introducing such cut-off is the loss of relativistic invariance [19] but it is possible to introduce some sophisticated cut-offs which maintain relativistic invariance [20]. Here we will not consider such cut-offs as we are not dealing with the relativistic aspects of the radiative corrections. All the summations over k written before and from now will be understood constrained by Eq. (2.2.8). The energy of the longitudinal field is then finite and given by [2]

$$\delta m_1 c^2 = \sum_{\mathbf{k}} \frac{e^2}{2\varepsilon_0 L^3 k^2}. \quad (2.2.10)$$

Transforming the summation into an integration,

$$\sum_{\mathbf{k}} \rightarrow \frac{L^3}{(2\pi)^3} \int_0^{k_M} d^3 k = \frac{L^3}{2\pi^2} \int_0^{k_M} k^2 dk, \quad (2.2.11)$$

we get

$$\begin{aligned} \delta m_1 c^2 &= \frac{e^2}{2\varepsilon_0 L^3} \frac{L^3}{2\pi^2} \int_0^{k_M} dk \\ &= \frac{\alpha}{\pi} \hbar\omega_M. \end{aligned} \quad (2.2.12)$$

where $\alpha \simeq 1/137$ is the fine structure constant. From now ω should be understood with the constraint of ω_M .

2.2.2.2 Electric Dipole approximation

To make the calculation simpler we will also consider the electric dipole approximation to avoid spatial variations of the fields interacting with the electron. In this approximation the binding potential energy localizes the electron in a volume centered on the origin with a linear dimension a much smaller than the wave length of the modes interacting with the electron and the cut-off k_M satisfies $k_M a \ll 1$. Using this approximation we can replace the fields $\mathbf{E}(\mathbf{R})$, $\mathbf{A}(\mathbf{R})$ described in Eq. (2.2.1) to Eq. (2.2.3) with the fields at the origin $\mathbf{E}(0)$ and $\mathbf{A}(0)$ without changing any physics [2].

2.2.3 The Electromagnetic field in presence of the particle

Using Eq. (2.2.6) we can write the Heisenberg equation of motion for $a_{\mathbf{k}\epsilon}(t)$

$$\dot{a}_{\mathbf{k}\epsilon}(t) = \frac{i}{\hbar} [H(t), a_{\mathbf{k}\epsilon}(t)] = -i\omega a_{\mathbf{k}\epsilon}(t) + \frac{ie}{m\hbar} \mathcal{A}_k \boldsymbol{\epsilon}^* \cdot \boldsymbol{\pi}(t), \quad (2.2.13)$$

where

$$\boldsymbol{\pi}(t) = \mathbf{p}(t) - e\mathbf{A}(0, t). \quad (2.2.14)$$

The solution of Eq. (2.2.13) is given by [2]

$$a_{\mathbf{k}\epsilon}(t) = a_{\mathbf{k}\epsilon}(t_0) e^{-i\omega(t-t_0)} + \frac{ie}{m\hbar} \mathcal{A}_k \int_{t_0}^t dt' e^{-i\omega(t-t')} \boldsymbol{\epsilon}^* \cdot \boldsymbol{\pi}(t'). \quad (2.2.15)$$

The time evolution of $a_{\mathbf{k}\epsilon}(t)$ has two terms: the first one corresponds to free evolution and the second term corresponds to forced evolution driven by the motion of the charge. Upon inserting Eq. (2.2.15) in the expansion of the transverse field, Eq. (2.2.3) to Eq. (2.2.1), we get two terms: the free field ($\mathbf{A}_0, \mathbf{E}_{\perp 0}$) and the source field ($\mathbf{A}_r, \mathbf{E}_{\perp r}$). The subscript zero stands for the free fields and r stands for radiation field or source field. It is sufficient to evaluate $\mathbf{A}(0)$ and $\mathbf{E}_{\perp}(0)$ by the use of the dipole approximation

$$\mathbf{A}(0, t) = \mathbf{A}_r(0, t) + \mathbf{A}_0(0, t), \quad (2.2.16)$$

$$\mathbf{E}_{\perp}(0, t) = \mathbf{E}_{\perp r}(0, t) + \mathbf{E}_{\perp 0}(0, t) \quad (2.2.17)$$

where

$$\mathbf{A}_0(0, t) = \sum_{\mathbf{k}, \epsilon} \mathcal{A}_k \boldsymbol{\epsilon} e^{-i\omega(t-t_0)} a_{\mathbf{k}\epsilon}(t_0) + \text{hc}, \quad (2.2.18)$$

$$\mathbf{A}_r(0, t) = \frac{4}{3} \frac{\delta m_1}{me} \boldsymbol{\pi}(t) - \frac{2}{3} \frac{e}{4\pi\epsilon_0 mc^3} \dot{\boldsymbol{\pi}}(t). \quad (2.2.19)$$

and

$$\mathbf{E}_{\perp 0}(0, t) = \sum_{\mathbf{k}, \epsilon} (\mathcal{E}_k \boldsymbol{\epsilon} e^{-i\omega(t-t_0)}) a_{\mathbf{k}\epsilon}(t_0) + \text{hc}, \quad (2.2.20)$$

$$\mathbf{E}_{\perp r}(0, t) = -\frac{4}{3} \frac{\delta m_1}{me} \dot{\boldsymbol{\pi}}(t) + \frac{2}{3} \frac{e}{4\pi\epsilon_0 mc^3} \ddot{\boldsymbol{\pi}}(t). \quad (2.2.21)$$

Detailed derivation of Eqs. (2.2.19) and (2.2.21) is given in Appendix A.

2.2.4 The Quantum Abraham-Lorentz equation

The Heisenberg equation of motion for electron operator \mathbf{r} and $\boldsymbol{\pi}$ are

$$m\dot{\mathbf{r}}(t) = \frac{im}{\hbar} [H(t), \mathbf{r}(t)] = \boldsymbol{\pi}(t), \quad (2.2.22)$$

$$\dot{\boldsymbol{\pi}}(t) = \frac{i}{\hbar} [H(t), \boldsymbol{\pi}(t)] \simeq e\mathbf{E}_{\perp}(0, t), \quad (2.2.23)$$

where we have only used the contribution of the last term in Eq. (2.2.6). Finally using Eqs. (2.2.20) and (2.2.21) we get

$$\begin{aligned} m\ddot{\mathbf{r}}(t) &= e\mathbf{E}_{\perp r}(0, t) + e\mathbf{E}_{\perp 0}(0, t) \\ &= -\frac{4}{3}\delta m_1\ddot{\mathbf{r}}(t) + \frac{2}{3}\frac{e^2}{4\pi\epsilon_0 c^3}\ddot{\mathbf{r}}(t) + e\mathbf{E}_{\perp 0}(0, t). \end{aligned} \quad (2.2.24)$$

This equation is the analogous quantum form of the Abraham-Lorentz equation which only contains the radiation contribution. The electron is subjected by two fields: the free field and its source field (its own field). The first term in Eq. (2.2.24) increases the mass of the electron from m to $m + \frac{4}{3}\delta m_1$ due to its interaction with the source field². The second term is the quantum analogue of the force which produces the radiative damping of the classical particle. Classically this term refers to the recoil force on an accelerating charged particle emitting electromagnetic radiation. The last term is the field which describes the coupling of the electron to the free field³. Contrary to the classical theory, in quantum mechanics $\mathbf{E}_{\perp}(0, t)$ is an operator and its vacuum expectation value is zero but its quadratic vacuum expectation value is positive. The modification of the electron dynamical properties arising from the free term (the last term in Eq. (2.2.24)) corresponds to the effect of vacuum fluctuations.

2.3 Spin dependence of the effective Hamiltonian

In the previous section, we calculated the renormalized mass ($m + \frac{4}{3}\delta m_1$) of the electron due to the effects of radiation reaction which modifies the kinetic energy part of the effective Hamiltonian. To get the total effective Hamiltonian we also need to modify the coupling of spin and magnetic field. In this section, we consider the modification of the coupling of electron spin and magnetic field by radiation field. This introduces extra terms to the Hamiltonian in Eq. (2.2.6). First, we consider the general case when an electron is irradiated

²The mass correction term here and Eq. (2.2.7) differ by a factor of $\frac{4}{3}$ which is due to the lack of covariance of the cut-off procedure [2]

³The free field is the field that would exist even in the absence of the particle. This field may be an incident radiation field.

by a monochromatic plane wave and submitted to constant (direct current, d.c.) electric and magnetic fields described by the fields \mathbf{E}_0 , \mathbf{B}_0 or the potential ϕ_0 , \mathbf{A}_0 . Here we are considering the general Hamiltonian where ϕ_0 is present but when we will discuss the free electron $g = 2$, they will not be relevant. Now using Foldy-Wouthuysen transformation with a modification to introduce quantized fields, in the Coulomb gauge the Hamiltonian is given by [21]

$$H_{FW} = \hbar\omega a^\dagger a + \frac{\boldsymbol{\pi}^2}{2m} + e\phi_0 - \frac{e\hbar}{2m}\boldsymbol{\sigma}\cdot\mathbf{B}_t - \frac{e\hbar^2}{8m^2c^2}\boldsymbol{\nabla}\cdot\mathbf{E}_t - \frac{e\hbar}{8m^2c^2}\boldsymbol{\sigma}\cdot(\mathbf{E}_t \times \boldsymbol{\pi} - \boldsymbol{\pi} \times \mathbf{E}_t) - \frac{1}{2mc^2}\left(\frac{\boldsymbol{\pi}^2}{2m} - \frac{e\hbar}{2m}\boldsymbol{\sigma}\cdot\mathbf{B}_t\right)^2. \quad (2.3.1)$$

Detailed derivation of H_{FW} is given in Appendix B. The subscript t stands for total field (static + plane wave) which includes both the incident field and the radiation field of the electron. $\boldsymbol{\pi} = \boldsymbol{\pi}_0 - e\mathbf{A}_r$, $\boldsymbol{\pi}_0 = \mathbf{p} - e\mathbf{A}_0$ and \mathbf{A}_r is defined by Eq. (2.2.2). As mentioned in the previous section, the subscript r stands for the radiation fields and zero stands for the incident field. Now separating the parts with various contributions in H_{FW} , we get

$$H_{FW} = H_0 + H_e + H_I, \quad (2.3.2)$$

where H_0 , H_e , H_I corresponds to the free, electron, and interaction Hamiltonian respectively. The free Hamiltonian

$$H_0 = \hbar\omega a^\dagger a, \quad (2.3.3)$$

corresponds to the last term in Eq. (2.2.6). The electron Hamiltonian is given by [21]

$$H_e = \frac{\boldsymbol{\pi}_0^2}{2m} + e\phi_0 - \frac{e\hbar}{2m}\boldsymbol{\sigma}\cdot\mathbf{B}_0 + \frac{e\hbar^2}{8m^2c^2}\Delta\phi_0 + \frac{e\hbar}{4m^2c^2}\boldsymbol{\sigma}\cdot(\boldsymbol{\nabla}\phi_0 \times \boldsymbol{\pi}_0) - \frac{1}{2mc^2}\left(\frac{\boldsymbol{\pi}_0^2}{2m} - \frac{e\hbar}{2m}\boldsymbol{\sigma}\cdot\mathbf{B}_0\right)^2. \quad (2.3.4)$$

The interaction Hamiltonian can be split into two parts so

$$H_I = H_I^1 + H_I^2, \quad (2.3.5)$$

where H_I^1 only contains linear power of the radiation field \mathbf{A}_r and H_I^2 contains \mathbf{A}_r^2 . They are given by [21]

$$H_I^1 = -\frac{e}{m}\mathbf{A}_r \cdot \boldsymbol{\pi}_0 - \frac{e\hbar}{2m}\boldsymbol{\sigma} \cdot \mathbf{B}_0 + \frac{e^2\hbar}{4m^2c^2}\boldsymbol{\sigma} \cdot (\mathbf{E}_0 \times \mathbf{A}_r) - \frac{e\hbar}{4m^2c^2}\boldsymbol{\sigma} \cdot (\mathbf{E}_r \times \boldsymbol{\pi}_0) + \frac{e}{2m^2c^2} \left\{ \mathbf{A}_r \cdot \boldsymbol{\pi}_0 \left(\frac{\boldsymbol{\pi}_0^2}{2m} - \frac{e\hbar}{2m}\boldsymbol{\sigma} \cdot \mathbf{B}_0 \right) + \text{h.c.} \right\}, \quad (2.3.6)$$

and

$$H_I^2 = \frac{1}{2m}e^2\mathbf{A}_r^2 + \frac{e^2\hbar}{4m^2c^2}\boldsymbol{\sigma} \cdot (\mathbf{E}_r \times \mathbf{A}_r) - \frac{e^2\mathbf{A}_r^2}{2m^2c^2} \left(\frac{\boldsymbol{\pi}_0^2}{2m} - \frac{e\hbar}{2m}\boldsymbol{\sigma} \cdot \mathbf{B}_0 \right) - \frac{e^2}{8m^3c^2} (2\mathbf{A}_r \cdot \boldsymbol{\pi}_0 - e\mathbf{A}_r^2)^2. \quad (2.3.7)$$

Now inserting the expressions for \mathbf{A}_r , \mathbf{E}_r and \mathbf{B}_r from Eq. (2.2.1) to Eq. (2.2.3) into the Hamiltonians mentioned in Eq. (2.3.4) to Eq. (2.3.7) and collecting the spin dependent parts we arrive at the spin dependent effective Hamiltonian

$$H_{\text{eff}}^{\text{spin}} = -\frac{e\hbar}{2m}\boldsymbol{\sigma} \cdot \mathbf{B}_0 - \frac{e\hbar}{4m^2c^2}\boldsymbol{\sigma} \cdot (\mathbf{E}_0 \times \boldsymbol{\pi}_0) + \frac{e\hbar}{4m^2c^2} \left(\frac{\boldsymbol{\pi}_0^2}{2m}\boldsymbol{\sigma} \cdot \mathbf{B}_0 + \boldsymbol{\sigma} \cdot \mathbf{B}_0 \frac{\boldsymbol{\pi}_0^2}{2m} \right) + \frac{E_V}{2mc^2} \frac{e\hbar}{2m} \{ 2(\boldsymbol{\kappa} \cdot \mathbf{B}_0)(\boldsymbol{\kappa} \cdot \boldsymbol{\sigma}) + (\boldsymbol{\epsilon}^* \cdot \mathbf{B}_0)(\boldsymbol{\epsilon} \cdot \boldsymbol{\sigma}) + (\boldsymbol{\epsilon} \cdot \mathbf{B}_0)(\boldsymbol{\epsilon}^* \cdot \boldsymbol{\sigma}) + 2\boldsymbol{\sigma} \cdot \mathbf{B}_0 - 2\boldsymbol{\sigma} \cdot \mathbf{B}_0 + (\boldsymbol{\epsilon}^* \cdot \mathbf{B}_0)(\boldsymbol{\epsilon} \cdot \boldsymbol{\sigma}) + (\boldsymbol{\epsilon} \cdot \mathbf{B}_0)(\boldsymbol{\epsilon}^* \cdot \boldsymbol{\sigma}) + 2[(\boldsymbol{\kappa} \times \boldsymbol{\epsilon}^*) \cdot \mathbf{B}_0][(\boldsymbol{\kappa} \times \boldsymbol{\epsilon}) \cdot \boldsymbol{\sigma}] + 2[(\boldsymbol{\kappa} \times \boldsymbol{\epsilon}) \cdot \mathbf{B}_0][(\boldsymbol{\kappa} \times \boldsymbol{\epsilon}^*) \cdot \boldsymbol{\sigma}] \}. \quad (2.3.8)$$

The energy E_V is expressed as

$$E_V = \frac{e^2}{2} \frac{E^2}{m\omega^2}, \quad (2.3.9)$$

This energy corresponds to the vibrational kinetic energy for any electric field described by Eq. (2.2.1). The last two terms of Eq. (2.3.8) vanish by considering $\boldsymbol{\kappa} = \frac{\mathbf{k}}{k}$ perpendicular to $\boldsymbol{\epsilon}$. The remaining terms of Eq. (2.3.8) in the braces can be written more compactly by defining the anisotropic Lande g factor as [21]

$$\frac{e\hbar}{2m} \sum_{i,j} \delta g_{ij} \sigma_i B_{0j}, \quad (2.3.10)$$

where

$$\delta g_{ij} = \frac{E_V}{mc^2} (\kappa_i \kappa_j - 2\delta_{ij}). \quad (2.3.11)$$

In deriving this definition, we have used the completeness relation for polarization of photon

$$\sum \epsilon_i \epsilon_j^* = \delta_{ij} - \kappa_i \kappa_j. \quad (2.3.12)$$

2.4 Effective Hamiltonian and electron $g - 2$

Now we are in a position to calculate the electron $g - 2$. The g factor is experimentally determined from the ratio of the Larmor frequency ω_L of the electron spin and the cyclotron frequency ω_C of the electron in the same field ($\frac{g}{2} = \frac{\omega_L}{\omega_C}$) [8]. Our goal here is to modify the Larmor and cyclotron frequency by including radiative corrections to the Hamiltonian. We suppose that an electron is subjected to a static and uniform external magnetic field \mathbf{B}_0 . In the absence of the potential ϕ_0 and considering only the linear terms, the electron Hamiltonian in Eq. (2.3.4) can be written as

$$H_e = \frac{\boldsymbol{\pi}_0^2}{2m} - \frac{e\hbar}{2m} \boldsymbol{\sigma} \cdot \mathbf{B}_0, \quad (2.4.1)$$

where $\boldsymbol{\pi}_0 = \mathbf{p}_0 - e\mathbf{A}_0$, $e\mathbf{A}_0$ is the static vector potential that corresponds to the static magnetic field \mathbf{B}_0 . The Larmor frequency and the cyclotron frequency without any modification is then given by

$$\omega_C = \frac{e}{m} B_0, \quad (2.4.2)$$

$$\omega_L = g \frac{e}{2m} B_0. \quad (2.4.3)$$

If $g = 2$ then $\omega_C = \omega_L$. Now to get the anomaly in the g factor it is necessary to modify ω_L and ω_C . To include mass correction term δm , we have to modify the kinetic energy term in Eq. (2.4.1) as

$$\frac{\boldsymbol{\pi}_0^2}{2m} \rightarrow \frac{\boldsymbol{\pi}_0^2}{2(m + \frac{4}{3}\delta m_1 + \delta m_2)} \simeq \frac{\boldsymbol{\pi}_0^2}{2m} \left(1 - \frac{4}{3} \frac{\delta m_1}{m} - \frac{\delta m_2}{m} \right), \quad (2.4.4)$$

where δm_1 is the mass correction due radiation reaction and from Eq. (2.2.24) we get the renormalized mass term ($m + \frac{4}{3} \frac{\delta m_1}{m}$) which represents the inertia of the self field that the electron carries when it moves. δm_2 is the mass correction due to vacuum fluctuation. The correction to the coupling of spin and magnetic moment comes from the anisotropic Lande

g factor mentioned in Eqs. (2.3.8) and (2.3.10). So the effective Hamiltonian becomes

$$H_{\text{eff}} = \frac{\pi_0^2}{2m} \left(1 - \frac{4}{3} \frac{\delta m_1}{m} - \frac{\delta m_2}{m} \right) - \frac{e\hbar}{2m} \left(\boldsymbol{\sigma} \cdot \mathbf{B}_0 + \sum_{i,j} \delta g_{ij} \sigma_i B_{0j} \right), \quad (2.4.5)$$

where δ_{ij} is defined by Eq. (2.3.11). It is to be noted that the second and third term of Eq. (2.3.8) are not included in Eq. (2.4.5). The second term of Eq. (2.3.8) vanishes as in this case there is no E_0 and the third term is neglected as for first order there is no cross term of $\frac{\pi_0^2}{2m}$ and $\boldsymbol{\sigma} \cdot \mathbf{B}_0$. We now want to write Eq. (2.4.5) in terms of the renormalized mass and for this purpose we only have to modify the term involving the Lande g factor. Substituting the value of E from Eq. (2.2.1) into Eq. (2.3.9) we get

$$E_V^0 = \frac{e^2}{2m} \frac{\hbar}{2\varepsilon_0 \omega L^3}. \quad (2.4.6)$$

We are denoting E_V by E_V^0 to specify that this energy in this context refers to electron vibration in the vacuum. More precisely E_V^0 is the vibrational kinetic energy associated with the electron vibrating in the vacuum fluctuations of mode $(\mathbf{k}, \boldsymbol{\epsilon})$. Now evaluating the summation in Eq. (2.3.11) using $\kappa_i \kappa_j \rightarrow \frac{\delta_{ij}}{3}$ we get a factor of $-\frac{5}{3} \frac{E_V^0}{mc^2}$. To first order there is no effect of mass renormalization due to self interaction in the mass term of $\frac{e\hbar}{2m} \boldsymbol{\sigma} \cdot \mathbf{B}_0$. As E_V^0 is associated with vacuum fluctuations, we can write $E_V^0 = \delta m_2 c^2$. Finally the effective Hamiltonian becomes

$$H_{\text{eff}} = \frac{\pi_0^2}{2m} \left(1 - \frac{4}{3} \frac{\delta m_1}{m} - \frac{\delta m_2}{m} \right) - \frac{e\hbar}{2m} \boldsymbol{\sigma} \cdot \mathbf{B}_0 \left(1 - \frac{5}{3} \frac{\delta m_2}{m} \right). \quad (2.4.7)$$

The cyclotron and Larmor frequency will then also be modified by the same factors to first order

$$\bar{\omega}_C = \omega_C \left(1 - \frac{4}{3} \frac{\delta m_1}{m} - \frac{\delta m_2}{m} \right), \quad (2.4.8)$$

$$\bar{\omega}_L = \omega_L \left(1 - 0 - \frac{5}{3} \frac{\delta m_2}{m} \right). \quad (2.4.9)$$

The first correction term in Eq. (2.4.8) and Eq. (2.4.9) corresponds to the contribution of radiation reaction and the second correction term contributes to the vacuum fluctuation. Now evaluating the fraction $\frac{\bar{g}}{2} = \frac{\bar{\omega}_L}{\bar{\omega}_C}$ to the first order, we get

$$\frac{\bar{g}}{2} = \frac{\bar{\omega}_L}{\bar{\omega}_C} \simeq 1 + \frac{4}{3} \frac{\delta m_1}{m} - \frac{2}{3} \frac{\delta m_2}{m}. \quad (2.4.10)$$

The first correction due to radiation reaction is positive and is much larger than the negative correction due to vacuum fluctuation which implies that the radiation reaction slows down the cyclotron motion of the charge more efficiently than the Larmor precession of the spin. Conventionally the factor referring to the anomalous magnetic moment of electron is defined as $a_e = \frac{\bar{g}-2}{2}$. So from our calculation, we get

$$\begin{aligned} a_e &= \frac{4}{3} \frac{\delta m_1}{m} - \frac{2}{3} \frac{\delta m_2}{m} \\ &= \frac{2}{3} \frac{\delta m_1}{m} \left(2 - \frac{\delta m_2}{\delta m_1} \right). \end{aligned} \quad (2.4.11)$$

As δm_2 is associated with vacuum fluctuation which is a higher order effect than mass correction due to self-energy, we can assume that in the non-relativistic domain and in the lowest order $\delta m_2 \ll \delta m_1$. So using Eq. (2.2.12) we can finally write

$$a_e \simeq \frac{4}{3} \frac{\alpha}{\pi} \frac{\hbar \omega_M}{mc^2}. \quad (2.4.12)$$

Now using $\omega_M = \frac{mc^2}{\hbar}$ for the cut-off value as mentioned in [22, 8], we get the contribution of non-relativistic modes to the anomalous magnetic moment

$$a_e \simeq \frac{4}{3} \frac{\alpha}{\pi}, \quad (2.4.13)$$

which agrees with [22].

2.5 Conclusion

In this chapter, we have reproduced the reasoning of [2, 3] to calculate the contribution of the non-relativistic modes to the anomaly of the electron magnetic moment. The total one-loop anomaly of the magnetic moment of the electron first obtained by Schwinger is [15]

$$\begin{aligned} a_e &= \frac{g-2}{2} \\ &= \frac{\alpha}{2\pi}. \end{aligned} \quad (2.5.1)$$

We can conclude that most of the contribution to the electron $g-2$ comes from the non-relativistic domain. We have seen that the Larmor frequency is only modified by the fluctuation of vacuum energy whereas the cyclotron frequency is modified by both vacuum fluctuation and radiation reaction. Due to the effect of radiation reaction and vacuum fluctuation,

both Larmor and cyclotron frequencies are reduced but the cyclotron frequency is reduced more than the Larmor frequency indicating that the modification of the cyclotron frequency weighs more in modifying the g factor of the electron. As the main contribution in modifying the cyclotron frequency comes from the self-energy or radiation reaction of the electron, we can safely conclude that most of the modification to the g factor of the electron is a non-relativistic effect and essentially due to the effect of self-interaction of the electron. In the next chapter, we will perform relativistic calculations using the effective Hamiltonian approach and obtain the total one-loop anomaly to the g factor of the electron.

Chapter 3

Relativistic effective Hamiltonian approach to electron $g - 2$

3.1 Introduction

In the previous chapter, we considered electron $g - 2$ in the non-relativistic domain. Although most of the contribution to the electron $g - 2$ comes from the non-relativistic modes, for completeness of the effective Hamiltonian approach, in this chapter we will calculate the full Schwinger factor $a_e = \frac{\alpha}{2\pi}$. We will do so by splitting the QED Hamiltonian into two parts, free and interaction Hamiltonian. The interaction Hamiltonian contains the electrostatic interaction (self-interaction of the particles with their own Coulomb field) and the interaction of the Dirac current with the transverse Maxwell field. Then we will take the matrix element of the Hamiltonian and identify the relevant processes for electron $g - 2$ which will give us the total effective Hamiltonian. From the total effective Hamiltonian we will then obtain the modified Larmor and cyclotron frequencies. We will work with standard S.I. units in this chapter.

3.2 Calculation of electron $g - 2$

In this section, we will calculate the electron $g - 2$ from relativistic consideration and reproduce the Schwinger factor $a_e = \frac{\alpha}{2\pi}$ [15]. We start with introducing the full QED Hamiltonian

$$H = H_0 + H_I, \tag{3.2.1}$$

where H_0 is the unperturbed part of the Hamiltonian which is the summation of free Maxwell field Hamiltonian H_0 and free Dirac field Hamiltonian H_D

$$H_0 = \sum_i \hbar\omega_i \left(a_i^\dagger a_i + \frac{1}{2} \right), \quad (3.2.2)$$

$$H_D = \int d^3r \Psi^\dagger(\mathbf{r}) \{ \beta mc^2 + c\boldsymbol{\alpha} \cdot \boldsymbol{\pi}_0 \Psi(\mathbf{r}) \}, \quad (3.2.3)$$

where Ψ^\dagger and Ψ are the quantized Dirac fields and $\boldsymbol{\pi}_0 = \mathbf{p} - e\mathbf{A}_0(\mathbf{r})$ and \mathbf{A}_0 is the static vector potential. The interaction Hamiltonian H_I can be spilt into two parts

$$H_I = V_{\text{Coul}} + U_\perp, \quad (3.2.4)$$

where V_{Coul} is the electrostatic interaction and is defined as [4]

$$V_{\text{Coul}} = \frac{e^2}{8\pi\epsilon_0} \iint d^3r d^3r' \frac{\rho(\mathbf{r})\rho(\mathbf{r}')}{|\mathbf{r} - \mathbf{r}'|}, \quad (3.2.5)$$

where $\rho(\mathbf{r}) = \Psi^\dagger(\mathbf{r})\Psi(\mathbf{r})$ and It corresponds to the same field caused by \mathbf{E}_\parallel described in Eq. (2.2.4). U_\perp is the interaction between the Dirac current $\mathbf{j}(\mathbf{r})$ where $\mathbf{j}(\mathbf{r}) = ec\Psi^\dagger(\mathbf{r})\boldsymbol{\alpha}\Psi(\mathbf{r})$ and the transverse Maxwell field $\mathbf{A}(\mathbf{r})$ [4]

$$\begin{aligned} U_\perp &= - \int d^3r \mathbf{j}(\mathbf{r}) \cdot \mathbf{A}(\mathbf{r}) \\ &= -ec \int d^3r \psi^\dagger(\mathbf{r}) \boldsymbol{\alpha} \psi(\mathbf{r}) \cdot \mathbf{A}(\mathbf{r}). \end{aligned} \quad (3.2.6)$$

3.2.1 Matrix element of the effective Hamiltonian

In this section, we will derive the matrix element of the Hamiltonian and arrive at the form from where we can figure out the relevant interactions for the process of electron $g - 2$. H_0 in Eq. (3.2.1) corresponds to states with an arbitrary number of noninteracting electron, positrons and photons and H_I describes the coupling between them. We need selection rules for describing virtual transition between different states. The quantized Dirac field operators are given by [4]

$$\Psi^\dagger(\mathbf{r}) = \sum_q c_q^\dagger u_q^\dagger(\mathbf{r}) + b_q v_q(\mathbf{r}), \quad (3.2.7)$$

$$\Psi(\mathbf{r}) = \sum_s c_s u_s(\mathbf{r}) + b_s^\dagger v_s(\mathbf{r}), \quad (3.2.8)$$

where c^\dagger, c are the creation and annihilation operators for electron and b^\dagger, b are the creation and annihilation operators for positron. u and v are the eigenspinors of the Hamiltonian

$$\mathcal{H}_D = \beta mc^2 + c\boldsymbol{\alpha}\cdot\boldsymbol{\pi}_0 \quad (3.2.9)$$

corresponding to positive and negative energy. The energy corresponding to \mathcal{H}_D with $\boldsymbol{\pi}_0 = 0$ is $E_0 + (N_e + N_p)mc^2$ where E_0 is the energy of the vacuum (non-observable) which will be subtracted later and N_e and N_p are the number operators for electron and positron and they are given by

$$N_e = \sum_q c_q^\dagger c_q \quad \text{and} \quad N_p = \sum_q b_q^\dagger b_q \quad (3.2.10)$$

The unperturbed energy levels of $\mathcal{H}_D = \beta mc^2$ for different number of electron and positrons is given in the following figure which follows [4]

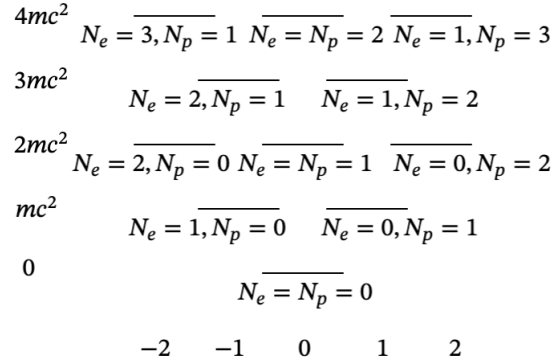


Figure 3.2.1: Unperturbed energy levels for $\mathcal{H}_D = \beta mc^2$ for different combinations of numbers of electrons and positrons. Energy is plotted vertically and the total charge ($N_p - N_e$) is plotted horizontally. The horizontal line ranges from -2 to 2 corresponding to states with 2 electrons or 2 positrons. The distance between two energy levels in the same column is $2mc^2$ which corresponds to creation or annihilation of electron-positron pairs.

The interaction Hamiltonian H_I only couples to energy levels in the same vertical column because of charge conservation and so the distance between two energy levels in the same column should be $2mc^2$ which corresponds to creation or annihilation of one or several pairs of electrons or positrons. So for a system that has a single electron, the minimum coupling because of H_I can occur between the states with energy mc^2 and $3mc^2$. Now for \mathcal{H}_D described in Eq. (3.2.9) which describes the dynamics of single slow electron with no incident photon, we start with a manifold \mathcal{E}_1 which describes the energy state mc^2 in Figure 3.2.1 where the perturbation V_{Coul} in Eq. (3.2.5) splits it into states n and n' . For the perturbation U_\perp in Eq. (3.2.6), the electron can now emit a virtual photon and virtually make a transition to manifold \mathcal{E}_2 from n state and return to n' state, $n' \rightarrow a \rightarrow n$. Here now we have one electron

and one photon in \mathcal{E}_2 . Finally, the manifold \mathcal{E}_4 which corresponds to the energy state $3mc^2$ in Figure 3.2.1 now with two electrons, one positron and one photon where again due to U_\perp the transition $n' \rightarrow b \rightarrow n$ occurs. The following figure depicts the analogous diagram corresponding to Figure 3.2.1 and it follows [4]

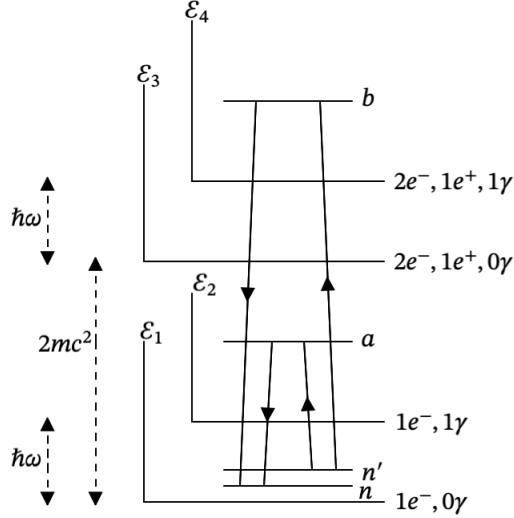


Figure 3.2.2: Relevant virtual energy levels of \mathcal{H}_D . The perturbation potential V_{Coul} splits the energy level \mathcal{E}_1 into states n and n' and for the perturbation potential U_\perp the electron makes a virtual transition ($n' \rightarrow a \rightarrow n$) to \mathcal{E}_2 . The energy level \mathcal{E}_4 corresponds to $3mc^2$ and due to U_\perp , the electron makes a similar transition $n' \rightarrow b \rightarrow n$.

We will now calculate the matrix element of the Hamiltonian between states n and n' in the manifold \mathcal{E}_1 and transition to state a and b from n and n' . The transition to n and n' is mediated by V_{Coul} described in Eq. (3.2.5) and transition from $n' \rightarrow a \rightarrow n$ and $n' \rightarrow b \rightarrow n$ is mediated by U_\perp Eq. (3.2.6). For a single particle state denoted as 1_n and $1_{n'}$ of \mathcal{E}_1 , we can now write the effective Hamiltonian as follows [4]

$$\begin{aligned}
\langle 1_n | H_{\text{eff}} | 1_{n'} \rangle &= \langle 1_n | V_{\text{Coul}} | 1_{n'} \rangle \\
&+ \frac{1}{2} \sum_{a \in \mathcal{E}_2} \langle 1_n | U_\perp | a \rangle \langle a | U_\perp | 1_{n'} \rangle \left[\frac{1}{E_n - E_a} + \frac{1}{E_{n'} - E_a} \right] \\
&+ \frac{1}{2} \sum_{b \in \mathcal{E}_4} \langle 1_n | U_\perp | b \rangle \langle b | U_\perp | 1_{n'} \rangle \left[\frac{1}{E_n - E_b} + \frac{1}{E_{n'} - E_b} \right], \tag{3.2.11}
\end{aligned}$$

where the first term describes virtual transition between states 1_n and $1_{n'}$ due to V_{Coul} and the last two terms describe the virtual transition due to U_\perp . For working out the matrix element of V_{Coul} we use the quantized Dirac field operators mentioned in Eqs. (3.2.7) and (3.2.8). From different combinations of the creation and annihilation operators we can vary the number

of particles by $\Delta N_1 = 0, \pm 2$ for the combination $\Psi^\dagger(\mathbf{r})\Psi(\mathbf{r})$ and same for the combination $\Psi^\dagger(\mathbf{r}')\Psi(\mathbf{r}')$ with $\Delta N_2 = 0, \pm 2$. For example c_q^\dagger creates an electron and c_s destroys one and so $\Delta N_1 = 0$; b_q destroys a positron and c_s destroys an electron and so $\Delta N_2 = -2$. For the purpose of charge conservation we need $\Delta N_1 + \Delta N_2 = 0$ and so out of eight combinations we get six terms altogether. The schematic diagram for various combinations follows from [4]

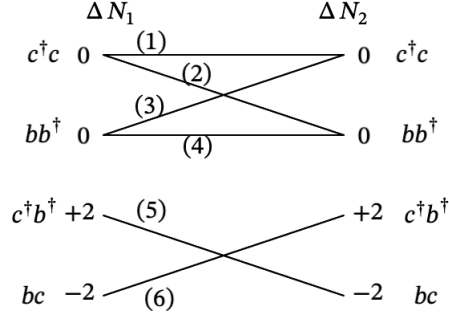


Figure 3.2.3: Various combinations of the creation and annihilation operators of electrons and positrons. c^\dagger, c are the creation and annihilation operators for electron and b^\dagger, b are the creation and annihilation operators for positron.

Analogously same for the matrix elements involving U_\perp but now with the presence of α matrices and polarizations.

3.2.2 Calculation of the matrix element of V_{Coul}

Now we calculate contribution from the various terms mentioned in Figure 3.2.3 and for this it is convenient to work with the Fourier transform of the V_{Coul} given by [4]

$$V_{\text{Coul}} = \frac{e^2}{16\pi^3\epsilon_0} \iiint d^3r d^3r' d^3k \frac{\rho(\mathbf{r}) \exp(i\mathbf{k}\cdot\mathbf{r}) \rho(\mathbf{r}') \exp(-i\mathbf{k}\cdot\mathbf{r}')}{k^2}, \quad (3.2.12)$$

where $\rho(\mathbf{r}) = \Psi^\dagger(\mathbf{r})\Psi(\mathbf{r})$.

3.2.2.1 Contribution of term 1

The first term is denoted as (1) in Figure 3.2.3. Subtracting the vacuum shift, we get

$$(1) = \frac{e^2}{16\pi^3\epsilon_0} \int \frac{d^3k}{k^2} \sum_q \sum_r \sum_s \sum_t \left(\int d^3r u_q^\dagger(\mathbf{r}) e^{i\mathbf{k}\cdot\mathbf{r}} u_r(\mathbf{r}) \right) \times \left(\int d^3r' u_s^\dagger(\mathbf{r}') e^{-i\mathbf{k}\cdot\mathbf{r}'} u_r(\mathbf{r}') \right) (\langle 1_n | c_q^\dagger c_r c_s^\dagger c_t | 1_{n'} \rangle - \delta_{nn'} \langle 0 | c_q^\dagger c_r c_s^\dagger c_t | 0 \rangle). \quad (3.2.13)$$

Now using

$$\langle 1_n | c_q^\dagger c_r c_s^\dagger c_t | 1_{n'} \rangle = \delta_{nq} \delta_{rs} \delta_{tn'}, \quad (3.2.14)$$

$$\langle 0 | c_q^\dagger c_r c_s^\dagger c_t | 0 \rangle = 0, \quad (3.2.15)$$

and from the matrix element $\langle u_q | e^{i\mathbf{k}\cdot\mathbf{r}} | u_r \rangle \langle u_s | e^{-i\mathbf{k}\cdot\mathbf{r}} \rangle$ obtained from the two integrals, we can rewrite Eq. (3.2.13) as

$$(1) = \frac{e^2}{16\pi^3\epsilon_0} \int d^3k \frac{1}{k^2} \langle u_n | e^{i\mathbf{k}\cdot\mathbf{r}} P_+ e^{-i\mathbf{k}\cdot\mathbf{r}} | u_{n'} \rangle, \quad (3.2.16)$$

where $P_+ = \sum_s |u_s\rangle \langle u_s|$. The process is shown in the diagram below taken from [4]

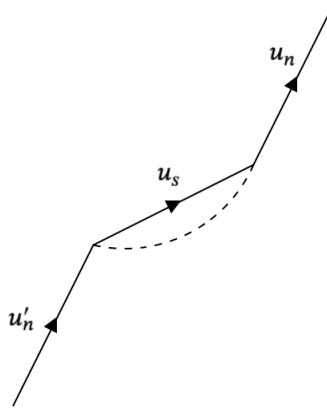


Figure 3.2.4: Diagram for term (1). The upwards arrow is for electron and the curve dotted line represents electrostatic interaction. This diagram represents interaction between electron and its Coulomb field with electron as the internal line.

3.2.2.2 Contribution of term 2 and 3

The second and third term denoted as (2) and (3) in Figure 3.2.3 can be written as

$$(2) = \frac{e^2}{16\pi^3\epsilon_0} \int \frac{d^3k}{k^2} \sum_q \sum_r \sum_s \sum_t \langle u_q | e^{i\mathbf{k}\cdot\mathbf{r}} | u_r \rangle \langle v_s | e^{-i\mathbf{k}\cdot\mathbf{r}} | v_t \rangle \times \left(\langle 1_n | c_q^\dagger c_r c_s b_t^\dagger | 1_{n'} \rangle - \delta_{nn'} \langle 0 | c_q^\dagger c_r c_s b_t^\dagger | 0 \rangle \right). \quad (3.2.17)$$

Using

$$\langle 1_n | c_q^\dagger c_r b_s b_t^\dagger | 1_{n'} \rangle = \delta_{st} \delta_{rn'} \delta_{qn}, \quad (3.2.18)$$

$$\langle 0 | c_q^\dagger c_r b_s b_t^\dagger | 0 \rangle = 0, \quad (3.2.19)$$

Eq. (3.2.17) becomes

$$(2) = \frac{e^2}{16\pi^3 \varepsilon_0} \int \frac{d^3 k}{k^2} \langle u_n | e^{i\mathbf{k}\cdot\mathbf{r}} | u_{n'} \rangle \sum_s \langle v_{\bar{s}} | e^{-i\mathbf{k}\cdot\mathbf{r}} | v_{\bar{s}} \rangle. \quad (3.2.20)$$

The term $\sum_s \langle v_{\bar{s}} | e^{-i\mathbf{k}\cdot\mathbf{r}} | v_{\bar{s}} \rangle$ is the Fourier transform of the charge distribution in the vacuum and the overall process describes the electrostatic interaction of the electron with the charge distribution in the vacuum and in the presence of uniform magnetic field, the contribution of terms 2 and 3 is zero because charge distribution in vacuum is uniform and static magnetic field is invariant under translation. The process is shown in the diagram below taken from[4]

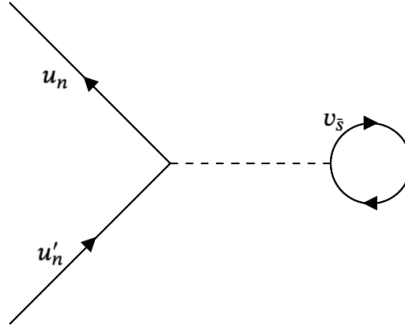


Figure 3.2.5: Diagram for term (2) and (3). The arrows represent electron, the straight dotted line represents electrostatic interaction and the circle is for charge distribution in vacuum. This diagram represents electrostatic interaction of the electron with the charge distribution in the vacuum.

3.2.2.3 Contribution of term 4

Denoted as (4) in Figure 3.2.3, the fourth term can be cast in the form

$$(4) = \frac{e^2}{16\pi^3 \varepsilon_0} \int \frac{d^3 k}{k^2} \sum_q \sum_r \sum_s \sum_t \langle v_{\bar{q}} | e^{i\mathbf{k}\cdot\mathbf{r}} | v_{\bar{r}} \rangle \langle v_{\bar{s}} | e^{-i\mathbf{k}\cdot\mathbf{r}} | v_{\bar{t}} \rangle \\ \times \left(\langle 1_n | b_q b_r^\dagger b_s b_t^\dagger | 1_{n'} \rangle - \delta_{nn'} \langle 0 | b_q b_r^\dagger b_s b_t^\dagger | 0 \rangle \right). \quad (3.2.21)$$

Both matrix elements of the bracket are equal to $\delta_{nn'} \delta_{qr} \delta_{st}$ and so contribution of term (4) is also zero. This term represents the electrostatic interaction in vacuum and is same in

presence and absence of the electron. When one subtracts the vacuum shift, then this term becomes zero. The process is shown in the diagram below taken from [4]

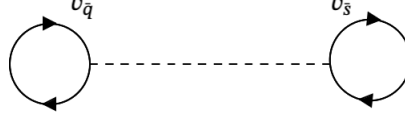


Figure 3.2.6: Diagram for term (4). The circles are the charge distribution in the vacuum and the dotted line represents the electrostatic interaction. This diagram represents electrostatic interaction in vacuum.

3.2.2.4 Contribution of term 5

Denoted as (5) is Figure 3.2.3, this term is proportional to

$$\langle 1_n | c_q^\dagger b_r^\dagger b_s c_t | 1_{n'} \rangle - \delta_{nn'} \langle 0 | c_q^\dagger b_r^\dagger b_s c_t | 0 \rangle, \quad (3.2.22)$$

which is equal to zero.

3.2.2.5 Contribution of term 6

In Figure 3.2.3, the sixth term is denoted as (6) and we can write it as

$$(6) = \frac{e^2}{16\pi^3\epsilon_0} \int \frac{d^3k}{k^2} \sum_q \sum_r \sum_s \sum_t \langle v_{\bar{q}} | e^{i\mathbf{k}\cdot\mathbf{r}} | u_r \rangle \langle u_s | e^{-i\mathbf{k}\cdot\mathbf{r}} \rangle \\ \times \left(\langle 1_n | b_q c_r c_s^\dagger b_t^\dagger | 1_{n'} \rangle - \delta_{nn'} \langle 0 | b_q c_r c_s^\dagger b_t^\dagger | 0 \rangle \right). \quad (3.2.23)$$

Now using $c_r c_s^\dagger = \delta_{rs} - c_s^\dagger c_r$ for the first term in the bracket

$$\langle 1_n | b_q c_r c_s^\dagger b_t^\dagger | 1_{n'} \rangle = \delta_{rs} \delta_{nn'} \delta_{qt} - \delta_{sn} \delta_{qt} \delta_{rn'}, \quad (3.2.24)$$

and the second term in the bracket

$$\delta_{nn'} \langle 0 | b_q c_r c_s^\dagger b_t^\dagger | 0 \rangle = \delta_{nn'} \delta_{rs} \delta_{qt}. \quad (3.2.25)$$

So Eq. (3.2.23) becomes

$$(6) = -\frac{e^2}{16\pi^3\epsilon_0} \int \frac{d^3k}{k^2} \langle u_n | e^{i\mathbf{k}\cdot\mathbf{r}} P_- e^{i\mathbf{k}\cdot\mathbf{r}} | u_{n'} \rangle, \quad (3.2.26)$$

where $P_- = \sum_q |v_{\bar{q}}\rangle \langle v_{\bar{q}}|$. The process is shown in the diagram below taken from [4]

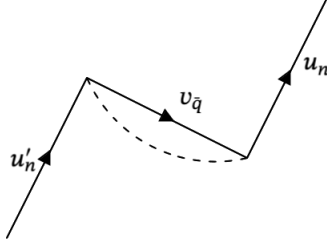


Figure 3.2.7: Diagram for term (6). The upwards arrow is for electron, the downward arrow is for positron and the dotted line represents electrostatic interaction. This diagram represents interaction between electron and its Coulomb field with positron as the internal line.

Combining all the contributions for term (1) – (6), we get

$$\langle 1_n | V_{\text{Coul}} | 1_{n'} \rangle = \frac{e^2}{16\pi^3 \epsilon_0} \int \frac{d^3 k}{k^2} \langle u_n | e^{i\mathbf{k}\cdot\mathbf{r}} (P_+ - P_-) e^{-i\mathbf{k}\cdot\mathbf{r}} | u_{n'} \rangle. \quad (3.2.27)$$

For $P_+ - P_-$ we can use the identity [4]

$$P_+ - P_- = \frac{\mathcal{H}_D}{\sqrt{\mathcal{H}_D^2}}, \quad (3.2.28)$$

where \mathcal{H}_D is defined by Eq. (3.2.9) and

$$\mathcal{H}_D^2 = m^2 c^4 + c^2 \boldsymbol{\pi}_0^2 - q \hbar c^2 \boldsymbol{\sigma} \cdot \mathbf{B}_0, \quad (3.2.29)$$

where for $(\boldsymbol{\alpha} \cdot \boldsymbol{\pi}_0)^2$ we have used Eq. (B.0.15). So first we have to evaluate

$$e^{i\mathbf{k}\cdot\mathbf{r}} \frac{\mathcal{H}_D}{\sqrt{\mathcal{H}_D^2}} e^{-i\mathbf{k}\cdot\mathbf{r}} = \frac{\beta m c^2 + c \boldsymbol{\alpha} \cdot (\boldsymbol{\pi}_0 - \hbar \mathbf{k})}{\sqrt{m^2 c^4 + c^2 (\boldsymbol{\pi}_0 - \hbar \mathbf{k})^2 - e \hbar c^2 \boldsymbol{\sigma} \cdot \mathbf{B}_0}}, \quad (3.2.30)$$

as the exponential factors transforms $\boldsymbol{\pi}_0$ to $\boldsymbol{\pi}_0 - \hbar \mathbf{k}$. Upon expanding the denominator of Eq. (3.2.30) in powers of $\boldsymbol{\pi}_0$ and $\boldsymbol{\sigma} \cdot \mathbf{B}_0$ and keeping terms in $\boldsymbol{\alpha} \cdot \boldsymbol{\pi}_0$, $\boldsymbol{\pi}_0^2$ and $\boldsymbol{\sigma} \cdot \mathbf{B}_0$ and then multiplying with the numerator and finally performing the angular integration we get

$$\langle 1_n | V_{\text{Coul}} | 1_{n'} \rangle = \langle u_n | \mathcal{V}_{\text{Coul}} | u_{n'} \rangle, \quad (3.2.31)$$

where

$$\mathcal{V}_{\text{Coul}} = \frac{\alpha}{\pi} \int_0^{x_M} dx \left\{ \beta m c^2 \frac{1}{\sqrt{1+x^2}} + c \alpha \cdot \boldsymbol{\pi}_0 \frac{1}{\sqrt{1+x^2}} \left(1 - \frac{x^2}{3(1+x^2)} \right) - \beta \frac{\boldsymbol{\pi}_0^2}{2m} \frac{1}{(1+x^2)^{5/2}} + \beta \frac{e\hbar}{2m} \boldsymbol{\sigma} \cdot \mathbf{B}_0 \frac{1}{(1+x^2)^{3/2}} \right\} \quad (3.2.32)$$

where α is the fine structure constant and x_M is the cut-off. Detailed calculation is given in Appendix C.1

3.2.3 Calculation of the matrix element of the transverse Photon (U_{\perp})

The calculation process involving U_{\perp} is similar to $\mathcal{V}_{\text{Coul}}$ as we can see from Eq. (3.2.6) that U_{\perp} has the same combination as $\mathcal{V}_{\text{Coul}}$. The differences are that now we have to take the matrix elements of $\boldsymbol{\alpha} \cdot \boldsymbol{\epsilon} \exp(i\mathbf{k} \cdot \mathbf{r})$ where $\boldsymbol{\epsilon}$ is the polarization of the transverse photon and we now have energy denominators from Eq. (3.2.11). We will denote the last two terms in Eq. (3.2.11) more compactly as $\langle 1_n | H_{\text{eff}}^{\perp} | 1_{n'} \rangle$.

3.2.3.1 Contribution of term 1

For the transverse photon, we start with \mathcal{E}_2 in Figure 3.2.1. So in the intermediate state we have one electron and one transverse photon. The process is shown in the diagram below taken from [4]

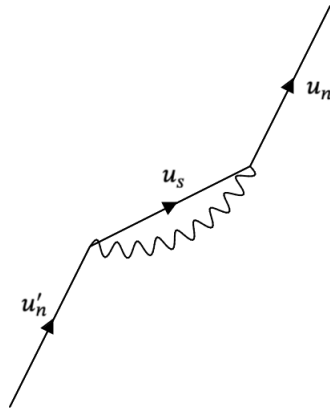


Figure 3.2.8: Contribution of term (1). The upwards arrow represents electron and the wavy line is for transverse photon. This diagram represents interaction between electron and its transverse radiation field with electron as the internal line.

3.2.3.2 Contribution of terms 2 and 3

The second and third term describes the interaction of the electron with the transverse field of the vacuum current. In a uniform magnetic field, the vacuum current is equal to zero. So the contribution of these two terms is zero. The process is shown in the diagram below taken from [4]

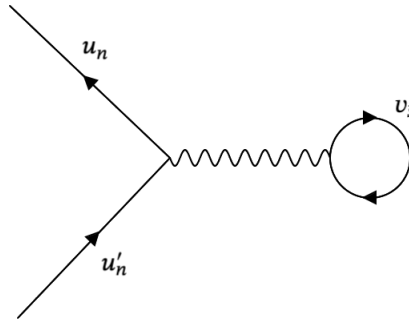


Figure 3.2.9: Diagrams for terms (2) and (3). The arrows are for electron, the straight wavy line represents interaction by transverse photon and the circle is charge in vacuum. This diagram represents the interaction of the electron with the transverse field of the vacuum current.

3.2.3.3 Contribution of term 4

This term describes the transverse interaction between the charges in the vacuum and it is same in presence or absence of the electron and so its contribution will not affect H_{eff}^{\perp} . The process is shown in the diagram below taken from [4]

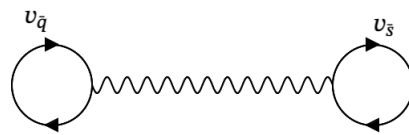


Figure 3.2.10: Diagram for term (4). This diagram represents transverse interaction in vacuum.

3.2.3.4 Contribution of term 5

It is equal to zero for the same reason as V_{Coul} .

3.2.3.5 Contribution of term 6

This term represents \mathcal{E}_4 in Figure 3.2.1 where in the intermediate state we now have two electrons, one positron and one transverse photon. The process is shown in the diagram

below taken from [4]

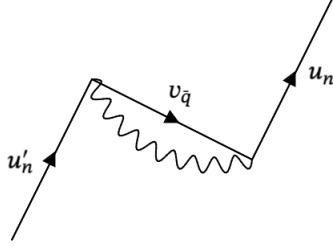


Figure 3.2.11: Diagram for term (6). The upward arrows are for electron, the downward arrow is for positron and the wavy line is for transverse photon. This diagram represents interaction between electron and its transverse radiation field with positron as the internal line.

So from terms (1) and (6) and using Eqs. (3.2.6) and (3.2.11) we get [4]

$$\begin{aligned}
\langle 1_n | H_{\text{eff}}^\perp | 1_{n'} \rangle &= \langle u_n | \mathcal{H}_{\text{eff}}^\perp | u_{n'} \rangle \\
&= \frac{e^2 c^2}{2} \int d^3 k \sum_\epsilon \frac{\hbar}{2 \epsilon_0 \omega (2\pi)^3} \\
&\times \langle u_n | (\boldsymbol{\epsilon} \cdot \boldsymbol{\alpha}) e^{i\mathbf{k} \cdot \mathbf{r}} \left(\frac{p_+}{E_n - \hbar\omega - \mathcal{H}_D} + \frac{P_-}{E_n + \hbar\omega - \mathcal{H}_D} \right) (\boldsymbol{\epsilon} \cdot \boldsymbol{\alpha}) e^{-i\mathbf{k} \cdot \mathbf{r}} | u_{n'} \rangle \\
&+ \text{same term with } E_n \rightarrow E_{n'}, \tag{3.2.33}
\end{aligned}$$

where we have used Eq. (2.2.2) for $\mathbf{A}(\mathbf{r})$ and the integration sign comes from converting the summation over k . Now

$$\begin{aligned}
\frac{p_+}{E_n - \hbar\omega - \mathcal{H}_D} + \frac{P_-}{E_n + \hbar\omega - \mathcal{H}_D} &= \frac{1}{E_n - \mathcal{H}_D - (P_+ - P_-)\hbar\omega} \\
&= \frac{E_n + \mathcal{H}_D + \hbar\omega \frac{\mathcal{H}_D}{\sqrt{\mathcal{H}_D^2}}}{E_n^2 - \left(\mathcal{H}_D^2 + \hbar^2 \omega^2 + 2\hbar\omega \sqrt{\mathcal{H}_D^2} \right)} \tag{3.2.34}
\end{aligned}$$

The exponential factors transform $\boldsymbol{\pi}_0$ to $\boldsymbol{\pi}_0 - \hbar\mathbf{k}$ and like V_{Coul} we expand the fraction of Eq. (3.2.34) in a power series of $\boldsymbol{\pi}_0$, $\boldsymbol{\sigma} \cdot \mathbf{B}_0$ and $E_n^2 - m^2 c^4$ and sum over $\boldsymbol{\epsilon}$ considering $\boldsymbol{\epsilon} \perp \mathbf{k}$.

After integrating over solid angle we get [4]

$$\begin{aligned}
\mathcal{H}_{\text{eff}}^{\perp} = & \frac{\alpha}{\pi} \int_0^{x_M} dx \left\{ \beta m c^2 \left(x - \frac{x^2}{\sqrt{1+x^2}} \right) \right. \\
& + c \boldsymbol{\alpha} \cdot \boldsymbol{\pi}_0 \left(\frac{2x}{3} - \frac{2x^2}{3\sqrt{1+x^2}} - \frac{3x^2+2}{3(1+x^2)^{3/2}} \right) \\
& - \beta \frac{\boldsymbol{\pi}_0^2}{2m} \left(\frac{4x}{3} - \frac{4x^2}{3\sqrt{1+x^2}} - \frac{x^2(2x^2+5)}{3(1+x^2)^{5/2}} \right) \\
& \left. + \beta \frac{e\hbar}{2m} \boldsymbol{\sigma} \cdot \mathbf{B}_0 \left(2x - \frac{2x^2}{\sqrt{1+x^2}} - \frac{3x^2+4}{3(1+x^2)^{3/2}} \right) \right\}. \tag{3.2.35}
\end{aligned}$$

3.2.4 Total effective Hamiltonian

Any Dirac Hamiltonian of the form

$$H = \beta m c^2 (1 + \epsilon) + c \boldsymbol{\alpha} \cdot \boldsymbol{\pi}_0 (1 + \epsilon') + \beta \mathcal{E} \tag{3.2.36}$$

can be transformed into [4]

$$\begin{aligned}
H = & \beta m c^2 (1 + \epsilon) + \frac{c^2 (\boldsymbol{\alpha} \cdot \boldsymbol{\pi}_0)^2 (1 + \epsilon')^2}{2m c^2 (1 + \epsilon)} + \beta \mathcal{E} \\
= & \beta \left(m c^2 (1 + \epsilon) + \mathcal{E} + \left(\frac{\boldsymbol{\pi}_0^2}{2m} - \frac{e\hbar}{2m} \boldsymbol{\sigma} \cdot \mathbf{B}_0 \right) (1 + 2\epsilon' - \epsilon) \right) \tag{3.2.37}
\end{aligned}$$

for $\epsilon, \epsilon' \ll 1$. We have used Eq. (B.0.15) and expanded $\frac{(1+\epsilon')^2}{(1+\epsilon)}$ neglecting squared terms. Now transforming the sum of Eqs. (3.2.32) and (3.2.35) like Eq. (3.2.37) we get one more $\left(\frac{\boldsymbol{\pi}_0^2}{2m} - \frac{e\hbar}{2m} \boldsymbol{\sigma} \cdot \mathbf{B}_0 \right)$ factor from the square of $c \boldsymbol{\alpha} \cdot \boldsymbol{\pi}_0$ terms from Eq. (3.2.37) and summing it with the existing $\left(\frac{\boldsymbol{\pi}_0^2}{2m} - \frac{e\hbar}{2m} \boldsymbol{\sigma} \cdot \mathbf{B}_0 \right)$ factor in Eqs. (3.2.32) and (3.2.35), we get [4]

$$\begin{aligned}
\mathcal{H}_{\text{eff}} = & m c^2 \left(1 + \frac{\alpha}{\pi} \int_0^{x_M} f_1(x) dx \right) \\
& + \frac{\boldsymbol{\pi}_0^2}{2m} \left(1 - \frac{\alpha}{\pi} \int_0^{x_M} f_2(x) dx \right) \\
& - \frac{e\hbar}{2m} \boldsymbol{\sigma} \cdot \mathbf{B}_0 \left(1 - \frac{\alpha}{\pi} \int_0^{x_M} f_3(x) dx \right), \tag{3.2.38}
\end{aligned}$$

where

$$f_1(x) = \frac{1}{\sqrt{1+x^2}} + x - \frac{x^2}{\sqrt{1+x^2}}, \quad (3.2.39)$$

$$f_2(x) = x \left(1 - \frac{x}{\sqrt{1+x^2}} + \frac{4}{3x\sqrt{1+x^2}} - \frac{x}{3(1+x^2)^{3/2}} - \frac{2x}{(1+x^2)^{5/2}} \right), \quad (3.2.40)$$

$$f_3(x) = x \left[\frac{5}{3} \left(1 - \frac{x}{\sqrt{1+x^2}} \right) + \frac{2}{3} \frac{x}{(1+x^2)^{3/2}} \right]. \quad (3.2.41)$$

3.2.5 Calculation of anomalous magnetic moment of electron

From Eq. (3.2.38), we can write the effective Hamiltonian for all modes as

$$\mathcal{H}_{\text{eff}} = \frac{\pi_0^2}{2m} \left(1 - \frac{\alpha}{\pi} \int_0^{x_M} f_2(x) dx \right) - \frac{e\hbar}{2m} \boldsymbol{\sigma} \cdot \mathbf{B}_0 \left(1 - \frac{\alpha}{\pi} \int_0^{x_M} f_3(x) dx \right). \quad (3.2.42)$$

The cyclotron and Larmor frequency will also be modified by the same factor. The modified cyclotron and Larmor frequency are

$$\bar{\omega}_C = \omega_C \left(1 - \frac{\alpha}{\pi} \int_0^{x_M} f_2(x) dx \right), \quad (3.2.43)$$

$$\bar{\omega}_L = \omega_L \left(1 - \frac{\alpha}{\pi} \int_0^{x_M} f_3(x) dx \right). \quad (3.2.44)$$

So the modified g factor is

$$\frac{\bar{g}}{2} = \frac{\bar{\omega}_L}{\bar{\omega}_C} = \frac{1 - \frac{\alpha}{\pi} \int_0^{x_M} f_3(x) dx}{1 - \frac{\alpha}{\pi} \int_0^{x_M} f_2(x) dx}. \quad (3.2.45)$$

In first order

$$\frac{\bar{g}}{2} = \left(1 - \frac{\alpha}{\pi} \int_0^{x_M} f_3(x) dx \right) \left(1 + \frac{\alpha}{\pi} \int_0^{x_M} f_2(x) dx \right). \quad (3.2.46)$$

Neglecting cross terms between $f_2(x)$ and $f_3(x)$, the anomalous magnetic moment now becomes

$$a_e = \frac{\bar{g} - 2}{2} = \frac{\alpha}{\pi} \int_0^{x_M} [f_2(x) - f_3(x)] dx. \quad (3.2.47)$$

After evaluating the integral for $x_M = \infty$, we get the same result as Schwinger [15]

$$a_e = \frac{\alpha}{2\pi}. \quad (3.2.48)$$

3.3 Justification of the obtained non-relativistic contribution of electron $g - 2$

In this section, we will take the non-relativistic limit of the relativistic calculation described in the previous section and show that it matches with our non-relativistic calculations done in section 2.4. For this purpose we start by expanding function $f_2(x)$ and $f_3(x)$ in Eqs. (3.2.40) and (3.2.41). Some terms of the expanded series is

$$f_2(x) = \frac{4}{3} + x - 4x^2 + \frac{13x^4}{2} + \mathcal{O}(x^6), \quad (3.3.1)$$

$$f_3(x) = 0 + \frac{5x}{3} - x^2 - \frac{x^4}{6} + \mathcal{O}(x^6). \quad (3.3.2)$$

Using the lowest order in the expansion and inserting them in Eq. (3.2.47) we get

$$\begin{aligned} a_e &\simeq \frac{4}{3} \frac{\alpha}{\pi} \int_0^{x_M} dx \\ &= \frac{4}{3} \frac{\alpha}{\pi} x_M. \end{aligned} \quad (3.3.3)$$

Here we can not use $x_M = \infty$ as the series is not convergent which indicates the lack of covariance in the non-relativistic formalism. After setting $\omega_M = \frac{mc^2}{\hbar}$, we get $x_M = 1$ and thus we reproduce our result in Eq. (2.4.13). This result justifies neglecting the effect of vacuum polarization in the non-relativistic calculation and we can now safely conclude that the main contribution comes from the non-relativistic modes and the effect of radiation reaction is significantly larger than vacuum fluctuation in the process regarding the anomalous magnetic moment of the electron.

3.4 Conclusion

In this chapter, we have reproduced [4] and calculated the Schwinger factor $a_e = \frac{\alpha}{2\pi}$ using relativistic effective Hamiltonian approach. We have seen that among several processes, only the interaction of the electron with the Coulomb photon (Figures 3.2.4 and 3.2.7) and transverse photons (Figures 3.2.8 and 3.2.11) contributes whereas no diagrams involving vacuum is relevant to the total one-loop electron $g - 2$. This justifies ignoring effects of vacuum fluctuation in our non-relativistic calculation of electron $g - 2$ discussed in the previous chapter. We have also taken the non-relativistic limit of our final result and justified our obtained result in the previous chapter. We can also see that the main contribution to the electron $g - 2$ comes from radiation reaction and not vacuum fluctuation. From the full

relativistic calculation, we can clearly see the main drawback of our non-relativistic approach. The covariant relativistic formalism discussed in this chapter does not need any cut-offs and the need of a cut-off in the non-relativistic calculation indicates the lack of covariance in that formalism. This concludes our discussion of the anomalous magnetic moment of the electron using the effective Hamiltonian approach. In the next chapter, we will see Luttinger's approach to electron $g - 2$ to get a new perspective of the radiation reaction [5].

Chapter 4

Luttinger's approach to the electron $g - 2$

4.1 Introduction

The anomalous magnetic moment of the electron and the discrepancy with the predicted value of the g factor by the Dirac equation was first theoretically explained by Schwinger in 1948 [23] and the detailed calculation was published in 1951 [15]. Schwinger considered the coupling between the electron and radiation field. The self-energy of electron introduces divergences in the theory and Schwinger used the concept of renormalization of the mass and the magnetic moment of the electron to get rid of the divergences. In 1948, Joaquin Luttinger provided an alternative approach to calculate the change in the magnetic moment without any reference to the subtraction formalism of renormalization [5]. Luttinger tackled the problem of electron $g - 2$ in the context of an electron in a homogenous magnetic field. The electron interacting with the zero point vibration of the quantized radiation field gives rise to infinite energies which are ascribed as change in mass and charge of the electron. Schwinger got rid of the infinite energies by his construct of subtraction formalism of renormalization. Luttinger wanted to avoid this artificial construct by targeting the corresponding energies which arise only because of the electron's interaction with magnetic field and avoiding the corresponding energies due to electron's self interaction. His insight was that the lowest eigenstate of the Dirac operator in homogenous magnetic field has an energy $E = m_e$ which does not depend on the applied field. For this state of the electron with $g = 2$, the energy from the orbital magnetic moment cancels the energy from the non-anomalous part of the spin magnetic moment. The change in energy for such a state due to change in mass and charge of the electron lies in the 0th power term upon employing perturbation theory in powers of the external field. This corresponds to the self-energy terms

$$\Delta E = \Delta E_{\text{self}}(0). \tag{4.1.1}$$

As ΔE_{self} is independent of the external field then the true change in energy must come from the higher order terms. All the divergent quantities are contained in the 0th power terms and then the linear and higher order terms in the external field will now contain the contributions from the anomalous magnetic moment of the electron. Here we will only consider the terms linear in the strength of the applied field. So, by isolating the terms linear in the applied field it is expected that we will get the alteration of the g -factor as a coefficient of the linear terms. The total change in energy ΔE will contain two terms ΔE_{static} and $\Delta E_{\text{dynamic}}$

$$\Delta E = \Delta E_{\text{static}} + \Delta E_{\text{dynamic}}. \quad (4.1.2)$$

The first term ΔE_{static} contains the contribution of the electrostatic energy of the electron and $\Delta E_{\text{dynamic}}$ contains the contribution of electrons interaction with the external field. In both cases we will use Dirac wave functions for electrons in magnetic field. We will consider natural units i.e. $\hbar = c = \epsilon_0 = 1$ in this chapter.

4.2 Defining terms for the calculation

The total hamiltonian of an electron interacting with magnetic field is given by

$$H = H_0 + H_1 + H_{\text{static}}. \quad (4.2.1)$$

where H_0 is the unperturbed Dirac Hamiltonian minimally coupled to the external field. H_1 and H_{static} are the perturbations corresponding to the interaction with radiation field and electrostatic energy from the interaction between all charge densities of the system respectively. Explicitly [5]

$$H_0 = \int \{ -\Psi^* \boldsymbol{\alpha} \cdot (-i\nabla - e\mathbf{A}_0) \Psi - im\Psi^* \beta \Psi \} d^3x + \frac{1}{2} \int (E^2 + B^2) d^3x, \quad (4.2.2)$$

$$H_1 = -e \int (\Psi^* \boldsymbol{\alpha} \Psi) \cdot \mathbf{A} d^3x, \quad (4.2.3)$$

$$H_{\text{static}} = \frac{e^2}{8\pi} \int \int \frac{\rho(\mathbf{x})\rho(\mathbf{x}')}{|\mathbf{x} - \mathbf{x}'|} d^3x d^3x', \quad (4.2.4)$$

where $\boldsymbol{\alpha}$ is the Dirac matrices, \mathbf{E} and \mathbf{B} are the electric and magnetic field (we will suppose $\mathbf{B} = B\hat{z}$), \mathbf{A}_0 is the vector potential of the external field (we will suppose $\mathbf{A}_0 = Bx\hat{y}$), \mathbf{A} is the dynamical radiation field and $\rho(x)$ is the charge density. Eqs. (4.2.3) and (4.2.4) corresponds to Eqs. (3.2.6) and (3.2.5) respectively. Now using $\Psi = \sum_n a_n \psi_n$, Eqs. (4.2.2)-

(4.2.4) can be written in quantized forms as [5]

$$H_0 = \sum_n a_n^* a_n E_n + \sum_s k_s c_s^* c_s, \quad (4.2.5)$$

$$H_1 = -\sum_{n,s} e A_s c_s^* a_n^* a_{n'} V_{nn'}^{(s)} + \text{hc}, \quad (4.2.6)$$

$$H_{\text{static}} = \frac{e^2}{8\pi} \sum_{n,n',l,l'} a_n^* a_{n'} a_l^* a_{l'} \times \int \int \frac{(\psi_n^*(\mathbf{x}) \psi_{n'}(\mathbf{x})) (\psi_l^*(\mathbf{x}') \psi_{l'}(\mathbf{x}'))}{|\mathbf{x} - \mathbf{x}'|} d^3x d^3x', \quad (4.2.7)$$

where hc denotes Hermitian conjugate and E_n , ψ_n are the eigenvalues and eigenfunction of the Dirac equation

$$\{\boldsymbol{\alpha} \cdot (-i\nabla - e\mathbf{A}_0) + \beta m\} \psi_n = E_n \psi_n. \quad (4.2.8)$$

a_n^* , a_n are creation and annihilation operators for electron in a state n and c_s^* , c_s are creation and annihilation operator for a photon with momentum \mathbf{k}_s and with a unit polarization vector $\hat{\mathbf{e}}$. The charge density is

$$\rho(\mathbf{x}) = \Psi^*(\mathbf{x}) \Psi(\mathbf{x}), \quad (4.2.9)$$

and the quantized form of the vector potential of the radiation field is

$$\mathbf{A} = \sum_s A_s (c_s e^{i\mathbf{k}_s \cdot \mathbf{x}} + c_s^* e^{-i\mathbf{k}_s \cdot \mathbf{x}}) \hat{\mathbf{e}}_s, \quad (4.2.10)$$

where $A_s = \left(\frac{1}{2k_s G}\right)^{1/2}$ with G being the normalization volume. With $\alpha_s \equiv \boldsymbol{\alpha} \cdot \hat{\mathbf{e}}$, $V_{nn'}^{(s)}$ is then

$$V_{nn'}^{(s)} = \int d^3x (\psi_n^* \alpha_s \psi_{n'}) e^{-i\mathbf{k}_s \cdot \mathbf{x}}, \quad (4.2.11)$$

Now with all the definitions lined up, we are in position to calculate ΔE_{static} and $\Delta E_{\text{dynamic}}$.

4.3 Calculation of ΔE_{static} and $\Delta E_{\text{dynamic}}$

To calculate ΔE_{static} , we consider the electron in state m where $E_m = m_e$. Here we will use the notation m_e for electron mass to differentiate from the state m . We now take the average

value of H_{static} for one particle in the state m with no photons present

$$\begin{aligned}
\langle H_{\text{static}}(m) \rangle &= \frac{e^2}{8\pi} \sum_{l, E_l > 0} \iint \frac{(\psi_m^*(\mathbf{x})\psi_l(\mathbf{x})) (\psi_l^*(\mathbf{x}')\psi_m(\mathbf{x}'))}{|\mathbf{x} - \mathbf{x}'|} d^3x d^3x' \\
&+ \frac{e^2}{8\pi} \sum_{n \neq m, E_n > 0, E_l < 0} \iint \frac{(\psi_n^*(\mathbf{x})\psi_l(\mathbf{x})) (\psi_l^*(\mathbf{x}')\psi_n(\mathbf{x}'))}{|\mathbf{x} - \mathbf{x}'|} d^3x d^3x' \\
&+ \frac{e^2}{4\pi} \sum_{l, E_l < 0} \iint \frac{(\psi_m^*(\mathbf{x})\psi_m(\mathbf{x})) (\psi_l^*(\mathbf{x}')\psi_l(\mathbf{x}'))}{|\mathbf{x} - \mathbf{x}'|} d^3x d^3x', \tag{4.3.1}
\end{aligned}$$

where the vacuum charge density is

$$\rho_0 = \sum_{l, E_l < 0} \psi_l^*(\mathbf{x}')\psi_l(\mathbf{x}'), \tag{4.3.2}$$

and the charge density of the particle in state m is

$$\rho_m = \psi_m^*(\mathbf{x})\psi_m(\mathbf{x}). \tag{4.3.3}$$

The third term represents interaction between the particle charge density and vacuum charge density and as homogenous magnetic field does not give rise to any polarization, it will be same whether there is any magnetic field or not and so it can be dropped. We now have to subtract the term when only vacuum is present as was done in chapter 3

$$\Delta E_{\text{static}} = \langle H_{\text{static}}(m) \rangle - \langle H_{\text{static}}(\text{vac}) \rangle, \tag{4.3.4}$$

where

$$\langle H_{\text{static}}(\text{vac}) \rangle = \frac{e^2}{8\pi} \sum_{n, l, E_n > 0, E_l < 0} \iint \frac{(\psi_n^*(\mathbf{x})\psi_l(\mathbf{x})) (\psi_l^*(\mathbf{x}')\psi_n(\mathbf{x}'))}{|\mathbf{x} - \mathbf{x}'|} d^3x d^3x' \tag{4.3.5}$$

Then ΔE_{static} will contain two terms representing positive and negative energy contribution in the context of hole theory. Writing in a compact way

$$\Delta E_{\text{static}} = \frac{e^2}{8\pi} \sum_l \delta_l \iint \frac{(\psi_m^*(\mathbf{x})\psi_l(\mathbf{x})) (\psi_l^*(\mathbf{x}')\psi_m(\mathbf{x}'))}{|\mathbf{x} - \mathbf{x}'|}, \tag{4.3.6}$$

with $\delta_l = +1$ for $E_l > 0$ and $\delta_l = -1$ for $E_l < 0$. Recalling the Dirac wave functions in a magnetic field from Appendix D, Eqs. (D.0.15) and (D.0.16), where for the state m the orbital and spin magnetic moment exactly cancel each other and $n = p_2 = p_3 = 0$ and

$$E_m = m_e,$$

$$\psi_m(x) = \frac{1}{G^{1/3}} \begin{pmatrix} 0 \\ I_0(x) \\ 0 \\ 0 \end{pmatrix}, \quad (4.3.7)$$

with $I_0(x) = e^{-eBx^2/2} \left(\frac{eB}{\pi}\right)^{1/4}$ from Eq. (D.0.11). For $n = l$ and $E_n \rightarrow m_e$, using the Dirac wave functions $\psi_l(x)$ described in Eqs. (D.0.15) and (D.0.16), Eq. (4.3.6) transforms as [5]

$$\Delta E_{\text{static}} = \frac{m_e e^2}{8\pi G^{4/3}} \sum_{p_2, p_3} \sum_n \frac{1}{E_n} \int \int \frac{\rho_n(\mathbf{x}) \rho_n^*(\mathbf{x}')}{|\mathbf{x} - \mathbf{x}'|}, \quad (4.3.8)$$

where $\rho_n(x) \equiv I_0(x) I_n(x) \exp i(p_2 y + p_3 z)$, $E_n = (m_e^2 + p_2^2 + p_3^2 + 2emB)^{1/2}$, and $I_n(x)$ is defined in Eq. (D.0.11). In the Fourier space

$$\rho_n(k) \equiv \int \rho_n(x) \exp[-i\mathbf{k} \cdot \mathbf{x}] d^3x. \quad (4.3.9)$$

Eq. (4.3.8) becomes

$$\Delta E_{\text{static}} = \frac{e^2 m_e}{2G^{7/3}} \sum_{p_2, p_3} \sum_n \frac{1}{E_n} \sum_k \frac{\rho_n(\mathbf{k}) \rho_n^*(\mathbf{k})}{k^2}, \quad (4.3.10)$$

because of [5]

$$\iint \frac{\rho_n(\mathbf{x}) \rho_n^*(\mathbf{x}')}{|\mathbf{x} - \mathbf{x}'|} = \frac{4\pi}{G} \sum_k \frac{\rho_n(\mathbf{k}) \rho_n^*(\mathbf{k})}{k^2}. \quad (4.3.11)$$

The result of Eq. (4.3.9) is [5]

$$\rho_n(\mathbf{k}) = G^{2/3} \delta_{k_2 p_2} \delta_{k_3 p_3} \frac{(-1)^n}{2^{n/2} (n!)^{1/2}} \left(\frac{p_2 + ik_1}{\sqrt{eB}} \right)^n \exp \left[-\frac{p_2^2 + k_1^2 + 2ip_2 k_1}{4eB} \right]. \quad (4.3.12)$$

Using the delta function in Eq. (4.3.12), k^2 can be written as $k^2 = k_1^2 + p_2^2 + p_3^2$. Then Eq. (4.3.10) becomes

$$\Delta E_{\text{static}} = \frac{e^2 m_e}{2G} \sum_{p_2, p_3} \sum_{n=0}^{\infty} \frac{1}{E_n} \sum_{k_1} \frac{1}{(k_1^2 + p_2^2 + p_3^2)} \frac{\left(\frac{p_2^2 + k_1^2}{eB}\right)^n}{2^n n!} \exp \left[\frac{-(p_2^2 + k_1^2)}{2eB} \right]. \quad (4.3.13)$$

Replacing the sums by integrals $\sum_{k_1} \frac{G^{1/3}}{2\pi} \rightarrow \int dk_1$ and similarly for p_2 and p_3 , Eq. (4.3.13) becomes

$$\Delta E_{\text{static}} = \frac{e^2 m_e}{16\pi^3} \sum_{n=0}^{\infty} \frac{1}{n!} \frac{1}{E_n} \int_{-\infty}^{\infty} \int_{-\infty}^{\infty} \int_{-\infty}^{\infty} dk_1 dp_2 dp_3 \frac{1}{k_1^2 + p_2^2 + p_3^2} \left(\frac{p_2^2 + k_1^2}{2eB} \right)^n \exp \left[\frac{-(p_2^2 + k_1^2)}{2eB} \right]. \quad (4.3.14)$$

Substituting the value of E_n from Eq. (D.0.13) and using polar coordinates ($r^2 = k_1^2 + p_2^2$ and $p_3 = p$; $k^2 = p^2 + r^2$), we can write Eq. (4.3.14) as

$$\Delta E_{\text{static}} = \frac{e^2 m_e}{8\pi^2} \int_{-\infty}^{\infty} dp \int_{-\infty}^{\infty} r dr \frac{1}{r^2 + p^2} f, \quad (4.3.15)$$

where

$$f \equiv \sum_{n=0}^{\infty} \frac{\eta^n}{n! \sqrt{(m_e^2 + p^2 + 2neB)}} e^{-\eta}, \quad \eta \equiv \frac{r^2}{2eB}. \quad (4.3.16)$$

Defining $g(n) \equiv \sqrt{(m_e^2 + p^2 + 2neB)}$ and Taylor expanding both f and $g(n)$, we get

$$f = g(\eta) + \left[\frac{ng''(n)}{2} \right] + \dots, \quad (4.3.17)$$

$$= \frac{1}{(m_e^2 + p^2 + r^2)^{1/2}} + \frac{3}{4} \left[\frac{eBr^2}{(m_e^2 + p^2 + r^2)^{5/2}} \right] + \dots \quad (4.3.18)$$

Then finally Eq. (4.3.15) becomes

$$\begin{aligned} \Delta E_{\text{static}} &= \frac{e^2 m_e}{8\pi^2} \int_{-\infty}^{\infty} dp \int_0^{\infty} r dr \frac{1}{(r^2 + p^2)(m_e^2 + p^2 + r^2)^{1/2}} \left[1 + \frac{3}{4} \frac{eBr^2}{(m_e^2 + p^2 + r^2)^2} + \dots \right], \\ &= \Delta E_{\text{static}}(0) + \frac{3e^2 m_e}{32\pi^2} \left(\int_{-\infty}^{\infty} dp \int_0^{\infty} r dr \frac{r^2}{m_e(r^2 + p^2)(m_e^2 + p^2 + r^2)^{5/2}} \right) eB + \dots, \\ &= \Delta E_{\text{static}}(0) + \frac{e^2}{12\pi^2} \left(\frac{e}{2m_e} \right) B + \dots \end{aligned} \quad (4.3.19)$$

From this equation we can see that $\Delta E_{\text{static}}(0)$ contains the self-energy or divergent terms which we do not care about and the next order terms are linear in order of magnetic field B . To calculate $\Delta E_{\text{dynamic}}$ we have to use second order perturbation theory on Eq. (4.2.6) and using Eq. (4.2.10) we get [5]

$$\Delta E_{\text{dynamic}} = -\frac{e^2}{2G} \sum_s \frac{1}{k_s} \sum_l \frac{|V_{ln}^{(s)}|^2}{\delta_l k_s + E_l - E_m}, \quad (4.3.20)$$

where $\delta_l = +1$ for $E_l > 0$ and $\delta_l = -1$ for $E_l < 0$. Treatment of $\Delta E_{\text{dynamic}}$ is quite similar to the calculation of ΔE_{static} . For the state $E_m = m_e$ and $E_m = -m_e$ [5]

$$\Delta E_{\text{dynamic}} = F(m_e) - F(-m_e), \quad (4.3.21)$$

where

$$F(m_e) \equiv \sum_{n=0}^{\infty} \frac{e^2}{16\pi^2} \int_{-\infty}^{\infty} dp \int_0^{\infty} \frac{\eta^n e^{-\eta}}{n!} \left\{ \frac{1 + \frac{p^2}{k^2}}{E_{n+1}(k + E_{n+1} - m_e)} + \frac{1 - \frac{p^2}{k^2}}{E_n(k + E_n - m_e)} \right\} r dr. \quad (4.3.22)$$

Most of the terms in this equation resembles the terms of Eqs. (4.3.15) and (4.3.16). The two terms here corresponds to $\delta_l = +1$ and $\delta_l = -1$. $\frac{1}{E_{n+1}}$ and $\frac{1}{E_n}$ terms comes from the two fold degenerate solutions of the Dirac equation and is similar to $\frac{1}{E_n}$ term in Eqs. (4.3.15) and (4.3.16). The terms $(k + E_{n+1} - m_e)$ and $(k + E_n - m_e)$ comes from the summation over l after putting the values of $\delta_l = +1, -1$ in Eq. (4.3.20). Now to evaluate $F(m_e)$ by following the same procedure in evaluation of ΔE_{static} , we arrive at [5]

$$\Delta E_{\text{dynamic}} = \Delta E_{\text{dynamic}}(0) - \frac{5e^2}{24\pi^2} \left(\frac{e}{2m_e} \right) B + \dots \quad (4.3.23)$$

From Eq. (4.1.2) and taking only terms that are linearly dependent on B , we get

$$\Delta E = \Delta E_{\text{static}}(0) + \Delta E_{\text{dynamic}}(0) - \frac{e^2}{8\pi^2} \left(\frac{e}{2m_e} \right) B. \quad (4.3.24)$$

Now discarding the divergent terms $\Delta E_{\text{static}}(0)$ and $\Delta E_{\text{dynamic}}(0)$ we get the true change in energy of an electron in homogenous external magnetic field. So the modification to the energy in the state m can be written as

$$E = -\frac{e}{2m_e} B \delta, \quad (4.3.25)$$

where $\delta = \frac{e^2}{8\pi^2}$. Now considering the modification to the g factor to be $g = 2(1 + \delta)$, we get

$$g = 2 \left(1 + \frac{e^2}{8\pi^2} \right). \quad (4.3.26)$$

Now using $\alpha = \frac{e^2}{4\pi}$, we get

$$a_e = \frac{g - 2}{2} = \frac{\alpha}{2\pi}, \quad (4.3.27)$$

which is the exact result obtained by Schwinger in [15].

4.4 Conclusion

In this chapter, we have discussed Luttinger's approach of calculating the anomalous magnetic moment of the electron. Luttinger's approach to calculate the anomalous magnetic moment of the electron differs from Schwinger's in terms of renormalization. Luttinger's approach is independent of any renormalization scheme or any cut-offs. In that sense, this approach is more natural. This approach is quite similar to that discussed in Chapter 3. Like in Chapter 3, here we also talk about the interaction of the Coulomb field and transverse field which corresponds to ΔE_{static} and $\Delta E_{\text{dynamic}}$ respectively. We also saw that Luttinger's approach does not depend on a choice of a cut-off like the relativistic effective Hamiltonian approach. Although these two approaches are more intuitive and natural but the calculation process is quite lengthy and not so practical in modern day quantum field theoretical calculations where the renormalization scheme proves quite useful. But from these approaches, we get a better and more intuitive understanding of the radiative corrections. This concludes our discussion of the anomalous magnetic moment of the electron. In the next chapter, we will discuss the Lamb shift and illustrate how fluctuating vacuum affects the motion of a bound electron.

Chapter 5

Calculation of the Lamb Shift

5.1 Introduction

Lamb shift is perhaps the most significant discovery presented at the Shelter Island conference in 1947 which implies the shortcoming of the Dirac theory. The Lamb-Retherford experiment in 1947 found a slight difference in energy, equivalent to the frequency of about 1000 MHz, between the levels $2s_{1/2}$ and $2p_{1/2}$ of the hydrogen atom. This energy shift is known as the Lamb shift [24]. In this chapter, we will present two approaches to the Lamb shift. Hans Bethe first theoretically explained the Lamb shift [16]. We thus first look at Bethe's calculation where he considered a bound electron's interaction with radiation field and then subtracted the free electron's interaction. The result contains a logarithmically enhanced term and this logarithmic effect is the primary feature of the Lamb shift. After Bethe, Theodore A. Welton provided a heuristic approach to the Lamb shift [9]. This approach provides an intuitive description of the Lamb shift. In this approach, one averages the Coulomb potential of the nucleus and the electron's vibrational motion in a vacuum.

5.2 Bethe's calculation of the Lamb Shift

In this section, we will briefly discuss Bethe's approach to the Lamb shift. Bethe's approach is non-relativistic where he considered self-interaction of the bound electron due to its interaction with transverse electromagnetic wave. We will first calculate the self-energy of a free electron and then generalize it to a bound electron. Then the difference between the self-energy of the free and bound electron will result in a logarithmic divergent quantity which is the Lamb shift. The self-energy graph is represented by the diagram

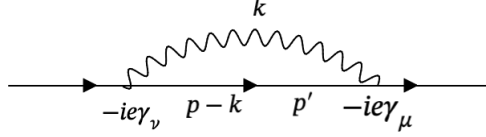


Figure 5.2.1: Self-energy Feynman diagram for free particle. The solid line represents fermions and the wavy line represents transverse photon.

The QED Feynman rules give the following expression for the above self-energy graph ,

$$\int d^4k \frac{\bar{u}(p) (-ie\gamma^\mu) i (-ig_{\mu\nu}) (-ie\gamma^\nu) u(p)}{(\not{p} - \not{k} - m + i\varepsilon) (k^2 + i\varepsilon)}, \quad (5.2.1)$$

which, in the non-relativistic limit after carrying out the integration over k_0 , gives to the first order

$$\begin{aligned} 4\pi e^2 \int \frac{d^3k}{(2\pi)^3} \frac{\bar{u}(p)\gamma^\mu u(p-k)g_{\mu\nu}\bar{u}(p-k)\gamma^\nu u(p)}{(E_p - E_{p-k} - |\mathbf{k}|)(2k^2)} \\ = 4\pi e^2 \int \frac{d^3k}{(2\pi)^3} \frac{\bar{u}_m\gamma^\mu u_n g_{\mu\nu}\bar{u}_n\gamma^\nu u_m}{(E_n - E_m - |\mathbf{k}|)(2k^2)}. \end{aligned} \quad (5.2.2)$$

Now considering $E_m, E_n \ll k$ for a free electron and using the projection $g_{\mu\nu} \rightarrow \epsilon_\mu\epsilon_\nu$ on the transversal photons with polarization ϵ and the velocity projection operator \mathbf{v} in the expression $u_m\gamma^\mu\epsilon(k)u_n \rightarrow \langle m|\hat{v}|n\rangle\epsilon(k)$, we can write the self-energy of the free electron as

$$E_0 = -4\pi e^2 \int \frac{d^3k}{(2\pi)^3} \frac{\sum_\lambda |\langle m|\mathbf{v}|n\rangle\epsilon(k)|^2}{2k^2} \quad (5.2.3)$$

$$= -4\pi e^2 \int \frac{d^3k}{(2\pi)^3} \frac{\mathbf{v}^2}{2k^2} |\epsilon(k)|^2, \quad (5.2.4)$$

where in the second line we have considered that the velocity projection operator has only diagonal elements for the free particle [16]. After performing the angular integration and using the Eq. (2.3.12) for the completeness relation for the photon, we get

$$E_0 = -\frac{2e^2}{3\pi} \int kdk \frac{\mathbf{v}^2}{k}. \quad (5.2.5)$$

For a bound electron, we can not assume $E_m - E_n \ll k$. Eq. (5.2.5) can be generalized for the bound case,

$$E_b = -\frac{2e^2}{3\pi} \int kdk \sum_n \frac{|\mathbf{v}_{mn}|^2}{E_n - E_m + k}, \quad (5.2.6)$$

where we have used the sum rule [16]

$$\mathbf{v}_{mm}^2 = \sum_n |\mathbf{v}_{mn}|^2. \quad (5.2.7)$$

Due to the self-interaction of the electron, electron's bare mass is increased with the addition of the electromagnetic mass. But the experimentally observed result contains the total mass, so to get the true energy shift we have to subtract the self-energy of the bound and free electron

$$\begin{aligned} E &= E_b - E_0 \\ &= \frac{2e^2}{3\pi} \int dk \sum_n \frac{|\mathbf{v}_{mn}|^2 (E_n - E_m)}{E_n - E_m + k} \end{aligned} \quad (5.2.8)$$

It is to be noted that both E_b and E_0 are both linearly divergent whereas E is logarithmically divergent. Now by introducing a cut-off K , the integration yields

$$E = \frac{2e^2}{3\pi} \sum_n |\mathbf{v}_{mn}|^2 (E_n - E_m) \ln \frac{K}{E_n - E_m}. \quad (5.2.9)$$

We now consider that the logarithmic divergence is approximately independent of n and then we only have to evaluate

$$\begin{aligned} \sum_n |\mathbf{v}_{mn}|^2 (E_n - E_m) &= \sum_n \left\{ \langle m | -i\nabla H | n \rangle \langle n | -i\nabla | m \rangle \right. \\ &\quad - \frac{1}{2} \langle m | -i\nabla | n \rangle \langle n | -i\nabla H | m \rangle \\ &\quad \left. - \frac{1}{2} \langle m | -iH\nabla | n \rangle \langle n | -i\nabla | m \rangle \right\}, \end{aligned} \quad (5.2.10)$$

which is equal to

$$\sum_n |\mathbf{v}_{mn}|^2 (E_n - E_m) = \langle m | \left[\nabla H \nabla - \frac{1}{2} \nabla^2 H - \frac{1}{2} H \nabla^2 \right] | m \rangle = \langle m | \frac{1}{2} [\nabla, [H, \nabla]] | m \rangle \quad (5.2.11)$$

$$= -\langle m | \nabla^2 V | m \rangle \quad (5.2.12)$$

Then using the Coulomb potential we get

$$\sum_n |\mathbf{v}_{mn}|^2 (E_n - E_m) = 2\pi Z e^2 \int \psi_m^* \delta(\mathbf{r}) \psi_m d\mathbf{r} = 2\pi Z e^2 \psi_m^2(0) \quad (5.2.13)$$

All wave function for $l \neq 0$ vanishes at the nucleus and so Lamb shift is only observable for states with $l = 0$. Now considering the normalized hydrogen wavefunction

$$\psi_n^2(0) = \frac{1}{\pi} \left(\frac{Z}{na} \right)^3, \quad (5.2.14)$$

where Z is the proton number, n is the principle quantum number, and a is the Bohr radius, we get

$$E = \frac{8}{3\pi} e^6 \text{Ry} \frac{Z^4}{n^3} \ln \frac{K}{\langle E_n - E_m \rangle_{av}}, \quad (5.2.15)$$

where Ry is the Rydberg constant. Using $K = mc^2$ for the cut-off and numerical value for the average excitation energy for the $2s$ state 17.8 Ry, Bethe got a numerical value 1040 MHz for the Lamb energy shift [16]. It is in excellent agreement with the observed result of 1000 MHz.

5.3 Welton's heuristic approach to the Lamb shift

In this section, we review Welton's heuristic explanation of the Lamb Shift [9]. The central theme of Welton's calculation of the Lamb shift considers how vacuum fluctuations of the electromagnetic field affect the electron in a hydrogen atom. The fluctuation of quantum states in their lowest energy state give rise to fluctuating electric field which pushes the electron causing the electron to move randomly. This is known as the position fluctuation of the electron. In other words, in a bound system (hydrogen atom) the fluctuating vacuum causes fluctuations in the position of the electron which modifies the Coulomb potential energy between the electron and nucleus which results in the Lamb shift. Now we consider the motion of electron in a static potential $\phi_0(\mathbf{r})$. The variation of the coordinate of the electron due to its random motion due to vacuum fluctuation changes the potential which can be expanded as

$$\phi_0(\mathbf{r} + \delta\mathbf{r}) = \left(1 + \delta\mathbf{r} \cdot \nabla + \frac{1}{2} (\delta\mathbf{r} \cdot \nabla)^2 + \dots \right) \phi_0(\mathbf{r}). \quad (5.3.1)$$

Since vacuum fluctuations are isotropic, we can write

$$\langle \delta\mathbf{r} \rangle_{\text{vac}} = 0, \quad (5.3.2)$$

$$\langle (\delta\mathbf{r} \cdot \nabla)^2 \rangle_{\text{vac}} = \frac{1}{3} \langle (\delta\mathbf{r})^2 \rangle_{\text{vac}} \nabla^2. \quad (5.3.3)$$

The expansion of the potential becomes

$$\langle \phi_0(\mathbf{r} + \delta\mathbf{r}) \rangle = \left(1 + \frac{1}{6} \langle (\delta\mathbf{r})^2 \rangle_{\text{vac}} \nabla^2 + \dots \right) \langle \phi(\mathbf{r}) \rangle. \quad (5.3.4)$$

We see that the fluctuation in electron's position modifies the potential in which it moves. The equation of motion for the electron's displacement by the fluctuating electric field for a single mode k can be written as

$$m \frac{d^2}{dt^2} (\delta\mathbf{r})_k = -e \mathbf{E}_k, \quad (5.3.5)$$

where the radiation field is defined by Eq. (2.2.1) but without the summation over ϵ . We consider the electron to be slow and for a field oscillating at ω we use the Ansatz (c.c. denotes complex conjugation)

$$\delta\mathbf{r}(t) = \delta\mathbf{r}(0) e^{-i\omega t} + \text{c.c.} \quad (5.3.6)$$

Inserting into Eq. (5.3.5), we get

$$(\delta\mathbf{r})_k \simeq \frac{e}{mc^2 k^2} \mathcal{E}_k (a_k e^{-i\omega t + i\mathbf{k}\cdot\mathbf{r}} + \text{h.c.}), \quad (5.3.7)$$

where $\mathcal{E}_k = \sqrt{\frac{\hbar\omega}{2\varepsilon_0 L^3}}$ as described in Eq. (2.2.1). So the $\langle (\delta\mathbf{r})^2 \rangle_{\text{vac}}$ term in Eq. (5.3.3) becomes

$$\begin{aligned} \langle (\delta\mathbf{r})^2 \rangle_{\text{vac}} &= \sum_k \left(\frac{e}{mc^2 k^2} \right)^2 \langle 0 | \mathbf{E}_k^2 | 0 \rangle \\ &= \sum_k \left(\frac{e}{mc^2 k^2} \right)^2 \left(\frac{\hbar ck}{2\varepsilon_0 L^3} \right) \\ &= \frac{1}{2\varepsilon_0 \pi^2} \left(\frac{e^2}{\hbar c} \right) \left(\frac{\hbar}{mc} \right)^2 \int \frac{dk}{k}, \end{aligned} \quad (5.3.8)$$

where in the last line we have converted the sum into integral by using Eq. (A.0.7). This result is divergent so we have to select lower and upper cut-offs to make it convergent. The lower limit arises from the condition that the wave length of the virtual photon should not exceed the size of the atom, $k > \frac{\pi}{a_0}$, where $a_0 = \frac{4\pi\varepsilon_0 \hbar^2}{me^2}$ is the Bohr radius. For the long wavelengths larger than the size of atom, the electric field oscillates so slowly that by the time it changes sign the electron will be at another place due to position fluctuation and so their contribution is zero. The upper limit is $k < \frac{mc}{\hbar}$. When the wavelengths get shorter than the Compton wavelength, the super energetic photons effectively do not push the electron but can create electron-positron pairs. After inserting the lower limit $\frac{\pi}{a_0}$ and the upper limit

$\frac{mc}{\hbar}$ into Eq. (5.3.8), we get

$$\langle (\delta \mathbf{r})^2 \rangle_{\text{vac}} = \frac{1}{2\varepsilon_0\pi^2} \left(\frac{e^2}{\hbar c} \right) \left(\frac{mc}{\hbar} \right)^2 \ln \frac{4\varepsilon_0\hbar c}{e^2}. \quad (5.3.9)$$

For evaluating $\nabla^2\phi(\mathbf{r})$, we will use Coulomb potential energy

$$\begin{aligned} \left\langle \nabla^2 \left(\frac{-e^2}{4\pi\varepsilon_0 r} \right) \right\rangle &= \frac{-e^2}{4\pi\varepsilon_0} \int d^3\mathbf{r} \psi^*(\mathbf{r}) \nabla^2 \left(\frac{1}{r} \right) \psi(\mathbf{r}) \\ &= \frac{e^2}{\varepsilon_0} |\psi(0)|^2, \end{aligned} \quad (5.3.10)$$

where $\psi(r)$ is the normalized hydrogen wave function and $\nabla^2 \left(\frac{1}{r} \right) = -4\pi\delta^3(\mathbf{r})$. So the energy shift now becomes

$$\begin{aligned} \langle \Delta\phi_0 \rangle &= \frac{1}{6} \langle (\delta \mathbf{r})^2 \rangle_{\text{vac}} \left\langle \nabla^2 \left(\frac{-e^2}{4\pi\varepsilon_0 r} \right) \right\rangle \\ &= \frac{4}{3} \frac{e^2}{4\pi\varepsilon_0} \frac{e^2}{4\pi\varepsilon_0\hbar c} \left(\frac{\hbar}{mc} \right)^2 \ln \frac{4\varepsilon_0\hbar c}{e^2} |\psi(0)|^2. \end{aligned} \quad (5.3.11)$$

Now using $\psi_{2s}(0) = \frac{1}{\sqrt{8\pi a_0^3}}$, we get the energy shift as

$$\langle \Delta\phi_0 \rangle = \alpha^5 mc^2 \frac{1}{6\pi} \ln \frac{1}{\pi\alpha}, \quad (5.3.12)$$

where α is the fine structure constant and the shift is about 500 MHz which is within an order of magnitude of the observed result of 1000 MHz.

5.4 Conclusion

In this chapter, we have discussed the Lamb shift using two different approaches. Bethe's approach considers the electron's self-energy in calculating the Lamb shift whereas Welton's approach considers the vibration of the electron in a fluctuating vacuum which modifies the Coulomb potential. At first glance, these two approaches may seem contradictory as one works with the self-interaction of the electron and the other works with the position fluctuation of the electron in the vacuum. Obviously there is no such controversy and this misunderstanding might arise from the word "vacuum". It should be made clear that we are not talking about vacuum fluctuation or the creation of electron-positron pairs in the vacuum. We are saying how a fluctuating vacuum can influence the motion of the electron which gives rise to the Lamb shift. The fluctuating electric field modifies the motion of

the electron causing position fluctuation. The electron radiates a transverse photon and the interaction of the electron and the transverse photon gives rise to the Lamb shift. Although Bethe's calculation gives a more accurate result than Welton's, Welton's calculation provides a more intuitive and clear explanation of the physics behind the Lamb shift.

We point out two primary features of the Lamb shift. One is that Lamb shift is logarithmically enhanced and other is that it primarily affects the s states ($l = 0$) of an atom, because of the delta function in the calculation when we take the Laplacian of the potential energy. This delta function signifies that the effect arises in the vicinity of the nucleus and as the wave functions for $l \neq 0$ vanishes at the nucleus, s states have the largest Lamb shift. This particular point should be noted as it will serve as our primary reasoning in refuting the claim of [1] that the next-to-leading order correction of the D-term has the same physics as the Lamb shift. This concludes our discussion of the well-known examples for interpreting radiative corrections, electron $g - 2$, and the Lamb shift. In the following chapters, we will explore the relatively new concept, the so-called D-term.

Chapter 6

Feynman rules for NRQED

6.1 Introduction

In this chapter, we will derive Feynman rules for non-relativistic quantum electrodynamics (NRQED). The proper way to derive these rules is by going back to the derivation of QED Feynman rules and re-deriving them in the non-relativistic limit. We will follow a simple approach where we will write down the QED Feynman rules for any process and then expand them in powers of \mathbf{p}/m [6]. The usual normalization convention is $\bar{u}(p)\gamma_0 u(p) = u^\dagger(p)u(p) = 2E$ but in non-relativistic physics it is conventional to normalize the states in a way that there is one particle per unit volume [6]. Throughout this chapter, we will use such normalization that the wave functions will contain a factor of $\frac{1}{\sqrt{2E}}$. We will also work with the Coulomb gauge, convenient in NRQED [6]. We will consider natural units i.e. $\hbar = c = \varepsilon_0 = 1$ in this chapter.

6.2 NRQED vertices

In this section, we derive the NRQED Feynman rules for vertices. We consider the interaction of an electron with a photon. Then the Feynman rules read

$$\bar{u}(p)ie\gamma_\mu u(p) = \sqrt{\frac{E'+m}{2E'}} \sqrt{\frac{E+m}{2E}} \left(\psi'^\dagger \quad \frac{\boldsymbol{\sigma}\cdot\mathbf{p}'}{E'+m} \psi'^\dagger \right) \gamma_0 ie \gamma_\mu \left(\begin{array}{c} \psi \\ \frac{\boldsymbol{\sigma}\cdot\mathbf{p}}{E'+m} \psi \end{array} \right). \quad (6.2.1)$$

We will consider the zeroth component and the three-momentum component of the vertex separately as the first couples to the Coulomb field and the later couples to the transverse

photon as demonstrated in Eq. (7.3.12). Then Eq. (6.2.1) becomes

$$\sqrt{\frac{E'+m}{2E'}}\sqrt{\frac{E+m}{2E}}ie\left(\psi'^{\dagger}\psi + \psi'^{\dagger}\frac{\boldsymbol{\sigma}\cdot\mathbf{p}'}{E'+m}\frac{\boldsymbol{\sigma}\cdot\mathbf{p}}{E+m}\psi\right). \quad (6.2.2)$$

We then obtained our first NRQED rule

$$ie, \quad (6.2.3)$$

which represents Coulomb interaction and can be represented graphically as

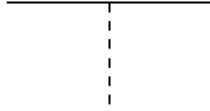


Figure 6.2.1: Graphical representation of Coulomb interaction where the solid line represents fermions and the dashed line represents Coulomb photon.

Now from the term

$$\sqrt{\frac{E'+m}{2E'}}\sqrt{\frac{E+m}{2E}}ie\psi'^{\dagger}\psi, \quad (6.2.4)$$

we get

$$\psi'^{\dagger}\psi \times ie\left(-\frac{\mathbf{p}^2}{8m^2} - \frac{\mathbf{p}'^2}{8m^2}\right) \quad (6.2.5)$$

where we have used

$$\sqrt{\frac{E+m}{2E}} \approx \left(1 - \frac{\mathbf{p}^2}{8m^2}\right). \quad (6.2.6)$$

Now in the same order the $\boldsymbol{\sigma}\cdot\mathbf{p}$ terms give

$$ie\psi'^{\dagger}\frac{\boldsymbol{\sigma}\cdot\mathbf{p}}{2m}\frac{\boldsymbol{\sigma}\cdot\mathbf{p}'}{2m}\psi = \left[e\psi'^{\dagger}\boldsymbol{\sigma}\cdot\frac{\mathbf{p}\times\mathbf{p}'}{4m^2}\psi + ie\psi'\frac{\mathbf{p}\cdot\mathbf{p}'}{4m^2}\psi\right] \quad (6.2.7)$$

where we have used Eq. (B.0.15). Now combining with Eq. (6.2.5) we obtain two more NRQED rules

$$-ie\frac{(\mathbf{p}-\mathbf{p}')^2}{8m^2} \quad e\boldsymbol{\sigma}\cdot\frac{(\mathbf{p}\times\mathbf{p}')}{4m^2}, \quad (6.2.8)$$

where the first one represents the Darwin interaction and the second one is spin-orbit interaction. The graphical representation is



Figure 6.2.2: Graphical representation of the Darwin and spin-orbit interactions. The first diagram represents Darwin interaction and the second diagram represents spin-orbit interactions. The solid line represents fermions and the wavy line represents transverse photon.

Now we will work with the γ_i parts. Then Eq. (6.2.1) becomes

$$\sqrt{\frac{E'+m}{2E'}} \sqrt{\frac{E+m}{2E}} ie \left(\psi'^{\dagger} \frac{\boldsymbol{\sigma} \cdot \mathbf{p}'}{E'+m} \sigma_j \psi + \psi'^{\dagger} \sigma_j \frac{\boldsymbol{\sigma} \cdot \mathbf{p}}{E+m} \psi \right). \quad (6.2.9)$$

Now using [6]

$$\boldsymbol{\sigma} \boldsymbol{\sigma} \cdot \mathbf{p} = i(\mathbf{p} \times \boldsymbol{\sigma}) + \mathbf{p}, \quad (6.2.10)$$

$$\boldsymbol{\sigma} \cdot \mathbf{p}' \boldsymbol{\sigma} = -i(\mathbf{p}' \times \boldsymbol{\sigma}) + \mathbf{p}', \quad (6.2.11)$$

we get

$$ie \psi'^{\dagger} \left[\frac{-i(\mathbf{p}' \times \boldsymbol{\sigma}) + \mathbf{p}}{2m} + \frac{i(\mathbf{p} \times \boldsymbol{\sigma}) + \mathbf{p}}{2m} \right] \psi, \quad (6.2.12)$$

which gives the following NRQED rules

$$ie \frac{\mathbf{p} + \mathbf{p}'}{2m} \quad e \frac{(\mathbf{p}' - \mathbf{p}) \times \boldsymbol{\sigma}}{2m}, \quad (6.2.13)$$

which represent dipole and magnetic interaction respectively. The graphical representation is



Figure 6.2.3: Graphical representation of the dipole and magnetic interactions. The first diagram represents dipole interaction and the second diagram represents magnetic interaction. The solid line represents fermions and the wavy line represents transverse photon.

For positron using

$$\bar{v}(p) ie \gamma_{\mu} v(-p) = \sqrt{\frac{E'+m}{2E'}} \sqrt{\frac{E+m}{2E}} \left(\chi'^{\dagger} \frac{\boldsymbol{\sigma} \cdot \mathbf{p}'}{E'+m} \chi'^{\dagger} \right) \gamma_0 ie \gamma_{\mu} \begin{pmatrix} \frac{\boldsymbol{\sigma} \cdot \mathbf{p}}{E+m} \chi \\ \chi \end{pmatrix}, \quad (6.2.14)$$

leads to the same NRQED rules except now \mathbf{p}' is the three momentum before the interaction.

6.3 Virtual Fermions

In this section, we derive the NRQED Feynman rules for internal lines or virtual fermions. The representative diagrams are



Figure 6.3.1: Representative diagrams for fermion (positron) as an internal line. The second diagram is the crossed diagram. The solid line represents fermions and the wavy line represents transverse photon.

In QED the propagator for the fermion is

$$\frac{i}{\not{p} - m + i\varepsilon} = i \frac{\not{p} + m}{p^2 - m^2 + i\varepsilon} \quad (6.3.1)$$

$$\approx \frac{i}{2p_0} \left(\frac{\not{p} + m}{p_0 - \sqrt{\mathbf{p}^2 + m^2} + i\varepsilon} + \frac{\not{p} + m}{p_0 + \sqrt{\mathbf{p}^2 + m^2} - i\varepsilon} \right). \quad (6.3.2)$$

In this expression p_0 is positive in the first term and negative in the second term. Now using Casimir trick, we get the fermion propagator containing both the propagation of particle (forward in time) and the anti-particle (backward in time) as

$$\frac{i}{2p_0} \left(\frac{\sum_{s=1,2} u_r^{(s)}(p) \bar{u}_r^{(s)}(p)}{p_0 - \sqrt{\mathbf{p}^2 + m^2} + i\varepsilon} - \frac{\sum_{s=1,2} v_r^{(s)}(-p) \bar{v}_r^{(s)}(-p)}{p_0 + \sqrt{\mathbf{p}^2 + m^2} - i\varepsilon} \right), \quad (6.3.3)$$

where we have used the index r to signify that we are working in relativistic domain like [6]. In non-relativistic normalization for the wave-functions, we will absorb the factor $\frac{1}{2p_0}$ due to the factor $\frac{1}{\sqrt{2E}}$ in our non-relativistic normalization but then we have to change the sign of the positron term [6]. We will also not include the terms concerning sum over spins as electron and positron are in the internal line. Now we consider the interaction of an electron with a photon of momentum k where the fermion line is an internal propagator. The electron

propagator is then

$$\frac{i}{p_0 + k_0 - \sqrt{(\mathbf{p} + \mathbf{k})^2 + m^2} + i\varepsilon} \approx \frac{i}{k_0 + \frac{\mathbf{p}^2}{2m} - \frac{(\mathbf{p} + \mathbf{k})^2}{2m} + i\varepsilon}, \quad (6.3.4)$$

and the positron propagator is

$$\frac{i}{p_0 + k_0 + \sqrt{(\mathbf{k} + \mathbf{p})^2 + m^2} - i\varepsilon} \approx \frac{i}{k_0 - \frac{\mathbf{p}^2}{2m} + \frac{(\mathbf{k} + \mathbf{p})^2}{2m} - i\varepsilon}. \quad (6.3.5)$$

Until now we have only considered photon rules for coupling of a particle with a particle or an anti-particle with an anti-particle. Now we will discuss coupling of particle and anti-particle. We will consider the interaction which connects a virtual positron to external electrons. To simplify calculation, we can set the momenta of the initial and final electron to be zero in the lowest order. We then have

$$\bar{u}ie\gamma_i v^{(s)} \approx \begin{pmatrix} \psi^\dagger & 0 \end{pmatrix} \gamma_0 ie\gamma_i \begin{pmatrix} \frac{\boldsymbol{\sigma} \cdot \mathbf{k}}{2m} \chi^{(s)} \\ \chi^{(s)} \end{pmatrix}, \quad (6.3.6)$$

where \mathbf{k} is the photon three-momentum. Which gives

$$ie\psi^\dagger \sigma_i \frac{\boldsymbol{\sigma} \cdot \mathbf{k}}{2m} \chi^{(s)}. \quad (6.3.7)$$

Similarly $\bar{v}^{(s)}ie\gamma_j u$ gives

$$ie\chi^{\dagger(s)} \frac{\boldsymbol{\sigma} \cdot \mathbf{k}}{2m} \sigma_j \psi. \quad (6.3.8)$$

So

$$\sum_s \bar{u}ie\gamma_i v^{(s)} \bar{v}^{(s)}ie\gamma_j u = -\frac{e^2}{4m^2} \mathbf{k}^2 \psi^\dagger \sigma_i \sigma_j \psi. \quad (6.3.9)$$

After adding the cross diagram ($i \leftrightarrow j$) and including the internal propagator for positron $\frac{i}{k_0 - \frac{\mathbf{k}^2}{2m}}$, we obtain

$$-\frac{ie^2}{2m^2} \frac{\mathbf{k}^2}{k_0 - \frac{\mathbf{k}^2}{2m}} \delta_{ij}. \quad (6.3.10)$$

The most important contribution comes from taking the fermion propagator pole instead of photon and so by taking $k_0 = -\frac{\mathbf{k}^2}{2m}$, we get [6]

$$\frac{ie^2}{2m} \delta_{ij}. \quad (6.3.11)$$

This NRQED rule represents seagull interaction and the corresponding diagram is



Figure 6.3.2: Seagull interaction where the solid line represents fermions and wavy line represents transverse photon.

6.4 Annihilation diagram

We have been considering NRQED rules for scattering up to now. Here in this section, we will work with annihilation diagrams. One example of this is positronium hyperfine splitting due to one photon annihilation channel [6]. The QED rule for this kind of process is [6]

$$\bar{v}(-p_1)ie\gamma_\mu u(p_2)\frac{-i}{q^2}\bar{u}(p_3)ie\gamma^\mu v(-p_4), \quad (6.4.1)$$

where the transferred momentum is $q = p_2 - p_1 = p_3 - p_4$. Considering $q = (m, \mathbf{0}) - (-m, \mathbf{0}) = (2m, \mathbf{0})$, we get

$$\bar{v}(0)ie\gamma_\mu u(0)\frac{-i}{4m^2}\bar{u}(0)ie\gamma^\mu v(0) = -\frac{ie^2}{4m^2}\chi^\dagger\boldsymbol{\sigma}\psi\cdot\psi^\dagger\boldsymbol{\sigma}\chi, \quad (6.4.2)$$

where we have taken $u(0) = \begin{pmatrix} \psi \\ 0 \end{pmatrix}$ and $v(0) = \begin{pmatrix} 0 \\ \chi \end{pmatrix}$. The spin average gives $\frac{-ie^2}{2m}$ in the ortho state where the spins are in the same direction and 0 for the para state where they are in different directions of positronium. The NRQED interaction can be represented by the following diagram

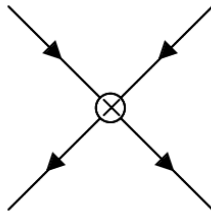


Figure 6.4.1: Annihilation contact interaction diagram where the solid line represents incoming and outgoing fermions.

6.5 Photon propagator

As photon travels at the speed of light, it is not possible to get a non-relativistic Feynman rule for photon. In QED, the photon propagator is $-\frac{ig_{\mu\nu}}{q^2+i\epsilon}$ in the Feynman gauge. But in NRQED calculations we use Coulomb gauge. So in this section, we will derive the photon propagator in the Coulomb gauge. We start from the definition of the four current operator of the Maxwell field

$$J^\nu(x) = \partial^2 A^\nu(x) - \partial^\nu (\partial_\mu A^\mu(x)). \quad (6.5.1)$$

A^μ can be written in terms of Green's function as

$$A^\mu(x) = \int d^4y (-i) G^{\mu\nu}(x-y) J_\nu(y). \quad (6.5.2)$$

First we start with the scalar potential $A^0(\mathbf{x}, t)$. In the Coulomb gauge i.e. $\nabla \cdot \mathbf{A} = 0$, we have

$$\begin{aligned} J^0 &= \partial^2 A^0 - \partial^0 (\partial_\mu A^\mu) \\ &= (\partial_0^2 - \nabla^2) A^0 - \partial^0 (\partial_0 A^0) \\ &= -\nabla^2 A^0, \end{aligned} \quad (6.5.3)$$

where we have used $\partial_\mu A^\mu = \partial_0 A^0 + \nabla \cdot \mathbf{A} = \partial_0 A^0$. The solution is just the Coulomb potential for the electric charge density $J^0(\mathbf{y}, t)$

$$A^0(\mathbf{x}, t) = \int d^3y \frac{J^0(\mathbf{y}, t)}{4\pi |\mathbf{x} - \mathbf{y}|}, \quad (6.5.4)$$

and in terms of Green's function it is

$$G^{00} = \frac{i\delta(x-y)}{4\pi |\mathbf{x} - \mathbf{y}|}, \quad (6.5.5)$$

which in momentum space becomes

$$G^{00} = \frac{i}{\mathbf{k}^2}, \quad (6.5.6)$$

which is the Coulomb photon propagator. Now we compute the propagator for the vector potential \mathbf{A} . The current is

$$\mathbf{J} = \partial^2 \mathbf{A} + \nabla (\partial_\mu A^\mu), \quad (6.5.7)$$

and in the Coulomb gauge

$$\partial_\mu A^\mu = \partial^0 A_0 = \frac{1}{\nabla^2} (\nabla \cdot \mathbf{J}), \quad (6.5.8)$$

where we have used Eq. (6.5.3) and electric current conservation $\partial_0 A^0 = -\nabla \cdot \mathbf{J}$. So Eq. (6.5.7) then becomes

$$(\partial_0^2 - \nabla^2) \mathbf{A} = \mathbf{J} - \nabla \frac{1}{\nabla^2} (\nabla \cdot \mathbf{J}), \quad (6.5.9)$$

or in the momentum space

$$-(k_0^2 - \mathbf{k}^2) A^i(k) = J^i - \frac{k^i k^j}{\mathbf{k}^2} \times J^j. \quad (6.5.10)$$

In terms of Green's function we get

$$G^{ij}(k) = \frac{i}{k_0^2 - \mathbf{k}^2} \left(\delta^{ij} - \frac{k^i k^j}{\mathbf{k}^2} \right), \quad (6.5.11)$$

which is the transverse photon propagator. We can regulate infrared divergences by introducing a small photon mass λ and then components of the photon propagator become

$$G^{00} = \frac{i}{k^2 + \lambda^2} \quad G^{ij}(k) = \frac{i}{k_0^2 - \mathbf{k}^2 + \lambda^2} \left(\delta^{ij} - \frac{k^i k^j}{\mathbf{k}^2} \right). \quad (6.5.12)$$

6.6 Conclusion

In this chapter, we have derived Feynman rules for non-relativistic quantum electrodynamics (NRQED) following [6]. We have derived the NRQED Feynman rules by expanding the QED Feynman rules in the power of $\frac{\mathbf{p}}{m}$. This way of deriving the NRQED Feynman rules is far simpler than the proper way which is rederiving the QED Feynman rules in the non-relativistic limit. The main drawback of this approach is that the end result obtained from these Feynman rules may differ by a factor of $\pm i$ or an overall phase [6]. If we had gone back to the derivation of the QED Feynman rules and rederived them in the non-relativistic limit, we would have fixed the overall sign of the imaginary factor as the usual rules come from the normal ordering which provides a minus sign for fermion loops [6]. But as most of the calculation in particle physics depends on taking the square of the matrix element of the scattering amplitude, the overall sign does not matter. In the next chapter, we will use these NRQED Feynman rules to calculate the next-to-leading order correction of the D-term.

Chapter 7

The D-term for hydrogen atom

7.1 Introduction

All particles generate gravity and gravity couples to matter through the energy-momentum tensor (EMT). In electromagnetism, matter interacts with the force field through a *vector* current, indicating that a photon carries spin 1. Analogously for gravity, the field is coupled to a source *tensor*, indicating a spin-2 graviton, the as yet undiscovered mediating particle of gravity [25]. In examining electromagnetic properties of a quantum mechanical system we take the matrix element of the total current operator which acts as a source for the electromagnetic field. Analogously mechanical structure of a particle is given in terms of the matrix element of the EMT between single particle states which describes the response of the system to a probing gravitational field [26]. Thus working with energy-momentum or stress-energy tensor is analogous to considering a scattering process by exchanging a graviton. The graviton-matter scattering process has been considered in the literature [27, 28, 29, 30].

Here in this thesis, we will work with the matrix element of the energy-momentum tensor. The matrix element of the EMT depends on fundamental properties of the particle namely mass and spin. When the matrix element is written in terms of EMT form factors, one more fundamental property of the particle emerges alongside mass and spin, the so-called D-term [10]. The D-term is often used in the context of quantum chromodynamics (QCD) and is referred to as the last unknown global property of the nucleon [10]. In the context of QCD, the D-term is related to the spatial components of the EMT and gives information about the pressure distribution inside the nucleon, structure, charge radius, and how the strong forces inside the nucleon balance to form a bound state [11]. In this thesis, we will not perform any QCD calculations. Instead of looking at the bound state of quarks and gluons inside the nucleon, we will consider an analogous bound system like hydrogen atom and perform QED calculations and obtain the D-term for hydrogen atom.

In this chapter, in section 7.2, we will start by discussing how the mass and spin of the particle can be obtained from the EMT without using form factors. Then we will discuss the symmetric stress-energy tensors. The vanishing matrix element of the diagonal terms of the symmetric stress-energy tensor is referred to as the self-stress [26]. As the self-stress vanishes for a symmetric and Lorentz invariant stress-energy tensor, we will clarify our reasoning for working with canonical EMT in a non-relativistic theory. Later in that section, we will write the EMT in terms of form factors and define the D-term and discuss the interpretation of the D-term. Then we will discuss an experimental procedure through which this so-called D-term can be measured indirectly. In the next two sections, we will calculate the leading and next-to-leading order correction to the D-term of hydrogen atom [7, 1]. The main goal is to verify the claim of [1] that the next-to-leading order correction to the D-term for hydrogen atom follows the same physics as the Lamb shift. We will see that although it has logarithmic divergence like the Lamb shift, it is actually quite different from the Lamb shift. We will work with natural units i.e. $\hbar = c = \epsilon_0 = 1$ in this chapter.

7.2 EMT form factors and the interpretation of the D-term

From the matrix elements of the EMT, we get information about the most fundamental properties of a particle, its mass and spin. In this section, first we will discuss how mass and spin of a particle can be read off from the EMT. If the system's Lagrangian density \mathcal{L} is known, we can find out the density of canonical EMT of the system from the well-known relation [31],

$$T^{\mu\nu} = \frac{\partial \mathcal{L}}{\partial(\partial_\mu \phi)} \partial^\nu \phi - g^{\mu\nu} \mathcal{L}, \quad (7.2.1)$$

where ϕ is the field variable and $g^{\mu\nu}$ is the metric tensor. Our reasoning of considering canonical EMT will be discussed in the next section. The total EMT of the system is conserved

$$\partial_\mu T^{\mu\nu} = 0. \quad (7.2.2)$$

In 4×4 matrix form, the T^{00} component is the energy density and T^{i0} components are the energy flux. The T^{0i} , T^{ii} and T^{ij} (where $i \neq j$) components correspond to momentum density, pressure and shear stress respectively. From the T^{00} and T^{0i} components of the EMT, we get information regarding the mass and spin of the particle as they correspond to the Hamiltonian and the angular momentum operator respectively. The Hamiltonian H is

defined as

$$H = \int d^3x T^{00}(x), \quad (7.2.3)$$

which corresponds to the energy $E = \sqrt{\mathbf{p}^2 + m^2}$ and for $\mathbf{p} = 0$, we get the mass of the particle. The matrix element of the angular momentum operator defined as [31]

$$J^i = \int d^3x \varepsilon^{ijk} x^j T^{0k}(x), \quad (7.2.4)$$

corresponds to the particle spin. More specifically the $T^{00}(x)$ and $T^{0k}(x)$ components of the EMT correspond to two Casimir operators of the Poincaré group. One is $m^2 = p^\mu p_\mu$ with the eigenvalue m^2 where m is the mass of the particle and p^μ is the four momentum. The other operator is $W^2 = W^\mu W_\mu$ where $W^\mu = \frac{1}{2} \varepsilon^{\mu\nu\sigma\tau} M_{\nu\sigma} p_\tau$ is the Pauli-Lubanski vector with $M_{\nu\sigma} = \int d^3x J_{0\nu\sigma}(x)$ and $J_{\mu\nu\sigma}(x) = T^{\mu\nu}(x) x_\sigma - T_{\mu\sigma}(x) x_\nu$. It has eigenvalues $(-m^2) s(s+1)$ where $s = 0, \frac{1}{2}, 1, \frac{3}{2}, \dots$ is the spin of the particle [31, 32]. We do not get any information regarding the spatial components $T^{ij}(x)$ of the EMT as they are not related to the Casimir operators of the Poincaré group. These spatial components correspond to the D-term. So, to get additional information of the system we will write the matrix element of the EMT in terms of form factors (EMT form factors).

7.2.1 Remarks about symmetric stress-energy tensor

Calculations in quantum field theory involve divergences due to self-energy interactions, vacuum polarization, and scattering of light by light [33]. To maintain Lorentz invariance and conservation of the energy and momentum, the matrix elements of the diagonal components of the stress-energy tensor (self-stress) vanishes [26]. In this section, we will briefly discuss some approaches in removing divergences from stress tensors arising from interaction involving self-energies in the context of relativistic theory. We will discuss how we can make the self-stress vanish and mention the reason for choosing canonical energy-momentum tensor for our calculation of the D-term.

In [34], it is mentioned that upon applying a boost in a certain direction the self-stress due to interaction with the electromagnetic energy would remain the same, and in case of a free particle with zero momentum (rest frame), it would become zero. But that paper got a finite result for the self-stress whereas Lorentz covariance demands that it must vanish [35]. This inconsistency was subsequently solved by other groups [33, 36, 35]. In [33], the vanishing of the self-stress was explicitly shown by going outside the framework of pure QED and introducing an auxiliary neutral vector meson field coupled to an electron by an imaginary coupling constant. That calculation splits the total stress-energy tensor into electron part

and radiation part involving vector mesons. It was shown that in the rest frame, matrix elements of all the components become zero.

Ref. [35] followed the same procedure as the renormalization scheme by Schwinger [15]. The idea is to identify the divergent integrals and interpret them as physical properties. For example, if some integrands differ only by translation, suppose one term contains $p' - k$ and other contains $p'' - k$, then the second term then can be made equal to the first term by the translation of the variable of integration ($k \rightarrow k + p' - p''$). This type of integration can then be eliminated and the remainder is either finite or interpreted as renormalization of some physical quantity. For maintaining energy conservation, in this way it is possible to make the self-stress vanish.

The stress tensor of any physical system must be symmetrical but the canonical tensor need not satisfy this requirement. It is easier to work with a canonical tensor for its simpler form. It is always possible to get the symmetric tensor with a straightforward calculations [35] using the Belifante procedure [37, 38] where we add a total derivative of a super-potential or couple the theory to a weak classical background gravitational field described by a symmetric metric tensor $g_{\mu\nu}$ [31]. The disappearance of the self-stress only applies for symmetric and Lorentz invariant stress-energy tensor and not for canonical tensors. In [39], the author claims that dealing with a symmetric energy momentum tensor is not natural in particle physics. From the canonical procedure based on Noether's theorem, one gets the canonical energy-momentum tensor which is neither symmetric nor gauge invariant [39]. So one might get inclined towards abandoning the canonical EMT and make it symmetric by the Belifante procedure. But in this procedure, there is no clear distinction between the spin and orbital angular momentum and also between the energy flow T^{i0} and momentum density T^{0i} [39]. But spin and orbital angular momentum are clearly distinguishable as spin is a Lorentz invariant quantity contrary to the orbital angular momentum [39]. The symmetry requirement comes from the classical theory of general relativity where gravity couples to the symmetric EMT. The absence of space-time torsion is the underlying background of the requirement of a symmetric EMT. But more general theories relax this assumption and do not require a symmetric EMT [39]. This argument justifies working with the canonical EMT.

7.2.2 EMT form factors

In this section, we will discuss the EMT form factors for a spin-0 and spin-1/2 particles by taking matrix elements of the EMT between the states $|P\rangle$ and $|P'\rangle$ and expressing the result in terms of the EMT form factors. For the spin-0 and spin-1/2 system we can write

the matrix element as [10, 11]

$$\begin{aligned}
\text{spin-0:} \quad & \langle P'|T^{\mu\nu}|P\rangle = \frac{P^\mu P^\nu}{2} A(q^2) + \frac{q^\mu q^\nu - g^{\mu\nu} q^2}{2} D(q^2) \\
\text{spin-1/2:} \quad & \langle P'|T^{\mu\nu}|P\rangle = u(P'S') \left[A(q^2) \frac{P^\mu P^\nu}{M} + J(q^2) \frac{i(P^\mu \sigma^{\nu\rho} + P^\nu \sigma^{\mu\rho}) q_\alpha}{2M} \right. \\
& \left. + \frac{(q^\mu q^\nu - g^{\mu\nu} q^2)}{4M} D(q^2) \right] u(PS)
\end{aligned} \tag{7.2.5}$$

where the normalization is $\langle P|P'\rangle = 2E(2\pi)^3 \delta^3(\mathbf{P}' - \mathbf{P})$, $q^\mu = P'^\mu - P^\mu$ is the transferred momentum and S' and S are the indices for spins. Particles with higher spin will have some additional form factors. All the fundamental properties of the particle can be obtained in the limit $q^2 \rightarrow 0$. These properties in this limit are called global properties [31]. In the limit $q^2 \rightarrow 0$ [31]

$$\lim_{q^2 \rightarrow 0} A(q^2) = A(0) = 1, \tag{7.2.6}$$

$$\lim_{q^2 \rightarrow 0} J(q^2) = J(0) = \frac{1}{2}, \tag{7.2.7}$$

$$\lim_{q^2 \rightarrow 0} D(q^2) = D(0) \equiv D. \tag{7.2.8}$$

The form factor $A(0)$ indicates the T^{00} component of the EMT whose eigenvalue at the rest frame of the particle gives the mass of the particle. The form factor $J(0)$ describes the spin of the particle. For the form factor $D(0)$ there is no such constraint and must be determined from experiment [10, 11]. The form factor $D(0)$ is referred to as the D-term. Like mass or spin, the D-term is also a fundamental property of the particle which is referred to as the last unknown global property of the nucleon [10, 11].

7.2.3 Interpretation of the D-term

In this section, we will describe how the D-term gives useful informations of the nucleon. The D-term is related to the spatial components of the energy-momentum tensor and the spatial components of the EMT or the D-term mainly refers to the pressure or shear force distribution of a system. The D-term for spin-1/2 system can be written as [31, 12]

$$D(0) = -\frac{2}{5}m \int d^3\mathbf{r} T_{ij}(\mathbf{r}) \left(r^i r^j - \frac{\mathbf{r}^2}{3} \delta^{ij} \right) \equiv D \tag{7.2.9}$$

The spatial part of the EMT or the stress tensor can be decomposed into a traceless part (shear force $s(r)$) and a trace part (pressure $p(r)$) [31, 12]

$$T_{ij}(\mathbf{r}) = \left(\frac{r_i r_j}{r^2} - \frac{1}{3} \delta_{ij} \right) s(r) + \delta_{ij} p(r), \quad (7.2.10)$$

The conservation of the static EMT $\nabla^i T_{ij} = 0$ implies the following differential equation relating $s(r)$ and $p(r)$ [31, 12]

$$\frac{2}{3} \frac{\partial s(r)}{\partial r} + \frac{2}{r} s(r) + \frac{\partial p(r)}{\partial r} = 0 \quad (7.2.11)$$

The explicit relation between shear force and pressure with the D-term is given by [31, 12]

$$D = -\frac{4}{15} m \int d^3 r r^2 s(r) = m \int d^3 r r^2 p(r). \quad (7.2.12)$$

The pressure satisfies the von Laue condition [40, 41]

$$\int_0^\infty dr r^2 p(r) = 0, \quad (7.2.13)$$

which gives information on how the internal forces balance out inside a composite particle [12]. The T^{ii} component of the EMT can be written as

$$T^{ii}(\mathbf{r}) = \frac{2}{3} s(r) + p(r). \quad (7.2.14)$$

$s(r)$ is related to the distribution of the shear force and $p(r)$ describes the radial distribution of the pressure inside the nucleon. Mechanical stability of the system requires the following inequalities [31]

$$T_{00}(r) \geq 0 \quad \text{and} \quad T_{ii}(r) \geq 0, \quad (7.2.15)$$

The information regarding the pressure and shear force can reveal several useful information about the nucleon such as mechanical mean square radius and force components inside the nucleon. The force components are related to the EMT by The normal component of the force on an infinitesimal area dA^i at distance \mathbf{r} can be written as

$$dF^i(\mathbf{r}) = T^{ij}(\mathbf{r}) dA^j, \quad (7.2.16)$$

The normal and tangential components of the pressure is then [12]

$$\frac{dF_r}{dA_r} = \frac{2}{3}s(r) + p(r) \quad (7.2.17)$$

$$\frac{dF_\theta}{dA_\theta} = \frac{dF_\phi}{dA_\phi} = -\frac{1}{3}s(r) + p(r) \quad (7.2.18)$$

The infinitesimal area element is $dA = dA_r \mathbf{e}_r + dA_\theta \mathbf{e}_\theta + dA_\phi \mathbf{e}_\phi$. To have a mechanically stable system the corresponding force must point outwards so $\frac{2}{3}s(r) + p(r) > 0$ which implies that for a stable system the D-term should be negative [12]. The mechanical radius of the nucleon is defined as [12]

$$\langle r^2 \rangle_{\text{mech}} = \frac{\int d^3r r^2 \left(\frac{2}{3}s(r) + p(r) \right)}{\int d^3r \left(\frac{2}{3}s(r) + p(r) \right)} = \frac{6D}{\int_{-\infty}^0 dt D(t)}, \quad (7.2.19)$$

and from this it is possible to measure the size of a nucleon. The remarks of the authors in the paper [7] differs from the statement of [12] regarding the relation between the sign of the D-term and mechanical stability. Their analogy is that if we thought of the momentum current T^{ij} as the radiation pressure, the surface experiences some force or pressure when the directional momentum current gets absorbed on the surface which can be measured from the momentum flux. Then negative pressure only implies that the direction of the momentum flow is negative with respect to a reference direction. As it depends on a reference frame, the direction of the force and thus the sign of the D-term does not give conclusive statement of the mechanical stability [7]. In [7], the D-term is defined in terms of momentum-current monopole or tensor monopole

$$T^{(0)} = \frac{1}{5} \int d^3\mathbf{r} T_{ij}(\mathbf{r}) \left(r^i r^j - \frac{\mathbf{r}^2}{3} \delta^{ij} \right), \quad (7.2.20)$$

and after comparing with Eq. (7.2.9), we get $\tau = -\frac{T(0)}{2} = \frac{D(0)}{4m}$.

7.2.3.1 D-term of a nuclei in the context of the liquid drop model

Here we will calculate the D-term of a nucleus. We will use the simplest model of the nucleus (liquid drop model) to gain physical intuition of the D-term. The pressure and shear force distributions in the liquid drop is given by [42]

$$p(r) = p_0 \theta(r - R) - \frac{p_0 R}{3} \delta(r - R), \quad (7.2.21)$$

$$s(r) = \gamma \delta(r - R), \quad (7.2.22)$$

where R is the radius of the drop, p_0 is the pressure inside the drop and γ is the surface tension coefficient related to p_0 and R by the Kelvin relation, $p_0 = \frac{2\gamma}{R}$ [42]. It satisfies the von Laue stability condition. The distribution of the normal pressure follows from Eq. (7.2.17) as [42]

$$\frac{dF_r}{dA_r} = \frac{2}{3}s(r) + p(r) = p_0\theta(r - R). \quad (7.2.23)$$

Finally inserting Eq. (7.2.22) into Eq. (7.2.12), we get the D-term

$$D = -\frac{16\pi}{15}m\gamma R^4. \quad (7.2.24)$$

If we consider γ depends slowly on the atomic number A , mass of the nucleus $m_A \propto A$, and radii $R_A \propto A^{1/3}$, then for a large nucleus $D_{\text{nucleus}} \propto A^{7/3}$.

7.2.4 Experimental procedure of measuring the D-term

In this section, we will discuss the reason for referring the D-term as the last unknown global property and experimental procedure for measuring the D-term. The basic mechanical properties of the nucleon are encoded in the gravitational form factors (GFFs) of the energy-momentum tensor. If we want to measure the EMT form factors directly from experiments, we have to probe it by gravity or consider a scattering process involving graviton [11]. Graviton-nucleon scattering is the direct way to measure these gravitational form factors [14]. But gravity is a much weaker force and with current technology and known physics, measuring the EMT form factors directly through the interaction of gravity is not possible and with the lack of any physical process from which the D-term can be measured indirectly, it received very little attention before the 1990s. Other global properties of the nucleon like mass, spin, charge, have been measured through other processes rather than the direct measurement from the coupling with gravity and are available in the Particle Data Book [43]. For this lack of knowledge regarding the D-term, it is referred to as the last unknown global property of the nucleon.

During 1990s, practical indirect processes to measure the EMT form factors especially the D-term were found [13, 12, 31]. Currently several experiments in CERN and in the Jefferson National Laboratory are looking to measure the D-term through Generalized Parton Distribution functions (GPDs) from indirect processes like Deeply Virtual Compton Scattering and hard exclusive meson production [12, 13, 14, 31]. Here we will briefly discuss the experiment done in the Jefferson National Laboratory which considers the deeply virtual Compton scattering (DVCS) [14].

In this process, high energy electrons are scattered from the proton in liquid hydrogen and

the scattered electron, proton, and photon are detected. The high energy virtual photon exchanged between the scattered electron and proton serves as a probe to the nucleon structure [14] and this process is called deeply virtual Compton scattering. The emitted real photon controls the momentum transfer to the the proton [14]. This process can be described in terms of Compton form factors (CFFs) and generalized parton distributions (GPDs) [14, 31]. The following figure depicts the Deeply Virtual Compton Scattering taken from[31]

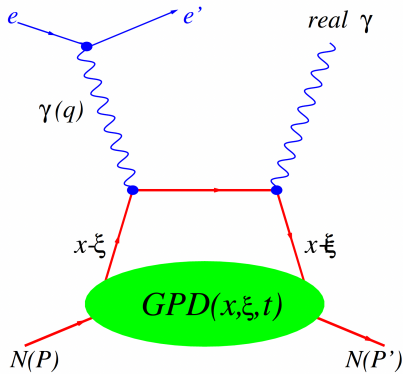


Figure 7.2.1: The leading order handbag diagram for the Deeply Virtual Compton Scattering ($\gamma^* N(p) \rightarrow \gamma N(p')$). Here x and ξ are the average and transferred momentum fractions. In this process, a highly virtual photon is created with momentum q and then it interacts with a nucleon with momentum P and results in a real photon and a nucleon with momentum P' . This process is described in terms of the GPDs and by measuring the GPDs it is possible to get information regarding the D-term.

The CFF are directly related to the experimental DVCS data which includes differential cross section [14]. The DVCS data are published in [44]. To get information about the D-term and pressure within the nucleus, it is necessary to fit theoretical D-term parameters to the experimental data through the relation between the GPDs, GFFs and CFF. The relation between the GPDs and GFFs are [13, 44]

$$\int x [H(x, \xi, t) + E(x, \xi, t)] dx = 2J(t), \quad (7.2.25)$$

$$\int x H(x, \xi, t) dx = A(t) + \frac{4}{5} \xi^2 d_1(t), \quad (7.2.26)$$

where t is the four momentum transfer to the proton, x and ξ are the average and transferred momentum fractions. H and E are the GPDs corresponding to the nucleon helicity conserving and spin flip processes respectively. $A(t)$, $J(t)$ are the GFFs related the mass and spin and $d_1(t)$ is the first Gegenbauer expansion of the D-term [14]. At $t = 0$ constraints applied to $A(t)$ and $J(t)$ gives mass and spin. The dispersion relation between the CFFs and the D-term

to the lowest order is [14]

$$\text{Re}\mathcal{H}(\xi, t) = D(t) + \mathcal{P} \int_{-1}^1 dx \left(\frac{1}{\xi - x} - \frac{1}{\xi + x} \right) \text{Im}\mathcal{H}(x, t), \quad (7.2.27)$$

where \mathcal{P} is the principle part of the integral and the subtraction constant is the D-term and as the average quark momentum is not observable it is integrated over. From these relations and the observed experimental DVCS data, it is now possible to relate the D-term to the experiment. The first Gegenbauer expansion of the D-term to fit the experimental result is [14]

$$d_1(t) = d_1(0) \left(1 - \frac{t}{M^2} \right)^{-\alpha}, \quad (7.2.28)$$

where the parameters M , α are to be adjusted to the data. Fits to the unpolarized cross-sections of DVCS and $d_1(t)$ are given in the following figures taken from [14]

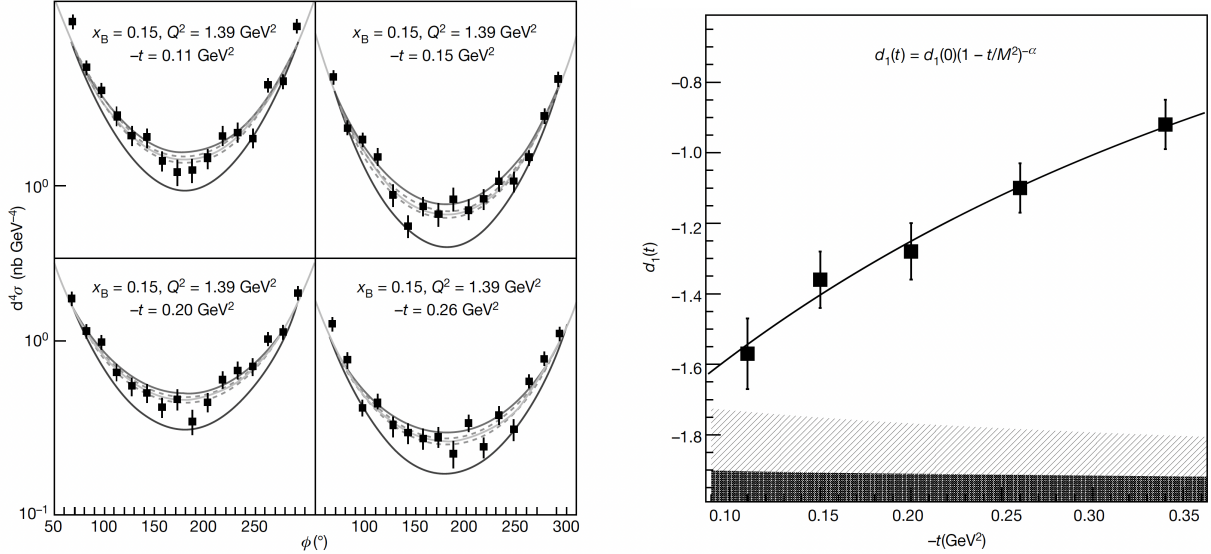


Figure 7.2.2: The figure on the left corresponds to the fits to the unpolarized DVCS cross-sections as a function of ϕ at fixed values of x_B and Q^2 . x_B is the momentum fraction of the quark and Q^2 is the virtuality of the exchanged photon. The black square represents the experimental DVCS cross-section, local fits with the parameter $d_1(t)$ at fixed $-t$ are shown by the light-grey curve. The upper dark-grey curves give global fits to $-t$ dependence of $d_1(t)$. The real part of the DVCS are calculated from the dispersion relation given in Eq. (7.2.27) and $d_1(t)$ is evaluated from the subtraction term $D(t)$. The right figure corresponds to the fit to $d_1(t)$. The error bars are obtained from the fit to the DVCS cross-section (left figure) at fixed $-t$. The light shaded area represents estimated uncertainty corresponding to fits to the regions without data and the dark shaded area corresponds to the projected uncertainties from a future experiment at 12 GeV. The current experiment was done at 6 GeV and uncertainties represent one standard deviation.

The fit results give $d_1(0) = -2.04$ with statistical uncertainty of 0.14 and systematic uncertainty of 0.33 [14]. As the D-term or the spatial components of the energy-momentum tensor give information about the shear force or pressure distribution, from the relation between GPDs, $d_1(t)$ and CFF, it is possible to get information about the pressure distribution in the proton. The fitted results to the experimental data regarding the pressure distribution in the proton is given in the following figure which was taken from [14]

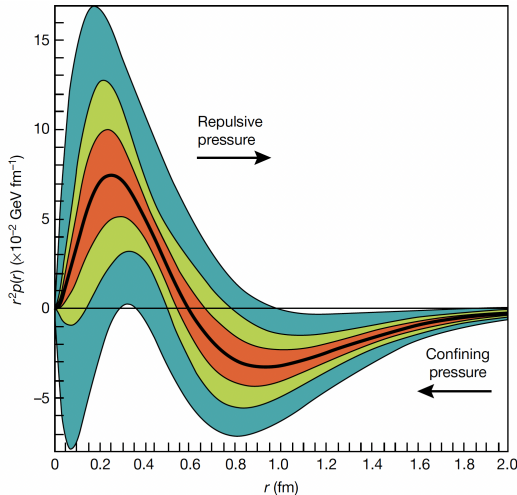


Figure 7.2.3: Radial pressure distribution in the proton. The figure shows the pressure distribution $r^2 p(r)$ vs the radial distance r from the center of the proton. The pressure distribution results from the interaction of the quarks in the proton. The pressure obtained from the D-term parameters fitted to the experimental data [14, 44] measured at 6 GeV is shown by the black line. The light-green shaded area and the blue are corresponds to the estimated uncertainties and all the data available before the 6 GeV experiment. The red area shaded area is a projection of future experiments at 12 GeV which will be performed using upgraded apparatus. Uncertainties are one standard deviation.

7.3 Relevant terms in the EMT in the context of QED

In the previous sections, we have provided a brief background on the D-term in the context of QCD. In this section, instead of considering the bound state of quarks and gluon inside a nucleon, we will consider the D-term in the context of QED for a bound state like hydrogen. First we will obtain the relevant components of the EMT for the hydrogen atom. We start with the non-relativistic Lagrangian density for an electron with background field from proton and electron [1]

$$\mathcal{L} = \phi^\dagger \left(iD_0 + \frac{D_i D_i}{2m_e} \right) \phi - \frac{1}{4} F_{\mu\nu} F^{\mu\nu}, \quad (7.3.1)$$

where we have neglected the spin contributions as the D-term gives the same physics for both spin-0 and spin-1/2 system. $D_0 = \partial_0 - ieV_e - ieV_p$ with V_e and V_p being the potential for electron and proton respectively and $D^i = \partial^i - ieA^i$. $F^{\mu\nu}$ is the electromagnetic field tensor with the definition $F^{\mu\nu} = \partial^\mu A^\nu - \partial^\nu A^\mu$. The relation between the EMT and Lagrangian density is given in Eq. (7.2.1). We will focus on the spatial components of the EMT as only they are relevant to the D-term. Now considering the proton to be infinitely heavy compared to the electron, the kinetic part of the EMT can be written as [1]

$$T_e^{ij} = -\frac{1}{4m_e} \left\{ \phi^\dagger D^i D^j \phi + (D^i D^j \phi)^\dagger \phi - (D^i \phi)^\dagger (D^j \phi) - (D^j \phi)^\dagger (D^i \phi) \right\}, \quad (7.3.2)$$

where m_e is the mass of the electron. The lowest order of kinetic contribution is

$$T_{e0}^{ij} = -\frac{1}{4m_e} (\phi^\dagger \partial^i \partial^j \phi + \partial^i \partial^j \phi^\dagger \phi - \partial^i \phi^\dagger \partial^j \phi - \partial^j \phi^\dagger \partial^i \phi), \quad (7.3.3)$$

where T_{e0}^{ij} is the contribution to the kinetic part of the EMT which contains the ∂^i parts of D^i . We now obtain the potential part of the EMT from the $-\frac{1}{4}F_{\mu\nu}F^{\mu\nu}$ term in Eq. (7.3.1) [34]

$$T_\gamma^{\mu\nu} = -F^{\rho\mu}F_\rho^\nu + \frac{1}{4}g^{\mu\nu}F^{\rho\sigma}F_{\rho\sigma}. \quad (7.3.4)$$

In more familiar terms $F^{j0} = E^j$, $F^{ij} = -\epsilon_{ijk}B^k$ and $\frac{1}{2}F^{\rho\sigma}F_{\rho\sigma} = \mathbf{B}^2 - \mathbf{E}^2$ and so Eq. (7.3.4) can be rewritten as

$$T_\gamma^{ij} = \frac{1}{2}\delta^{ij}(\mathbf{E}^2 + \mathbf{B}^2) - B^i B^j - E^i E^j, \quad (7.3.5)$$

with $\mu_0 = \epsilon_0 = 1$. There are several fields at play and we can take different combinations of them to get various terms for the potential part of the EMT. We can decompose T_γ^{ij} as

$$T_\gamma^{ij} = T_{\gamma||}^{ij} + T_{\gamma||\perp}^{ij} + T_{\gamma\perp}^{ij}, \quad (7.3.6)$$

where the subscript γ indicates the photon field. $T_{\gamma||}^{ij}$, $T_{\gamma\perp}^{ij}$ and $T_{\gamma||\perp}^{ij}$ corresponds to pure Coulomb field, transverse radiative fields and mixture of Coulomb and transverse radiative fields respectively and they are [1]

$$T_{\gamma||}^{ij} = -\partial^i V_e \partial^j V_e + \frac{1}{2}\delta^{ij} \partial^k V_e \partial^k V_e, \quad (7.3.7)$$

$$T_{\gamma||\perp}^{ij} = \partial^i V_e \partial^0 A^j + \partial^j V_e \partial^0 A^i - \delta^{ij} \partial^k V_e \partial^0 A^k, \quad (7.3.8)$$

$$T_{\gamma\perp}^{ij} = T_{\gamma E}^{ij} + T_{\gamma B}^{ij}. \quad (7.3.9)$$

and

$$T_{\gamma E}^{ij} = -\partial^0 A^i \partial^0 A^j + \frac{1}{2} \delta^{ij} \partial^0 A^k \partial^0 A^k, \quad (7.3.10)$$

$$T_{\gamma B}^{ij} = (\partial^i A^k - \partial^k A^i) (\partial^j A^k - \partial^k A^j) - \frac{1}{2} \delta^{ij} (\partial^k A^l \partial^k A^l - \partial^k A^l \partial^l A^k), \quad (7.3.11)$$

where we have considered the gauge $\nabla \cdot \mathbf{A} = 0$ and in this gauge the electric field is separated into longitudinal (Coulomb) and transverse (radiative) parts denoted as \mathbf{E}_{\parallel} and \mathbf{E}_{\perp} respectively

$$\mathbf{E} = \mathbf{E}_{\parallel} + \mathbf{E}_{\perp}, \quad (7.3.12)$$

where $\mathbf{E}_{\parallel} = -\nabla V_e$ and $\mathbf{E}_{\perp} = -\partial^0 \mathbf{A}$. These EMT's represent interaction between electron and photon field. Now, we are left with the mixed contribution between the photon field and proton's electric field, and the EMT of the proton. The mixed contribution between the proton and photon field can be decomposed in two parts, one involving the longitudinal and other for transverse field [1]

$$T_{\gamma P}^{ij} = T_{\perp P}^{ij} + T_{\parallel P}^{ij}, \quad (7.3.13)$$

where

$$T_{\parallel P}^{ij} = \delta^{ij} \nabla V_p \cdot \nabla V_e - \partial^i V_e \partial^j V_p - \partial^i V_p \partial^j V_e, \quad (7.3.14)$$

$$T_{\perp P}^{ij} = \partial^i V_p \partial^0 A^j + \partial^j V_p \partial^0 A^i - \delta^{ij} \partial^k V_p \partial^0 A^k. \quad (7.3.15)$$

$T_{\parallel P}^{ij}$ corresponds to mixing between electron's Coulomb field and proton's electric field and $T_{\perp P}^{ij}$ corresponds the mixing between the radiative field and proton's electric field. Finally the EMT of the proton is derived from the classical electric field of the proton ($E^i = \frac{er^i}{4\pi r^3}$) which in momentum space is [1]

$$T_P^{ij}(\mathbf{q}) = (q^i q^j - \delta^{ij} q^2) \frac{\alpha\pi}{16|q|}, \quad (7.3.16)$$

7.4 Leading order calculation of the D-term for hydrogen atom

From the EMTs obtained in the previous section, we are now in position to calculate the D-term for the hydrogen atom. In this section, we will calculate the leading order D-term in

the infrared region $r \sim \frac{1}{\alpha}$ or $|q| \leq \mathcal{O}(\alpha m_e)$. We will determine the D-term for hydrogen in terms of tensor monopole moment mentioned in the subsection 7.2.3

$$\tau = -\frac{T(0)}{2} = \frac{D(0)}{4m}. \quad (7.4.1)$$

In SI units the tensor monopole moment of a free spin-0 boson reads [7]

$$\tau_{\text{boson}} = -\frac{\hbar^2}{4m}. \quad (7.4.2)$$

which motivated the authors in [7] to work in the unit $\tau_0 = \frac{\hbar^2}{4m}$. We will also work with the same unit as [7]. Now with all the definitions lined up, we start our calculation of the D-term for hydrogen. We start with the Schrödinger equation

$$\left(-\frac{1}{2m_e} \nabla^2 - eV_p \right) \phi(\mathbf{r}) = E\phi(\mathbf{r}), \quad (7.4.3)$$

where e is the charge of the proton and $\phi(\mathbf{r}) = \sqrt{\frac{\alpha^3}{\pi}} e^{-\alpha r}$ is the normalized ground state Hydrogen wave function. The potential for the static charge of proton is the Coulomb potential $V_p = \frac{e}{4\pi r}$ which satisfies the Laplace equation $\nabla^2 V_p = -e\delta^3(r)$. V_e is the static potential for the electron [7]

$$V_e(r) = \frac{ee^{-2\alpha r} (1 + \alpha r - e^{2\alpha r})}{4\pi r}, \quad (7.4.4)$$

which satisfies the Poisson equation $\nabla^2 V_e(r) = e|\phi(\mathbf{r})|^2$. The leading order EMT for the hydrogen comprise of the kinetic contribution from the electron T_{e0}^{ii} and mixing between electron's Coulomb field and proton's electric field $T_{||p}^{ii}$. The total EMT is then $T_{e0+||p}^{ii} = T_{e0}^{ii} + T_{||p}^{ii}$ where T_{e0}^{ii} and $T_{||p}^{ii}$ is described by Eq. (7.3.3) and Eq. (7.3.14) respectively. The total EMT is

$$T_{e0+||p}^{ii} = |\phi|^2 \left(\frac{E + eV_p}{2} \right) + \frac{1}{4m_e} \nabla \phi^\dagger \cdot \nabla \phi + \nabla V_p \cdot \nabla V_e, \quad (7.4.5)$$

From Eq. (7.2.1), we see that the form factor corresponding to the D-term, $D(q^2)$ is related to the EMT by

$$T^{ij}(\mathbf{q}) = (q^i q^j - \delta^{ij} q^2) \frac{D(q^2)}{4m}. \quad (7.4.6)$$

or in position space

$$T^{ij}(\mathbf{r}) = (\delta^{ij} \nabla^2 - \nabla^i \nabla^j) \frac{D(\mathbf{r})}{4m}. \quad (7.4.7)$$

So taking $i = j$ for this process the relation between $D(q^2)$ and EMT becomes

$$T_{e0+||P}^{ii} = 2\nabla^2 \frac{D_{e0+||p}(r)}{4m_e}, \quad (7.4.8)$$

The solution in the position space is [7]

$$\frac{D_{e0+||p}(r)}{4m_e} = \frac{e^{-2\alpha r} \alpha (1 + 2\alpha r)}{16\pi r^2} - \frac{\alpha}{16\pi r^2}, \quad (7.4.9)$$

and in momentum space by taking Fourier transformation, we get

$$\frac{D_{e0+||P}(q^2)}{4m_e} = \frac{1}{2m_e \left(\frac{q^2}{\alpha^2 m_e^2} + 4 \right)} - \frac{\alpha\pi}{8|q|} + \frac{\alpha}{4|q|} \tan^{-1} \frac{q}{2\alpha m_e}. \quad (7.4.10)$$

The second term in both of these equations is called the Coulomb tail which prevents a finite D-term in the limit $q \rightarrow 0$. But the self-energy contribution of both electron and proton will cancel this Coulomb tail and we will obtain a finite D-term at $q \rightarrow 0$. The self energy contribution of the electron comes from the interaction of the electron with its longitudinal field described in Eq. (7.3.7). We will now calculate the self-energy contribution of the electron in the infrared region $r \sim \frac{1}{\alpha}$ and in this region by expanding the exponent in V_e described in Eq. (7.4.4) to first order of α , we get the electron potential $V_e = -\frac{e}{4\pi r}$. From Eq. (7.3.7), the self-energy contribution of the electron is then

$$T_{\gamma||}^{ij} = \frac{1}{2} \nabla V_e \cdot \nabla V_e = (\delta^{ij} \partial^2 - \partial^i \partial^j) \frac{\alpha}{32\pi r^2}. \quad (7.4.11)$$

Now for a bound state of hydrogen atom, the self-energy contribution of the free electron will get dressed by the bound state wave function described as [1]

$$\frac{16\alpha^4}{\left(\frac{q^2}{m_e^2} + 4\alpha^2 \right)^2} = \int \frac{d^3\mathbf{p}}{(2\pi)^3} \phi^\dagger \left(\mathbf{p} - \frac{\mathbf{q}}{2} \right) \phi \left(\mathbf{p} + \frac{\mathbf{q}}{2} \right). \quad (7.4.12)$$

So the self-energy contribution of the electron to $D(q^2)$ is then

$$\frac{D_{\gamma||}(q^2)}{4m_e} = \frac{\alpha\pi}{16|q|} \frac{16\alpha^4}{\left(\frac{q^2}{m_e^2} + 4\alpha^2 \right)^2}, \quad (7.4.13)$$

where the first term is the Fourier transform of $\frac{\alpha}{32\pi r^2}$ corresponding to the free electron contribution and the second factor is the dressing in bound state wave function. Now from

Eq. (7.3.16), we obtain $D(q^2)$ for proton

$$\frac{D_P(q^2)}{4M} = \frac{\alpha\pi}{16|q|}, \quad (7.4.14)$$

where M is the mass of the proton. Now gathering all the $D(q^2)$ (Eqs. (7.4.10), 7.4.13, and 7.4.14), we get the total $D_H^{(0)}(q^2)$ for the hydrogen in the region $|q| \leq \mathcal{O}(\alpha m_e)$ as

$$\frac{D_H^{(0)}(q^2)}{4m_e} = \frac{D_{e0+|p}(q^2)}{4m_e} + \frac{D_{\gamma||}(q^2)}{4m_e} + \frac{D_P(q^2)}{4M} \quad (7.4.15)$$

$$= \frac{1}{2m_e \left(\frac{q^2}{\alpha^2 m_e^2} + 4 \right)} - \frac{\alpha\pi}{8|q|} + \frac{\alpha}{4|q|} \tan^{-1} \frac{q}{2\alpha m_e} + \frac{\alpha\pi}{|q|} \frac{1}{\left(\frac{q^2}{\alpha^2 m_e^2} + 4 \right)^2} + \frac{\alpha\pi}{16|q|}. \quad (7.4.16)$$

The superscript 0 refers to the leading order calculation. In the limit $q^2 \rightarrow 0$, we can see that the self-energy of the electron and proton cancels the Coulomb tail. Finally by expanding the \tan^{-1} term to the first order and expressing the D-term in terms of tensor monopole moment using the relation $\tau = \frac{D^{(0)}}{4m}$ from subsection 7.2.3, we get

$$\tau_H^{(0)} = \frac{D_H^{(0)}(0)}{4m_e} = \tau_0 [1 + \mathcal{O}(\alpha \ln \alpha)]. \quad (7.4.17)$$

where $\tau_0 = \frac{\hbar^2}{4m_e}$ and the small logarithmic correction comes from the next-to-leading order terms which we will calculate in the next section.

7.5 Logarithmic correction to the D-term for hydrogen atom

The main goal of this section is to calculate the logarithmic divergent term for the next-to-leading order correction to the D-term of hydrogen and confirm our claim that although it has logarithmic divergence, the physics is not the same as the Lamb shift of energy levels and thus refute the claim of [1]. We will give an overview of the calculation scheme of [1] and not go into detail calculation for the terms that are not logarithmic divergent. Our purpose is to understand the origin of the logarithmic divergent terms to check whether the physics behind these terms is the same as the Lamb shift or not. For our calculation, we will incorporate the concept of dimensional regularization (DR) to calculate the loop integrals. Among various approaches to regularize divergent loop integrals such as cut-off, Wilson regularization, Pauli–Villars regularization, etc., dimensional regularization is the most appropriate one for our purposes as it preserves all the symmetries of the theory [45].

In DR one works with a non-integer dimension instead of the usual 4-dimensional space-time to regularize a divergent integral [45, 46]. As we are working in the non-relativistic domain, we will use the standard dimensional regularization with $D = 3 - 2\epsilon$ as [1]. The remaining EMTs in section 7.3 are the contribution of the pure transverse radiative fields (Eq. (7.3.9) and Eqs. (7.3.10), and 7.3.11) and mixed contribution of the Coulomb and transverse radiative fields (Eq. (7.3.14)).

7.5.1 Photonic contribution and matching to QED

We start our calculation with the photonic contribution of the EMT which can be later generalized for the bound system calculation. When using dimensional regularization using $D = 3 - 2\epsilon$, the final result will contain a term involving $\frac{1}{\epsilon}$ indicating UV divergence. The photonic contribution of the EMT in NRQED will give the required coefficient when matching with the full QED result obtained from several literatures [27, 28, 1]. When it is subtracted from the bound state NRQED calculation, we will get a divergent free result in the UV sector. The photonic contribution comes from the following diagrams [1]

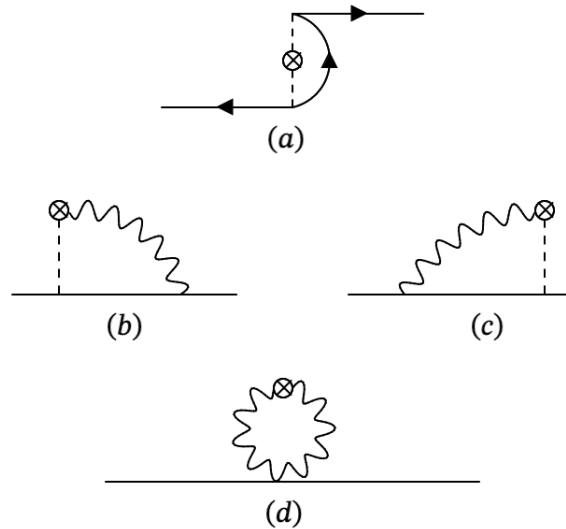


Figure 7.5.1: The photonic contribution of T_{γ}^{ij} (Eq. (7.3.6)). The dashed lines represent Coulomb interaction and radiative interactions are given by the wavy lines. Diagram (a) represents pure Coulomb interaction, diagrams (b) and (c) are the mixed contribution of Coulomb and transverse photon and diagram (d) is the tadpole diagram originated from pure transverse radiative fields (Eq. 7.3.9).

Before proceeding with calculating these Feynman diagrams, it should be mentioned first that in dimensional regularization, integrals of the type $\int \frac{d^D k}{(k^2)^n}$ is considered to be zero. This

type of integrals are refereed as scaleless integral and this conjecture is known as 't Hooft-Veltman conjecture [47]. Now setting the scaleless integral to be zero, the Feynman rules for the diagram 7.5.1(a) reads

$$\langle T_{\gamma||}^{ij} \rangle_a = -e^2 Q^2 \int \frac{d^D k}{(2\pi)^D} \frac{1}{(\mathbf{k} + \mathbf{Q})^2 (\mathbf{k} - \mathbf{Q})^2}, \quad (7.5.1)$$

where we have used the Coulomb propagator derived in Eq. (6.5.12). Now using standard Feynman parameters, we get

$$\begin{aligned} \langle T_{\gamma||}^{ij} \rangle_a &= -e^2 Q^2 \frac{1}{16|Q|} \\ &= \frac{\alpha\pi}{8|Q|} (Q^i Q^j - \delta^{ij} Q^2). \end{aligned} \quad (7.5.2)$$

So this diagram does not have any logarithmic divergence. Diagrams 7.5.1(b and c) will give logarithmic contributions. The Feynman rules for these diagrams give [1]

$$\begin{aligned} \langle T_{\gamma||\perp}^{ij} \rangle_{b,c} &= e^2 \mu^{2\epsilon} \int \frac{d^D k}{(2\pi)^D} \frac{(k - Q)^i P^{jk} (\mathbf{k} + \mathbf{Q}) Q^k + (i \leftrightarrow j)}{m_e |\mathbf{k} - \mathbf{Q}|^2 |\mathbf{k} - \mathbf{Q}|} \\ &\quad - e^2 \delta^{ij} \mu^{2\epsilon} \int \frac{d^D k}{(2\pi)^D} \frac{(k - Q)^l P^{lk} (\mathbf{k} + \mathbf{Q}) Q^k}{m_e |\mathbf{k} - \mathbf{Q}|^2 |\mathbf{k} - \mathbf{Q}|}, \end{aligned} \quad (7.5.3)$$

where μ is the fictitious mass of the photon and we have used the transverse photon propagator given in Eq. (6.5.12) where

$$P^{ij} = \delta^{ij} - \frac{k^i k^j}{k^2}, \quad (7.5.4)$$

We have used the Feynman rules for the standard triple vertex from Eq. (6.2.13) and the relation $P^{jk} (\mathbf{k} + \mathbf{Q}) (Q - k)^k = 2p^{jk} (\mathbf{k} + \mathbf{Q}) Q^k$ [1]. One can decompose the above expression into two scalar integrals and using the property of the scaleless integral we get [1]

$$\langle T_{\gamma||\perp}^{ii} \rangle_{b,c} = 2e^2 (D - 2) \mu^{2\epsilon} \int \frac{d^D k}{(2\pi)^D} \frac{Q^i P^{ij} Q^j}{m_e |\mathbf{k} - \mathbf{Q}|^2 |\mathbf{k} - \mathbf{Q}|}, \quad (7.5.5)$$

$$Q^i \langle T_{\gamma||\perp}^{ij} \rangle_{b,c} Q^j = 2e^2 \mu^{2\epsilon} \int \frac{d^D k}{(2\pi)^D} \frac{\mathbf{k} \cdot \mathbf{Q} Q^i P^{ij} Q^j}{m_e |\mathbf{k} - \mathbf{Q}|^2 |\mathbf{k} - \mathbf{Q}|}. \quad (7.5.6)$$

The result of these loop integrals are

$$\langle T_{\gamma||\perp}^{ii} \rangle_{\text{b,c}} = \frac{e^2}{3m_e\pi^2} Q^2 \left[\frac{1}{\epsilon} - \ln \frac{Q^2}{\mu^2} + \gamma_E - 5 + \ln 4 + \ln \pi + 2\psi \left(\frac{5}{2} \right) \right], \quad (7.5.7)$$

$$Q^i \langle T_{\gamma||\perp}^{ij} \rangle_{\text{b,c}} = \frac{e^2}{15m_e\pi^2\epsilon} Q^4 \left[-\frac{1}{\epsilon} + \ln \frac{Q^2}{\mu^2} - \gamma_E + 3 - \ln 4 - \ln \pi - 2\psi \left(\frac{7}{2} \right) \right], \quad (7.5.8)$$

where γ_E is the Euler–Mascheroni constant and $\psi(z)$ is the digamma function which can be evaluated using the relation [1]

$$\psi \left(n + \frac{1}{2} \right) = -\gamma_E - \ln 4 + \sum_{k=1}^n \frac{2}{2k-1}. \quad (7.5.9)$$

These terms contain logarithmic IR divergence i.e. $\ln Q^2$. Detail calculation for evaluating these loop integrals is presented in Appendix E. It is to be noted that Eq. (7.5.5) represents conserved or trace part and Eq. (7.5.6) represent non-conserved part. Because for a diagram that depends on Q and two indices i and j , the conserved part represent the structure $Q^i Q^j - \delta^{ij} Q^2$ as when contracted with Q^i it gives zero. But this structure has a non-zero trace. The coefficient of the other possible linear combination can be obtained by contracting with Q^i and Q^j which represents the non-conserved part. The next job is calculate the tadpole diagram in 7.5.1(d). The contribution of the non-conserved part of the tadpole diagram cancels the non-conserved Eq. (7.5.6) [1]. The trace or conserved part of the tadpole diagram is given by [1]

$$\langle T_{\gamma\perp}^{ii} \rangle_{\text{d}} = -\frac{Q^2 e^2}{18m_e\pi^2} (1 - 6\ln 4). \quad (7.5.10)$$

Now the total EMT is conserved. The EMT in terms of the form factor $D(Q^2)$ is defined as

$$\langle T^{ij} \rangle = (Q^i Q^j - \delta^{ij} Q^2) \frac{D(Q^2)}{4m_e}$$

and so gathering the terms from Eq. (7.5.5) and Eq. (7.5.10), we get

$$\frac{D(Q^2)}{4m_e} = \frac{\alpha\pi}{8|Q|} + \frac{e^2}{6m_e\pi^2} \left(-\frac{1}{\epsilon} + \ln \frac{Q^2}{\mu^2} + \gamma_E - \ln \pi - \frac{7}{6} \right) \quad (7.5.11)$$

The form factor $D(Q^2)$ has been obtained in several papers [27, 28, 1]

$$\frac{D_{\text{QED}}(Q^2)}{4m_e} = \frac{\alpha\pi}{8|Q|} + \frac{e^2}{6m_e\pi^2} \ln \frac{4Q^2}{m_e^2} - \frac{11e^2}{72m_e\pi^2}. \quad (7.5.12)$$

To match with the full QED, we write the total T_{NRQED}^{ij} in terms of tree level and a correction

which contains a coefficient d_0

$$T_{\text{NRQED}}^{ij} = T_{\text{tree}}^{ij} + d_0 (\partial^i \partial^j - \delta^{ij} \partial^2) \psi^\dagger \psi, \quad (7.5.13)$$

where d_0 contains only logarithm in μ and m_e and given by [1]

$$d_0 = -\frac{\alpha}{6\pi m_e} \left(\frac{1}{\epsilon} + \ln \frac{4\mu^2}{m_e^2} - \gamma_E + \ln \pi + \frac{1}{4} \right). \quad (7.5.14)$$

we will later see that when d_0 is subtracted from the bound state results, we will get rid of ϵ and get a finite result.

7.5.2 Bound state calculation for $\mathcal{O}(\alpha)$ correction to the D-term

In this section, we will calculate the bound state $\mathcal{O}(\alpha)$ correction to the D-term for hydrogen and identify the origin of the logarithmic divergent term. The Feynman diagrams for the bound state contribution to $\mathcal{O}(\alpha)$ correction in non-relativistic reduction is given by [1]

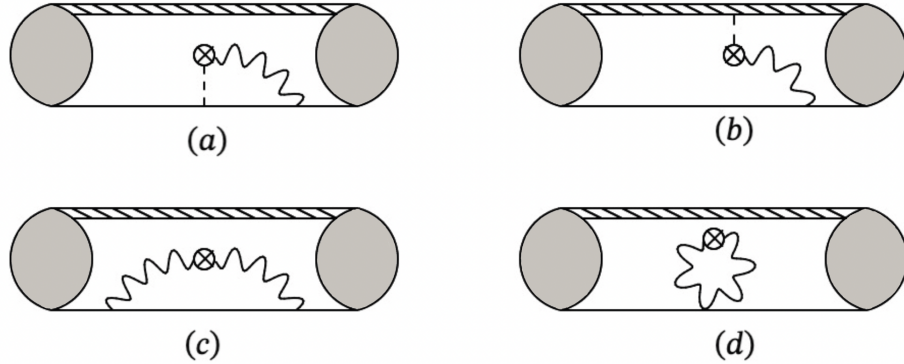


Figure 7.5.2: Bound state contribution to $T_{\gamma}^{ij} + T_{\gamma P}^{ij}$ (Eqs. (7.3.6) and (7.3.13)) to calculate order $\mathcal{O}(\alpha)$ correction to the D-term. The dashed line represents Coulomb photon and the wavy line represents transverse photon. The double shaded line represents the nucleus line and the thin line represents electron line. Diagram (a) and (b) represents the mixed contribution of radiative and transverse photon from electron and proton line respectively in a bound state. Diagram (c) represents purely radiative contribution and diagram (d) is the tadpole diagram. The shaded circle represents the bound state wave functions.

In the bound state, the obtained IR divergence i.e. $\ln Q^2$ discussed in the previous section 7.5.1 will be regulated by binding energy difference in the bound state[1]. Diagrams 7.5.2(a) and 7.5.2(b) are the interference diagrams containing mixed contribution of the Coulomb

and radiative fields and as shown in the previous section 7.5.1, they will contain logarithmic divergent terms but the IR divergences $\ln Q^2$ will be now get regulated by the binding energy difference. In Diagram 7.5.2(b), the Coulomb photon is emitted from the proton line and vanishes [1]. As earlier, diagram 7.5.2(a) will have both conserved and non-conserved parts. The tadpole diagram 7.5.2(d) which represents pure transverse radiative fields is independent of the bound state and the same as the free state and as the non-conserved part of this diagram has $\ln Q^2$ dependence, it will not be able to cancel the non-conserved part of the mixed diagram 7.5.2(a) as $\ln Q^2$ in the mixed diagram will now be replaced by the binding energy contribution [1]. But the diagram 7.5.2(c) also represents pure transverse photons and it will also have conserved and non-conserved part. The non-conserved part of the 7.5.2(c) will cancel both the non-conserved part of tadpole and mixed diagram [1]. So, now we have the conserved part of diagrams 7.5.2(a), (c), and (d) which indicates that the total EMT is conserved. Analogously to the earlier discussion, only conserved part of the diagram 7.5.2(a) has the logarithmic contribution and 7.5.2(c) and (d) will only contribute to the constants. The Feynman rules for the conserved or trace part of the diagram 7.5.2(a) reads [1]

$$\begin{aligned} \langle T_{\gamma||\perp}^{ii} \rangle_a &= 2e^2 (D-2) \mu^{2\epsilon} \frac{1}{D} \sum_M i (\mathbf{v}_{0M} \cdot \mathbf{x}_{M0} - \mathbf{x}_{0M} \cdot \mathbf{v}_{M0}) \\ &\times \int \frac{d^D k}{(2\pi)^D} \frac{Q^i P^{ij} Q^j}{|\mathbf{k} - 2\mathbf{Q}|^2 (|\mathbf{k}| + E_M - E_0)}. \end{aligned} \quad (7.5.15)$$

The integral is analogous to the integral in Eq. (7.5.5). The exceptions are the insertion of the term $\frac{1}{D} \sum_M i (\mathbf{v}_{0M} \cdot \mathbf{x}_{M0} - \mathbf{x}_{0M} \cdot \mathbf{v}_{M0})$ which indicates taking matrix element in the bound state. It comes from the dipole expansion of the matrix elements defined in[1]

$$\mathbf{v}_{NM}(\mathbf{k}) = \int d^D k \psi_N^\dagger(\mathbf{x}) \frac{-i\nabla}{m_e} \psi_M(\mathbf{x}) e^{-i\mathbf{k}\cdot\mathbf{x}}, \quad (7.5.16)$$

$$\rho_{NM}(\mathbf{k}) = \int d^D k \psi_N^\dagger(\mathbf{x}) \psi_M(\mathbf{x}) e^{-i\mathbf{k}\cdot\mathbf{x}}, \quad (7.5.17)$$

and the dipole expansion gives [1]

$$v^i(\mathbf{k}) = v_{MN}^i + \mathcal{O}(\alpha), \quad (7.5.18)$$

$$\rho_{MN}(\mathbf{k}) = \delta_{MN} - i\mathbf{k} \cdot \mathbf{x}_{MN} + \mathcal{O}(\alpha). \quad (7.5.19)$$

In Eq. (7.5.15), we have considered interaction between intermediate state M and the ground state. The commutation relation in the term $\frac{1}{D} \sum_M i (\mathbf{v}_{0M} \cdot \mathbf{x}_{M0} - \mathbf{x}_{0M} \cdot \mathbf{v}_{M0})$ any dimension

gives [1]

$$\frac{1}{D} \sum_M i (\mathbf{v}_{0M} \cdot \mathbf{x}_{M0} - \mathbf{x}_{0M} \cdot \mathbf{v}_{M0}) \equiv \frac{1}{m_e} \equiv \sum_M 2 \frac{\mathbf{v}_{M0} \cdot \mathbf{v}_{0M}}{D(E_M - E_0)}. \quad (7.5.20)$$

The evaluation of the integral in Eq. (7.5.15) is identical to the evaluation of Eq. (7.5.5) which was shown in details in Appendix E. The result reads [1]

$$\langle T_{\gamma||\perp}^{ii} \rangle_a = \frac{e^2}{3\pi^2} Q^2 \sum_M 2 \frac{\mathbf{v}_{M0} \cdot \mathbf{v}_{0M}}{D(E_M - E_0)} \left(\frac{1}{\epsilon} - \ln \frac{(E_M - E_0)^2}{\mu^2} - \gamma_E + \ln \pi - \frac{1}{3} \right), \quad (7.5.21)$$

which has the same ϵ dependency as Eq. (7.5.7) and the IR divergence $\ln Q^2$ is now being regulated by the binding energy difference. The conserve part of the diagrams 7.5.2(c) and (d) reads [1]

$$\langle T_{\gamma\perp}^{ii} \rangle_c = -\frac{e^2}{3\pi^2} Q^2 \sum_M 2 \frac{\mathbf{v}_{M0} \cdot \mathbf{v}_{0M}}{D(E_M - E_0)} \ln 4, \quad (7.5.22)$$

$$\langle T_{\gamma\perp}^{ii} \rangle_d = -\frac{e^2}{18\pi^2} Q^2 \sum_M 2 \frac{\mathbf{v}_{M0} \cdot \mathbf{v}_{0M}}{D(E_M - E_0)} (1 - 6 \ln 4), \quad (7.5.23)$$

Now combining Eqs. (7.5.21), (7.5.22), and (7.5.23), we get the full EMT as

$$\langle T_{\gamma||\perp}^{ii} \rangle = \frac{e^2}{6\pi^2} (-2Q^2) \sum_M 2 \frac{\mathbf{v}_{M0} \cdot \mathbf{v}_{0M}}{D(E_M - E_0)} \left[-\frac{1}{\epsilon} + \ln \frac{(E_M - E_0)^2}{\mu^2} + \gamma_E - \ln \pi + \frac{1}{2} \right]. \quad (7.5.24)$$

Now from the relation between EMT and the form factor $D(Q^2)$

$$\langle T^{ij} \rangle = (Q^i Q^j - \delta^{ij} Q^2) \frac{D(Q^2)}{4m_e}, \quad (7.5.25)$$

$$\langle T^{ii} \rangle = (-2Q^2) \frac{D(Q^2)}{4m_e}, \quad (7.5.26)$$

we get

$$\frac{D_H^{(1)}(0)}{4m_e} = \frac{e^2}{6\pi^2} \sum_M 2 \frac{\mathbf{v}_{M0} \cdot \mathbf{v}_{0M}}{D(E_M - E_0)} \left[-\frac{1}{\epsilon} + \ln \frac{(E_M - E_0)^2}{\mu^2} + \gamma_E - \ln \pi + \frac{1}{2} \right], \quad (7.5.27)$$

where the superscript 1 stands for next-to-leading order correction to the D-term for hydrogen. Now to match with QED, one needs to subtract $4d_0$ [1] and finally we get the D-term

of hydrogen in terms of tensor monopole moment as

$$\tau_H = \frac{1}{4m_e} + \frac{\alpha}{6\pi} \sum_M 2 \frac{\mathbf{v}_{M0} \cdot \mathbf{v}_{0M}}{D(E_M - E_0)} \left[\ln \frac{(E_M - E_0)^2}{m_e^2} - \frac{1}{4} \right], \quad (7.5.28)$$

where there is no ϵ and μ dependency. We have also added the leading order D-term for hydrogen from Eq. (7.4.17). We can see from Eq. (7.5.20) that the term involving summation scales as $\frac{1}{m_e}$ and the ground state energy of the hydrogen atom scales as $-\frac{m\alpha^2}{2}$. Using these facts we can rescale Eq. (7.5.28) as

$$\tau_H = \frac{1}{4m_e} + \frac{\alpha}{6\pi m_e} [\ln \alpha^4 + \text{cons.}]. \quad (7.5.29)$$

7.6 Discussion

From our above discussion, we can clearly see that only the conserved part of the diagram 7.5.2(a) contributes to the logarithmic divergence in terms of energy levels like the logarithmic divergence shown in Bethe's calculation scheme of the Lamb shift discussed in section 5.2. The authors in [1] interpreted this logarithmic divergence as the same as the Lamb shift. Although it is logarithmically divergent, the physics is not the same as Lamb shift. From Welton's calculation shown in section 5.3, we get a clear physical picture of the Lamb shift. In a bound system, the fluctuating vacuum creates fluctuating electric field which modifies the motion of the electron causing position fluctuation. The position fluctuation modifies the Coulomb potential energy between the electron and nucleus which give rise to the Lamb shift. So, one main feature of the Lamb shift is the fluctuating electric field. The diagram 7.5.2(a) refers to mixed contribution of Coulomb and transverse photon and it refers to the EMT in Eq. (7.3.14) and this term is referred as the interference term which signifies the interference between the Coulomb and transverse photon [1]. In the $\mathcal{O}(\alpha \ln \alpha)$ term, α comes from the vertex factors and the $\ln \alpha$ term regularizes the IR divergence. In this regard, the physics is not the same as the Lamb shift.

Another feature of the Lamb shift is that it primarily affects the s states because of the delta function when taking Laplacian of the Coulomb potential. For this delta function, the Lamb shift arises in the vicinity of the nucleus and only the s states does not vanish at the origin. But in obtained next-to-leading order result for the D-term does not have such constraints. The only part where the wave functions can play a role is the matrix elements \mathbf{v} and ρ in Eqs. (7.5.16) and (7.5.17). But in the calculation, we have considered the combination $\sum_M 2 \frac{\mathbf{v}_{M0} \cdot \mathbf{v}_{0M}}{D(E_M - E_0)}$ to scale as $\frac{1}{m_e}$ and so this result is applicable to all possible states. This also indicates that the next-to-leading order correction to the D-term is not

Lamb shift of energy levels.

7.7 Conclusion

In this chapter, we have provided a brief background to the D-term. The D-term is a relatively rarely discussed topic in theoretical physics but is on the same footing as the other fundamental properties like the mass and spin of a particle. We have discussed how the D-term provides us with information about the pressure and shear force distribution of a bound system. From the knowledge of pressure distribution inside a proton, it is possible to get information about the charge radius of the proton and how the interaction between quarks and gluons creates a bound system like a proton. There is still dispute about the proper interpretation of the D-term regarding the mechanical stability of a system. Proper interpretation and knowledge of the D-term can provide us with information about the fundamental gravitational properties of the proton and might be possible to get knowledge about how deconfined quarks and gluons in the early universe transitioned into a state of confinement to produce a stable proton [14]. In this chapter, we have considered the D-term in the context of QED and calculated the leading and next-to-leading order D-term for the hydrogen atom. Using our intuition about radiative corrections developed in earlier chapters, we have refuted the statement of [1] that the next-to-leading order correction has the same physics as the Lamb shift. In one sentence, the summary would be that the Lamb shift is logarithmic divergent in energy levels but not all logarithmic divergence in energy levels is a Lamb shift.

Chapter 8

Conclusion

In chapter 2 of this thesis, we have calculated the non-relativistic contribution to the electron $g - 2$ using effective Hamiltonian approach. We have seen that most of the contribution to the electron $g - 2$ comes from the non-relativistic domain and essentially due to the self-interaction of the electron. In chapter 3, we have performed full relativistic calculation to obtain the total anomalous magnetic moment of the electron using effective Hamiltonian approach. We have seen that the relativistic calculation does not require a cut-off as the non-relativistic calculation due to the covariance of the relativistic theory.

We justified our result obtained in chapter 2 by taking the non-relativistic limit. The main point of this chapter was to understand the processes that causes the anomaly in the g factor of the electron which is the self-interaction of the electron with its Coulomb and radiative fields. In this effective Hamiltonian approach, one finds the modified Larmor and cyclotron frequency and their ratio gives the electron $g - 2$. In this regard, this approach is relevant to experimental procedure of measuring this anomaly.

In chapter 4, we provided another scheme of calculating the electron $g - 2$. Luttinger's approach is more intuitive and natural in a sense that it does not introduce the artificial concept of renormalization like Schwinger's. In this approach, when employing perturbation in powers of external fields, all the divergent terms lies in the 0th order term which can be discarded. In Luttinger's approach, one understands the electron $g - 2$ in terms of energy differences caused by the external fields. The interpretation of this approach is quite similar to the relativistic effective Hamiltonian approach as here one also considers electron's interaction with its Coulomb and radiative fields. We get an intuitive interpretation of the self-interaction and electron $g - 2$ from all of these approaches. As a future project, it would be interesting to calculate the bound state electron $g - 2$ by generalizing these approaches.

In 5, we have discussed Bethe's and Welton's approach to calculate the Lamb shift. We have seen that the Lamb shift arises from the position fluctuation of the electron caused by

the fluctuating vacuum. This chapter provides an intuitive explanation about the Lamb shift which is essential to reach our main conclusion of the thesis that the next-to-leading order correction to the D-term is not the same as Lamb shift. In this regard, this chapter serves as a pivot for this thesis.

In chapter 6, we have derived the NRQED Feynman rules which is used to calculate the logarithmic divergent contribution to the D-term of hydrogen. Chapter 7 is the main part of this thesis. This chapter discusses about another fundamental property of a nucleon, the so-called D-term. We have interpreted the D-term in terms of pressure, shear force distribution, and the charge radius. The proper interpretation of the D-term's sign is still being disputed regarding the relation to the mechanical stability of a bound system. We have also discussed how this fundamental property can be measured experimentally. In this thesis, we have calculated the D-term for hydrogen atom in the context of QED. We identified relevant components of the energy-momentum tensor and calculated the leading and next-to-leading order correction to the D-term for hydrogen atom. As a main result of this thesis, we have shown that the physics of the next-to-leading order correction to the D-term is not the same as the Lamb shift as the origin of the logarithmic divergent term is the interference of Coulomb and transverse radiative photon whereas Lamb shift arises from fluctuating electric field caused by the fluctuating vacuum and thus we disproved a statement of [1].

The D-term is an exiting field to explore. As a future project, to understand the proper interpretation of the D-term, I would like to calculate the D-term for a classical body like a star or a black hole.

Bibliography

- [1] X. Ji and Y. Liu, *Gravitational tensor-monopole moment of hydrogen atom to order $\mathcal{O}(\alpha)$* , arXiv preprint arXiv:2208.05029 (2022).
- [2] J. Dalibard, J. Dupont-Roc, and C. Cohen-Tannoudji, *Vacuum fluctuations and radiation reaction: Identification of their respective contributions*, Journal de Physique **43**, 1617–1638 (1982).
- [3] J. Dupont-Roc, C. Fabre, and C. Cohen-Tannoudji, *Physical interpretations for radiative corrections in the non-relativistic limit*, Journal of Physics B: Atomic and Molecular Physics (1968-1987) **11**, 563 (1978).
- [4] J. Dupont-Roc and C. Cohen-Tannoudji, *Effective hamiltonian approach to $g-2$ relativistic calculation*, in *Les Houches Summer School on Theoretical Physics: New Trends in Atomic Physics* (1982).
- [5] J. Luttinger, *A note on the magnetic moment of the electron*, Physical Review **74**, 893 (1948).
- [6] P. Labelle, *Order α^2 nonrelativistic corrections to positronium hyperfine splitting and decay rate using nonrelativistic quantum electrodynamics*, Ph.d. thesis, Cornell University (1994).
- [7] X. Ji and Y. Liu, *Momentum-current gravitational multipoles of hadrons*, Physical Review D **106**, 034028 (2022).
- [8] C. Cohen-Tannoudji and D. Guéry-Odelin, *Advances in Atomic Physics: An Overview*, World scientific (2011).
- [9] T. A. Welton, *Some observable effects of the quantum-mechanical fluctuations of the electromagnetic field*, Physical Review **74**, 1157 (1948).
- [10] J. Hudson and P. Schweitzer, *D term and the structure of pointlike and composed spin-0 particles*, Physical Review D **96**, 114013 (2017).

- [11] M. V. Polyakov and P. Schweitzer, *D-term, strong forces in the nucleon, and their applications*, arXiv preprint arXiv:1801.05858 (2018).
- [12] M. V. Polyakov and P. Schweitzer, *Forces inside hadrons: pressure, surface tension, mechanical radius, and all that*, International Journal of Modern Physics A **33**, 1830025 (2018).
- [13] X. Ji, *Deeply virtual compton scattering*, Physical Review D **55**, 7114 (1997).
- [14] V. Burkert, L. Elouadrhiri, and F. Girod, *The pressure distribution inside the proton*, Nature **557**, 396–399 (2018).
- [15] J. Schwinger, *On gauge invariance and vacuum polarization*, Physical Review **82**, 664 (1951).
- [16] H. A. Bethe, *The electromagnetic shift of energy levels*, Physical Review **72**, 339 (1947).
- [17] C. d. C. Rodegheri, K. Blaum, H. Kracke, S. Kreim, A. Mooser, W. Quint, S. Ulmer, and J. Walz, *An experiment for the direct determination of the g-factor of a single proton in a penning trap*, New Journal of Physics **14**, 063011 (2012).
- [18] P. Kusch and H. Foley, *The magnetic moment of the electron*, Physical Review **74**, 250 (1948).
- [19] J. French and V. Weisskopf, *The electromagnetic shift of energy levels*, Physical Review **75**, 1240 (1949).
- [20] R. P. Feynman, *Relativistic cut-off for quantum electrodynamics*, Physical Review **74**, 1430 (1948).
- [21] P. Avan, C. Cohen-Tannoudji, J. Dupont-Roc, and C. Fabre, *Effect of high frequency irradiation on the dynamical properties of weakly bound electrons*, Journal de Physique **37**, 993–1009 (1976).
- [22] V. Arunasalam, *The electromagnetic shift of landau levels and the magnetic moment of the electron*, American Journal of Physics **37**, 877–881 (1969).
- [23] J. Schwinger, *On quantum-electrodynamics and the magnetic moment of the electron*, Physical Review **73**, 416 (1948).
- [24] W. E. Lamb Jr and R. C. Retherford, *Fine structure of the hydrogen atom by a microwave method*, Physical Review **72**, 241 (1947).

- [25] R. Feynman, *Feynman lectures on gravitation*, CRC Press (2018).
- [26] H. Pagels, *Energy-momentum structure form factors of particles*, Physical Review **144**, 1250 (1966).
- [27] K. A. Milton, *Quantum-electrodynamic corrections to the gravitational interaction of the photon*, Physical Review D **15**, 2149 (1977).
- [28] F. A. Berends and R. Gastmans, *Quantum electrodynamical corrections to graviton-matter vertices*, Annals of Physics **98**, 225–236 (1976).
- [29] H. Saif, *Graviton-electron interactions*, Physical Review D **44**, 1140 (1991).
- [30] I. Y. Kobzarev and L. Okun, *On gravitational interaction of fermions*, Zh. Eksperim. i Teor. Fiz. **43** (1962).
- [31] J. Hudson, *D-terms in bosonic and fermionic Systems*, Ph.d. thesis, University of Connecticut (2019).
- [32] J. Schwichtenberg, *Physics from symmetry*, Springer (2015).
- [33] F. Rohrlich, *The self-stress of the electron*, Physical Review **77**, 357 (1950).
- [34] A. Pais and S. Epstein, *Note on relativistic properties of self-energies*, Reviews of Modern Physics **21**, 445 (1949).
- [35] S. Borowitz and W. Kohn, *On the stress tensor of the electron*, Physical Review **86**, 985 (1952).
- [36] F. Villars, *On the energy-momentum tensor of the electron*, Physical Review **79**, 122 (1950).
- [37] F. J. Belinfante, *On the spin angular momentum of mesons*, Physica **6**, 887–898 (1939).
- [38] F. J. Belinfante, *On the current and the density of the electric charge, the energy, the linear momentum and the angular momentum of arbitrary fields*, Physica **7**, 449–474 (1940).
- [39] C. Lorcé, *The light-front gauge-invariant energy-momentum tensor*, Journal of High Energy Physics **2015**, 1–23 (2015).
- [40] M. von Laue, *Zur Dynamik der Relativitätstheorie*, Annalen Phys. **340**, 524–542 (1911).

- [41] M. von Laue, *Die Relativitätstheorie. Erster Band: Das Relativitätsprinzip der Lorentz-transformation*, Vieweg, Braunschweig (1921).
- [42] M. Polyakov, *Generalized parton distributions and strong forces inside nucleons and nuclei*, Physics Letters B **555**, 57–62 (2003).
- [43] M. Tanabashi et al., *Particle data group*, Phys. Rev. D **98**, 030001 (2018).
- [44] H.-S. Jo, F. Girod, H. Avakian, V. Burkert, M. Garçon, M. Guidal, V. Kubarovsky, S. Niccolai, P. Stoler, K. Adhikari, et al., *Cross sections for the exclusive photon electroproduction on the proton and generalized parton distributions*, Physical review letters **115**, 212003 (2015).
- [45] V. Ilisie, *Concepts in Quantum Field Theory*, Springer (2016).
- [46] F. Mandl and G. Shaw, *Quantum field theory*, John Wiley & Sons (2010).
- [47] D. Capper and G. Leibbrandt, *On a conjecture by't hooft and veltman*, Journal of Mathematical Physics **15**, 86–87 (1974).
- [48] W. Greiner et al., *Relativistic Quantum Mechanics*, volume 2, Springer (2000).
- [49] K. Bhattacharya, *Solution of the dirac equation in presence of an uniform magnetic field*, arXiv preprint arXiv:0705.4275 (2007).
- [50] J. J. Sakurai, *Advanced quantum mechanics*, Pearson Education India (2006).
- [51] V. Radovanovic, *Problem book in quantum field theory*, Springer (2006).

Appendix A

Calculation of the source fields

In this appendix, we will present the detail calculation of the source fields discussed in chapter 2. More specifically we will derive Eqs. (2.2.19) and (2.2.21). From Eqs. (2.2.1) and (2.2.2) we get the expression for $\mathbf{E}_\perp(0, t)$ and $\mathbf{A}(0, t)$ with the condition $|\mathbf{k}| < k_M$

$$\mathbf{A}(0, t) = \sum_{\mathbf{k}, \epsilon} \mathcal{A}_k \epsilon a_{\mathbf{k}\epsilon} + \text{hc}, \quad (\text{A.0.1})$$

$$\mathbf{E}_\perp(0, t) = \sum_{\mathbf{k}, \epsilon} \mathcal{E}_k \epsilon a_{\mathbf{k}\epsilon} + \text{hc}. \quad (\text{A.0.2})$$

Inserting Eq. (2.2.15) to these two equations we get

$$\mathbf{A}_r(0, t) = \sum_{\mathbf{k}, \epsilon} \frac{i\mathcal{A}_k^2 e}{m\hbar} \int_{t_0}^t dt' e^{-i\omega(t-t')} \epsilon(\epsilon^* \cdot \boldsymbol{\pi}(t')) + \text{hc}, \quad (\text{A.0.3})$$

$$\mathbf{E}_{\perp r}(0, t) = \sum_{\mathbf{k}, \epsilon} \frac{i\mathcal{A}_k \mathcal{E}_k e}{m\hbar} \int_{t_0}^t dt' e^{-i\omega(t-t')} \epsilon(\epsilon^* \cdot \boldsymbol{\pi}(t')) + \text{hc}. \quad (\text{A.0.4})$$

To evaluate these equations first consider the summation over ϵ

$$\begin{aligned} \pi^j \sum_{\epsilon} \epsilon^i \epsilon^{*j} &= \left(\delta^{ij} - \frac{k^i k^j}{k^2} \right) \pi^j \\ &= \frac{2}{3} \pi^i, \end{aligned} \quad (\text{A.0.5})$$

where we have averaged over all directions of κ^i with $\boldsymbol{\kappa} = \frac{\mathbf{k}}{k}$ using

$$\kappa^i \kappa^j \rightarrow \frac{\delta^{ij}}{3}. \quad (\text{A.0.6})$$

Now we do the summation over \mathbf{k}

$$\sum_{\mathbf{k}} \rightarrow \frac{L^3}{(2\pi)^3} \int d^3k \rightarrow \frac{L^3}{(2\pi)^3} 4\pi \int k^2 dk \rightarrow \frac{L^3}{2\pi^2} \int_0^{\omega_M} \frac{\omega^2 d\omega}{c^3}, \quad (\text{A.0.7})$$

where we have used the cut-off ω_M . Now using the definitions of \mathcal{A}_k , \mathcal{E}_k and using the factors from the summations we get

$$\begin{aligned} \mathbf{A}_r(0, t) &= -\frac{e}{3\varepsilon_0 m c^3} \left(\frac{-i}{2\pi^2} \right) \int_{t_0}^t dt' \int_0^{\omega_M} d\omega \omega e^{-i\omega(t-t')} \pi(t') \\ &= -\frac{e}{3\pi\varepsilon_0 m c^3} \int_0^\infty d\tau \pi(t - \tau) \delta'_M(\tau), \end{aligned} \quad (\text{A.0.8})$$

where we have used the definition of the δ function

$$\delta_M(\tau) = \frac{1}{2\pi} \int_{-\omega_M}^{+\omega_M} d\omega e^{-i\omega\tau}. \quad (\text{A.0.9})$$

and took $\tau = t - t'$ where $t_0 = -\infty$. Similarly for $\mathbf{E}_{\perp r}(0, t)$ we get

$$\begin{aligned} \mathbf{E}_{\perp r}(0, t) &= -\frac{e}{3\varepsilon_0 m c^3} \left(\frac{1}{2\pi^2} \right) \int_{t_0}^t dt' \int_0^{\omega_M} d\omega \omega^2 e^{-i\omega(t-t')} \pi(t') \\ &= \frac{e}{3\pi\varepsilon_0 m c^3} \int_0^\infty d\tau \pi(t - \tau) \delta''_M(\tau). \end{aligned} \quad (\text{A.0.10})$$

Now integrating by parts we get

$$\mathbf{A}_r(0, t) = \frac{e}{3\pi\varepsilon_0 c^3 m} \delta_M(0) \boldsymbol{\pi}(t) - \frac{e}{3\pi\varepsilon_0 c^3 m} \int_0^\infty d\tau \dot{\boldsymbol{\pi}}(t - \tau) \delta_M(\tau), \quad (\text{A.0.11})$$

$$\mathbf{E}_{\perp r}(0, t) = -\frac{e}{3\pi\varepsilon_0 c^3 m} \delta_M(0) \dot{\boldsymbol{\pi}}(t) - \frac{e}{3\pi\varepsilon_0 c^3 m} \int_0^\infty d\tau \ddot{\boldsymbol{\pi}}(t - \tau) \delta_M(\tau). \quad (\text{A.0.12})$$

The characteristic time evolution of $\boldsymbol{\pi}(t)$ are very long compared to the width of $\delta(\tau)$ which is $1/\omega_M$ and so we can replace $\dot{\boldsymbol{\pi}}(t - \tau)$ and $\ddot{\boldsymbol{\pi}}(t - \tau)$ by $\dot{\boldsymbol{\pi}}(t)$ and $\ddot{\boldsymbol{\pi}}(t)$. The integral of the $\delta_M(\tau)$ is equal to 1/2 because $\delta_M(\tau)$ is a symmetric function. So we obtain

$$\mathbf{A}_r(0, t) = \frac{e\omega_M}{3\pi^2\varepsilon_0 c^3 m} \boldsymbol{\pi}(t) - \frac{e}{6\pi\varepsilon_0 c^3 m} \dot{\boldsymbol{\pi}}(t), \quad (\text{A.0.13})$$

$$\mathbf{E}_{\perp r}(0, t) = -\frac{e\omega_M}{3\pi^2\varepsilon_0 c^3 m} \dot{\boldsymbol{\pi}}(t) - \frac{e}{6\pi\varepsilon_0 c^3 m} \ddot{\boldsymbol{\pi}}(t). \quad (\text{A.0.14})$$

Finally using the expression for δm_1 from Eq. (2.2.12) we get our desired expressions for Eqs. (2.2.19) and (2.2.21).

Appendix B

The Foldy-Wouthuysen Transformation

In this appendix, we will perform standard Foldy-Wouthuysen transformation on the Dirac equation in external fields with vector potential \mathbf{A} (minimally coupled) and scalar potential ϕ . The Hamiltonian of the system is

$$\begin{aligned} H &= \boldsymbol{\alpha} \cdot (\mathbf{p} - e\mathbf{A}) + \beta m + e\phi \\ &= \beta m + \mathcal{O} + \epsilon \end{aligned} \tag{B.0.1}$$

where $\mathcal{O} = \boldsymbol{\alpha} \cdot (\mathbf{p} - e\mathbf{A})$ and $\epsilon = e\phi$. We now consider the transformation

$$\psi' = e^{iS}\psi \tag{B.0.2}$$

There will be mixture of particle and anti-particle states in the hamiltonian and so it will not be possible to make the hamiltonian diagonal for all order and so we have to be content with the non-relativistic expansion of the transformed hamiltonian in a power series of $1/m$. Then the Schrödinger equation reads

$$\left(i \frac{\partial \psi'}{\partial t} \right) = \left[e^{iS} \left(H - i \frac{\partial}{\partial t} \right) e^{-iS} \right] = H' \psi'. \tag{B.0.3}$$

Now using the Baker–Campbell–Hausdorff formula to a desired order of accuracy H' becomes

$$H' = H + i[S, H] - \frac{1}{2}[S, [S, H]] - \frac{i}{6}[S, [S, [S, H]]] + \frac{1}{24}[S, [S, [S, [S, H]]]] - \dot{S} - \frac{i}{2}[S, \dot{S}] + \frac{1}{6}[S, [S, \dot{S}]]. \tag{B.0.4}$$

Using $\{\alpha, \beta\} = 0$, then $\beta\mathcal{O} = -\mathcal{O}\beta$ and $\beta^2 = 1$, the result of the commutator relations are

$$i[S, H] = -\mathcal{O} + \frac{\beta}{2m}[\mathcal{O}, \epsilon] + \frac{1}{m}\beta\mathcal{O}^2, \quad (\text{B.0.5})$$

$$\frac{i^2}{2}[S, [S, H]] = -\frac{\beta\mathcal{O}^2}{2m} - \frac{1}{8m^2}[\mathcal{O}, [\mathcal{O}, \epsilon]] - \frac{1}{2m^2}\mathcal{O}^2, \quad (\text{B.0.6})$$

$$\frac{i^3}{3!}[S, [S, [S, H]]] = \frac{\mathcal{O}^3}{6m^2} - \frac{1}{6m^2}\beta\mathcal{O}^4, \quad (\text{B.0.7})$$

$$\frac{i^4}{4!}[S, [S, [S, [S, H]]]] = \frac{\beta\mathcal{O}^4}{24m^2}, \quad (\text{B.0.8})$$

$$-\dot{S} = \frac{i\beta\dot{\mathcal{O}}}{2m}, \quad (\text{B.0.9})$$

$$-\frac{i}{2}[S, \dot{S}] = -\frac{i}{8m^2}[\mathcal{O}, \dot{\mathcal{O}}]. \quad (\text{B.0.10})$$

So H' becomes

$$\begin{aligned} H' &= \beta \left(m + \frac{\mathcal{O}^2}{2m} - \frac{\mathcal{O}^4}{8m^2} \right) + \epsilon - \frac{1}{8m^2}[\mathcal{O}, [\mathcal{O}, \epsilon]] - \frac{i}{8m^2}[\mathcal{O}, \dot{\mathcal{O}}] \\ &+ \frac{\beta}{2m}[\mathcal{O}, \epsilon] - \frac{\mathcal{O}^3}{3m^2} + \frac{i\beta\dot{\mathcal{O}}}{2m} = \beta + \mathcal{O}' + \epsilon'. \end{aligned} \quad (\text{B.0.11})$$

For further reduction, by applying a second Foldy-Wouthuysen transformation using the same procedure, we find

$$H'' = e^{iS'} \left(H' - i\frac{\partial}{\partial t} \right) e^{-iS'} = \beta m + \epsilon' + \mathcal{O}'', \quad (\text{B.0.12})$$

where \mathcal{O} is now in order of $1/m^2$ and $S' = -\frac{i\beta\mathcal{O}'}{2m}$. Finally with $S'' = -\frac{i\beta\mathcal{O}''}{2m}$ a third transformation gives

$$\begin{aligned} H''' &= e^{iS''} \left(H'' - i\frac{\partial}{\partial t} \right) e^{-iS''} \\ &= \beta \left(m + \frac{\mathcal{O}^2}{2m} - \frac{\mathcal{O}^4}{8m^3} \right) + \epsilon - \frac{1}{8m^2}[\mathcal{O}, [\mathcal{O}, \epsilon]] - \frac{i}{8m^2}[\mathcal{O}, \dot{\mathcal{O}}]. \end{aligned} \quad (\text{B.0.13})$$

Now

$$\begin{aligned} \frac{\mathcal{O}^2}{2m} &= \frac{(\boldsymbol{\alpha} \cdot (\mathbf{p} - e\mathbf{A}))^2}{2m} \\ &= \frac{1}{2m}(\mathbf{p} - e\mathbf{A})^2 - \frac{e}{2m}\boldsymbol{\Sigma} \cdot \mathbf{B}, \end{aligned} \quad (\text{B.0.14})$$

where $\Sigma_i = \begin{pmatrix} \sigma_i & 0 \\ 0 & \sigma_i \end{pmatrix}$ and σ 's are the Pauli Matrices and we have used the relation [48]

$$(\boldsymbol{\alpha} \cdot \mathbf{A})(\boldsymbol{\alpha} \cdot \mathbf{B}) = \mathbf{A} \cdot \mathbf{B} + i\boldsymbol{\Sigma} \cdot (\mathbf{A} \times \mathbf{B}). \quad (\text{B.0.15})$$

and $\nabla \times \mathbf{A} = \mathbf{B}$. For the next terms in Eq. (B.0.13)

$$\frac{1}{8m^2} \left([\mathcal{O}, \epsilon] + i\dot{\mathcal{O}} \right) = \frac{e}{8m^2} \left(-i\boldsymbol{\alpha} \cdot \nabla \Phi - i\boldsymbol{\alpha} \cdot \dot{\mathbf{A}} \right) = \frac{ie}{8m^2} \boldsymbol{\alpha} \cdot \mathbf{E} \quad (\text{B.0.16})$$

where we have considered \mathbf{A} to be constant and $\mathbf{E} = -\nabla\phi$. Now

$$\begin{aligned} \left[\mathcal{O}, \frac{ie}{8m^2} \boldsymbol{\alpha} \cdot \mathbf{E} \right] &= \frac{ie}{8m^2} [\boldsymbol{\alpha} \cdot \mathbf{p}, \boldsymbol{\alpha} \cdot \mathbf{E}] \\ &= \frac{e}{8m^2} \nabla \cdot \mathbf{E} + \frac{ie}{8m^2} \boldsymbol{\Sigma} \cdot (\nabla \times \mathbf{E}) + \frac{e}{4m^2} \boldsymbol{\Sigma} \cdot (\mathbf{E} \times \mathbf{p}) \end{aligned} \quad (\text{B.0.17})$$

here we have used Eq. (B.0.15) and substituted $-i\nabla$ for \mathbf{p} . Now gathering Eq. (B.0.14) to Eq. (B.0.17), Eq. (B.0.13) becomes

$$\begin{aligned} H''' &= \beta \left(m + \frac{(\mathbf{p} - e\mathbf{A})^2}{2m} - \frac{\mathbf{p}^4}{8m^3} \right) + e\phi - e\frac{1}{2m} \beta \boldsymbol{\Sigma} \cdot \mathbf{B} \\ &\quad - \frac{e}{8m^2} \nabla \cdot \mathbf{E} - \frac{ie}{8m^2} \boldsymbol{\Sigma} \cdot (\nabla \times \mathbf{E}) - \frac{e}{4m^2} \boldsymbol{\Sigma} \cdot (\mathbf{E} \times \mathbf{p}) \end{aligned} \quad (\text{B.0.18})$$

where we have considered \mathbf{A}^4 as very small and $\epsilon = e\phi$. Now to get Eq. (2.3.1) in a complete non-relativistic form Eq. (B.0.18) can be modified by discarding the β matrix and $\boldsymbol{\Sigma}$ then converts to just $\boldsymbol{\sigma}$. For a constant magnetic field $\nabla \times \mathbf{E} = 0$ and adding the quantized free field $\hbar\omega a^\dagger a$, we get

$$H''' = \hbar\omega a^\dagger a + \frac{\boldsymbol{\pi}^2}{2m} + \frac{\boldsymbol{\pi}^4}{8m^3} + e\phi_0 - \frac{e}{2m} \boldsymbol{\sigma} \cdot \mathbf{B} - \frac{e}{8m^2} \nabla \cdot \mathbf{E} - \frac{e}{4m^2} \boldsymbol{\sigma} \cdot (\mathbf{E} \times \mathbf{p}) \quad (\text{B.0.19})$$

where $\boldsymbol{\pi} = \mathbf{p} - e\mathbf{A}$. This is analogous to the standard Foldy-Wouthuysen Transformation [48]. We can now perform another modification by not considering \mathbf{A}^4 as small as previously mentioned. So there would be a term $(\mathbf{p} - e\mathbf{A})^4$ in case of \mathbf{p}^4 in Eq. (B.0.18). Then from Eq. (B.0.13)

$$\begin{aligned} \frac{\mathcal{O}^4}{8m^3} &= \frac{1}{2m} \frac{(\boldsymbol{\alpha} \cdot (\mathbf{p} - e\mathbf{A}))^4}{4m^2}, \\ &= \frac{1}{2m} \frac{(\boldsymbol{\alpha} \cdot (\mathbf{p} - e\mathbf{A}))^2}{2m} \frac{(\boldsymbol{\alpha} \cdot (\mathbf{p} - e\mathbf{A}))^2}{2m}. \end{aligned} \quad (\text{B.0.20})$$

Now using Eq. (B.0.14) we get

$$\frac{\mathcal{O}^4}{8m^3} = \frac{1}{2m} \left(\frac{\boldsymbol{\pi}^2}{2m} - \frac{e}{2m} \boldsymbol{\Sigma} \cdot \mathbf{B} \right)^2. \quad (\text{B.0.21})$$

Inserting it back to Eq. (B.0.19) by converting $\boldsymbol{\Sigma}$ to $\boldsymbol{\sigma}$ and using the subscript t for total field, we arrive at Eq. (2.3.1). We have restored \hbar and c .

Appendix C

Calculation of the matrix elements

C.1 Calculation of $\mathcal{V}_{\text{Coul}}$

In this appendix, we will provide the derivation of the Coulomb part $\mathcal{V}_{\text{Coul}}$ of the total effective Hamiltonian described in chapter 3. More specifically we will derive Eq. (3.2.32). We can write the denominator in Eq. (3.2.30) as

$$\begin{aligned} & (m^2c^4(1+x^2) + \boldsymbol{\pi}_0^2c^2 - 2\hbar c^2\boldsymbol{\pi}_0\cdot\mathbf{k} + \hbar^2k^2c^2 - e\hbar c^2\boldsymbol{\sigma}\cdot\mathbf{B}_0)^{-1/2}, \\ &= \frac{1}{mc^2} \frac{1}{\sqrt{1+x^2}} \left\{ 1 + \frac{\boldsymbol{\pi}_0^2}{m^2c^2(1+x^2)} - \frac{2\hbar\boldsymbol{\pi}_0\cdot\mathbf{k}}{m^2c^2(1+x^2)} - \frac{e\hbar\boldsymbol{\sigma}\cdot\mathbf{B}_0}{m^2c^2(1+x^2)} \right\}^{-1/2} \end{aligned} \quad (\text{C.1.1})$$

where we have used $m^2c^4 + \hbar^2k^2c^2 = m^2c^4(1+x^2)$. Now we expand in terms of $\boldsymbol{\pi}_0^2$, $\boldsymbol{\sigma}\cdot\mathbf{B}_0$

$$\frac{1}{mc^2} \frac{1}{\sqrt{1+x^2}} \left\{ 1 - \frac{\boldsymbol{\pi}_0^2}{2m^2c^2(1+x^2)^2} + \frac{2\hbar\boldsymbol{\pi}_0\cdot\mathbf{k}}{2m^2c^2(1+x^2)} + \frac{e\hbar\boldsymbol{\sigma}\cdot\mathbf{B}_0}{2m^2c^2(1+x^2)} \right\} \quad (\text{C.1.2})$$

Now we multiply with the numerator in Eq. (3.2.30) and finally get the terms

$$\begin{aligned} e^{i\mathbf{k}\cdot\mathbf{r}} \frac{\mathcal{H}_D}{\sqrt{\mathcal{H}_D^2}} e^{-i\mathbf{k}\cdot\mathbf{r}} &= \frac{1}{mc^2} \left\{ \frac{\beta mc^2}{\sqrt{1+x^2}} + \frac{c\boldsymbol{\alpha}\cdot\boldsymbol{\pi}_0}{\sqrt{1+x^2}} - c\boldsymbol{\alpha}\cdot\boldsymbol{\pi}_0 \frac{x^2}{3(1+x^2)^{3/2}} \right. \\ &\quad \left. - \beta \frac{\boldsymbol{\pi}_0^2}{2m} \frac{1}{(1+x^2)^{5/2}} + \beta \frac{e\hbar}{2m} \boldsymbol{\sigma}\cdot\mathbf{B}_0 \frac{1}{(1+x^2)^{3/2}} \right\} \end{aligned} \quad (\text{C.1.3})$$

All the other terms are just trivial multiplication, the only non-trivial term is $c\boldsymbol{\alpha}\cdot\boldsymbol{\pi}_0\frac{x^2}{3(1+x^2)^{3/2}}$, which comes from the multiplication of

$$\begin{aligned} \left(\frac{\hbar c\boldsymbol{\alpha}\cdot\mathbf{k}}{mc^2\sqrt{(1+x^2)}}\right)\left(\frac{\hbar\boldsymbol{\pi}_0\cdot\mathbf{k}}{m^2c^2(1+x^2)}\right) &= \frac{\hbar^2c\boldsymbol{\alpha}\cdot\boldsymbol{\pi}_0\frac{\omega^2}{3c^2}}{mc^2(1+x^2)^{3/2}\times 2m^2c^2} \\ &= \frac{c\boldsymbol{\alpha}\cdot\boldsymbol{\pi}_0}{mc^2}\frac{x^2}{3(1+x^2)^{3/2}}. \end{aligned} \quad (\text{C.1.4})$$

So the final form of Eq. (3.2.27) becomes

$$\langle 1_n | V_{\text{Coul}} | 1_{n'} \rangle = \frac{e^2}{16\pi^3\varepsilon_0} \int_0^{k_M} \frac{d^3k}{k^2} \langle u_n | e^{i\mathbf{k}\cdot\mathbf{r}} \frac{\mathcal{H}_D}{\sqrt{\mathcal{H}_D^2}} e^{-i\mathbf{k}\cdot\mathbf{r}} | u_{n'} \rangle. \quad (\text{C.1.5})$$

For convenience we will work only with the factor outside the integration and the integration variables

$$\frac{e^2}{16\pi^3\varepsilon_0} \frac{4\pi}{mc^2} = \frac{\alpha\hbar}{\pi} \frac{1}{mc}, \quad (\text{C.1.6})$$

where the factor 4π comes from the angular integration, α is the fine structure constant and $\frac{1}{mc^2}$ comes from Eq. (C.1.3). Now changing the integration variable from dk to dx using $dk = \frac{mc}{\hbar}dx$, we arrive at Eq. (3.2.32).

C.2 Calculation of $\mathcal{H}_{\text{eff}}^\perp$

In this appendix, we will provide a brief overview of the calculation of the transverse part of the effective Hamiltonian $\mathcal{H}_{\text{eff}}^\perp$ described in Eq. (3.2.35). We can write the numerator of Eq. (3.2.34) including the $\boldsymbol{\alpha}$ matrices in Eq. (3.2.33)

$$\begin{aligned} \beta mc^2 \left(1 - \frac{x}{\sqrt{1+x^2}}\right) + c\boldsymbol{\alpha}\cdot\boldsymbol{\pi}_0 \left(1 - \frac{1}{\sqrt{1+x^2}} \left(1 - \frac{x^2}{3(1+x^2)}\right)\right) \\ - \hbar c\boldsymbol{\alpha}\cdot\mathbf{k} - \beta \frac{\boldsymbol{\pi}_0^2}{2m} \frac{1}{(1+x^2)^{5/2}} + \beta \frac{e\hbar}{2m} \boldsymbol{\sigma}\cdot\mathbf{B}_0 \frac{1}{(1+x^2)^{3/2}}, \end{aligned} \quad (\text{C.2.1})$$

where we have used Eq. (C.1.3) for $\hbar\omega\frac{\mathcal{H}_D}{\sqrt{\mathcal{H}_D^2}}$. Now we will evaluate the denominator and after expanding the denominator becomes

$$\begin{aligned} E_n^2 - \hbar^2\omega^2 - m^2c^4 \left[\left(1 + x^2 + \frac{\boldsymbol{\pi}_0^2}{m^2c^2} - \frac{2\hbar\boldsymbol{\pi}_0\cdot\mathbf{k}}{m^2c^2} - \frac{e\hbar\boldsymbol{\sigma}\cdot\mathbf{B}_0}{m^2c^2}\right) \right. \\ \left. \left\{ 1 + \frac{2x}{\sqrt{1+x^2}} \left(1 - \frac{\boldsymbol{\pi}_0^2}{2m^2c^2(1+x^2)^2} + \frac{2\hbar\boldsymbol{\pi}_0\cdot\mathbf{k}}{2m^2c^2(1+x^2)} + \frac{e\hbar\boldsymbol{\sigma}\cdot\mathbf{B}_0}{2m^2c^2(1+x^2)}\right) \right\} \right] \end{aligned} \quad (\text{C.2.2})$$

Now taking m^2c^4 as a common factor and expanding this term again as it is in denominator, we get

$$\left\{ 1 + \frac{2x}{\sqrt{1+x^2}} \left(1 - \frac{\pi_0^2}{2m^2c^2(1+x^2)^2} + \frac{2\hbar\pi_0 \cdot \mathbf{k}}{2m^2c^2(1+x^2)} + \frac{e\hbar\boldsymbol{\sigma} \cdot \mathbf{B}_0}{2m^2c^2(1+x^2)} \right) \right\}, \quad (\text{C.2.3})$$

with whole factor is multiplied by $\frac{1}{m^2c^4}$. Now the factor outside the integration becomes

$$\begin{aligned} \frac{e^2c^2}{2} \frac{\hbar}{2\varepsilon_0\omega(2\pi)^3} 4\pi k^2 dk &= \frac{e^2c^2}{2} \frac{\hbar}{2\varepsilon_0\omega(2\pi)^3} 4\pi \left(\frac{mc}{\hbar}\right)^3 x^2 dx \\ &= \frac{\alpha}{2\pi} x dx \end{aligned} \quad (\text{C.2.4})$$

Another factor of 2 will come from the same calculation involving $E_n \rightarrow E_{n'}$ as described in Eq. (3.2.33) and the term x gets multiplied with the numerator. Now finally we multiply the numerator with the denominator and after summing over polarization using the completeness relation of polarization using Eq. (A.0.5) we arrive at the same expression as Eq. (3.2.35).

Appendix D

Dirac equation in magnetic field

In this appendix, we will derive the energy levels and Dirac wave functions for a particle subjected by a homogenous magnetic field. For a particle of mass m and charge e , the Dirac equation in the presence of a homogenous magnetic field \mathbf{A}_0 is

$$i\frac{d\psi}{dt} = [\boldsymbol{\alpha} \cdot (-i\nabla - e\mathbf{A}_0) + \beta m] \psi, \quad (\text{D.0.1})$$

with $\boldsymbol{\alpha}$ and β are the Dirac matrices. The wave function can be written in terms of two-component spinors

$$\psi = e^{-iEt} \begin{pmatrix} \phi \\ \chi \end{pmatrix}. \quad (\text{D.0.2})$$

where ϕ and χ are two component spinors and Eq. (D.0.1) can be written as

$$(E - m)\phi = \boldsymbol{\sigma} \cdot (-i\nabla - e\mathbf{A}_0)\chi \quad (\text{D.0.3})$$

$$(E + m)\chi = \boldsymbol{\sigma} \cdot (-i\nabla - e\mathbf{A}_0)\phi \quad (\text{D.0.4})$$

now by eliminating χ we arrive at

$$(E^2 - m^2)\phi = [\boldsymbol{\sigma} \cdot (-i\nabla - e\mathbf{A}_0)]^2 \phi. \quad (\text{D.0.5})$$

we now use the prescription $\mathbf{B} = B\hat{z}$ and $\mathbf{A}_0 = Bx\hat{y}$. With this choice Eq. (D.0.5) reduces to

$$(E^2 - m^2) = \left[-\nabla^2 + (eB)^2 x^2 + eB \left(2ix \frac{\partial}{\partial y} + \sigma_3 \right) \right] \phi, \quad (\text{D.0.6})$$

where σ_3 is the diagonal Pauli matrix. Noticing that co-ordinates y and z appear in the equation only through the derivatives, the solution can be then written as

$$\phi = e^{i(p_2 y + p_3 z)} f(x), \quad (\text{D.0.7})$$

where $f(x)$ is a two-component matrix. There are two independent solutions of $f(x)$ where $\sigma_3 f_s = s f$ with $s = \pm 1$ and

$$f_+(x) = \begin{pmatrix} F_+(x) \\ 0 \end{pmatrix}, \quad f_-(x) = \begin{pmatrix} 0 \\ F_-(x) \end{pmatrix} \quad (\text{D.0.8})$$

The differential equation Eq. (D.0.6) can now be written in terms of F_s as

$$\left[\frac{d^2 \xi}{d\xi^2} - \xi^2 + a_s \right] F_s = 0, \quad (\text{D.0.9})$$

where $\xi = \sqrt{eB} \left(x - \frac{p_2}{eB} \right)$ and $a_s = \frac{E^2 - m^2 - p_3^2 - eBs}{eB}$. The solutions exist for $a_s = 2\nu + 1$ for $\nu = 0, 1, 2, \dots$. Then the energy eigenvalue can be written as [49]

$$\begin{aligned} E^2 &= m^2 + p_3^2 + (2\nu + 1 + s)eB, \\ &= m^2 + p_3^2 + 2eB \left(\nu + \frac{1 + s}{2} \right). \end{aligned} \quad (\text{D.0.10})$$

Here we are choosing that for $s = 1$, $E^2 = m^2 + p_3^2 + 2(n + 1)eB$ and for $s = -1$, $E^2 = m^2 + p_3^2 + 2neB$ with $\nu = n$. Solutions for F_s are [49]

$$I_\nu(\xi) \equiv N_\nu e^{-\xi^2/2} H_\nu(\xi), \quad (\text{D.0.11})$$

where H_n are Hermite polynomials of order ν and N_ν is the normalization [49]

$$N_\nu = \left(\frac{\sqrt{eB}}{\nu! 2^\nu \sqrt{\pi}} \right)^{1/2}. \quad (\text{D.0.12})$$

From Eq. (D.0.10), the energy levels can be written as

$$E_m^2 = m^2 + p_3^2 + 2meB, \quad (\text{D.0.13})$$

for $m = n$ or $m = n + 1$. The first term in Eq. (D.0.8) then corresponds to the energy for $s = 1$ and the second term for $s = -1$. To write the general solutions of the Dirac wave functions in magnetic field, we will have to compare them with the free particle solutions of

the Dirac equation. The free particle solutions are given by [50]

$$\begin{aligned}
\text{for } E = \sqrt{\mathbf{p}^2 + m^2} > 0: \quad u^{(1)}(\mathbf{p}) &= N \begin{pmatrix} 1 \\ 0 \\ \frac{p_3}{E+m} \\ \frac{p_1+ip_2}{E+m} \end{pmatrix}, & u^{(2)}(\mathbf{p}) &= N \begin{pmatrix} 0 \\ 1 \\ \frac{p_1-ip_2}{E+m} \\ -\frac{p_3}{E+m} \end{pmatrix}, \\
\text{for } E = -\sqrt{\mathbf{p}^2 + m^2} < 0: \quad v^{(1)}(\mathbf{p}) &= N \begin{pmatrix} -\frac{p_3}{-E+m} \\ -\frac{p_1+ip_2}{-E+m} \\ 1 \\ 0 \end{pmatrix}, & v^{(2)}(\mathbf{p}) &= N \begin{pmatrix} -\frac{p_1-ip_2}{-E+m} \\ \frac{p_3}{-E+m} \\ 0 \\ 1 \end{pmatrix},
\end{aligned} \tag{D.0.14}$$

where $N = \sqrt{\frac{E+m}{2EV}}$ is the normalization constant with V being the normalization volume. Now comparing the energy levels in Eqs. (D.0.13) and (D.0.14), the combination of momentum components p_1 and p_2 can be replaced by $-\sqrt{2neB}$. The spinors $\begin{pmatrix} 1 \\ 0 \end{pmatrix}$ will be replaced by $f_+^{(n)}(x)$ and $\begin{pmatrix} 0 \\ 1 \end{pmatrix}$ will then be replaced by $f_-^{(n)}(x)$. Then for $E = E_m$, $m = n + 1$ for U_+ and $m = n$ for U_- , we get

$$U_+(x, n, \mathbf{p}) = N \begin{pmatrix} I_n(\xi) \\ 0 \\ \frac{p_3}{E+m} I_n(\xi) \\ -\frac{\sqrt{2neB}}{E+m} I_{n+1}(\xi) \end{pmatrix}, \quad U_-(x, n, \mathbf{p}) = N \begin{pmatrix} 0 \\ I_n(\xi) \\ -\frac{\sqrt{2neB}}{E+m} I_{n-1}(\xi) \\ -\frac{p_3}{E+m} I_n(\xi) \end{pmatrix}, \tag{D.0.15}$$

and for $E = -E_m$ and $m = n + 1$ for V_+ and $m = n$ for V_- , we get

$$V_+(x, n, \mathbf{p}) = N \begin{pmatrix} \frac{p_3}{E+m} I_n(\tilde{\xi}) \\ \frac{\sqrt{2neB}}{E+m} I_{n-1}(\tilde{\xi}) \\ I_n(\tilde{\xi}) \\ 0 \end{pmatrix}, \quad V_-(x, n, \mathbf{p}) = N \begin{pmatrix} \frac{\sqrt{2neB}}{E+m} I_{n+1}(\tilde{\xi}) \\ -\frac{p_3}{E+m} I_n(\tilde{\xi}) \\ 0 \\ I_n(\tilde{\xi}) \end{pmatrix}, \tag{D.0.16}$$

here $\tilde{\xi}$ is ξ changing the sign of the p_2 term and $N = \sqrt{\frac{E+m}{2EG^{2/3}}}$ is the normalization where G is the normalization volume. We will get the Dirac wave functions in a magnetic field by substituting these spinors in Eq. (D.0.7).

Appendix E

Calculation of the loop integrals

In this appendix, we will present detailed derivation of Eqs. (7.5.7) and (7.5.8). We have to solve the integrals

$$\langle T_{\gamma||\perp}^{ii} \rangle_{b,c} = 2e^2 (D-2) \mu^{2\epsilon} \int \frac{d^D k}{(2\pi)^D} \frac{Q^i P^{ij} Q^j}{m_e |\mathbf{k} - \mathbf{Q}|^2 |\mathbf{k} - \mathbf{Q}|}, \quad (\text{E.0.1})$$

$$Q^i \langle T_{\gamma||\perp}^{ij} \rangle_{b,c} Q^j = 2e^2 \mu^{2\epsilon} \int \frac{d^D k}{(2\pi)^D} \frac{\mathbf{k} \cdot \mathbf{Q} Q^i P^{ij} Q^j}{m_e |\mathbf{k} - \mathbf{Q}|^2 |\mathbf{k} - \mathbf{Q}|}, \quad (\text{E.0.2})$$

where

$$P^{ij} = \delta^{ij} - \frac{k^i k^j}{k^2}. \quad (\text{E.0.3})$$

To solve the integrals, we first shift the $\mathbf{k} - \mathbf{Q}$ to \mathbf{k} and the integrals become

$$\langle T_{\gamma||\perp}^{ii} \rangle_{b,c} = 2e^2 (D-2) \mu^{2\epsilon} \int \frac{d^D k}{(2\pi)^D} \frac{Q^i P^{ij} Q^j}{m_e |\mathbf{k} - 2\mathbf{Q}|^2 |\mathbf{k}|}, \quad (\text{E.0.4})$$

$$Q^i \langle T_{\gamma||\perp}^{ij} \rangle_{b,c} Q^j = 2e^2 \mu^{2\epsilon} \int \frac{d^D k}{(2\pi)^D} \frac{(\mathbf{Q} \cdot \mathbf{k} - \mathbf{Q} \cdot \mathbf{Q}) Q^i P^{ij} Q^j}{m_e |\mathbf{k} - 2\mathbf{Q}|^2 |\mathbf{k}|}. \quad (\text{E.0.5})$$

For the contraction of $Q^i P^{ij} Q^j$, we have used the programming language FORM and this contraction provides a structure like

$$\begin{aligned} I &= \int \frac{d^D k}{(2\pi)^D} \frac{(\mathbf{k} \cdot \mathbf{k})^m}{(k^2 - 4kQ + 4Q^2) (k^2)^{1/2}} \\ &= \int \frac{d^D k}{(2\pi)^D} \frac{1}{(k^2 - 4kQ + 4Q^2) (k^2)^{\frac{1-2m}{2}}}, \end{aligned} \quad (\text{E.0.6})$$

where $n = 1$ and $m = -1, 0, 1$ for Eq. (E.0.4) and $m = -1, 0, 1, 2$ for Eq. (E.0.5). We first solve the above integral for general n and m . Using the Feynman parameters [51]

$$\frac{1}{a^\alpha b^\beta} = \frac{1}{B(\alpha, \beta)} \int_0^1 dx \frac{x^{\alpha-1} (1-x)^{\beta-1}}{[xa + (1-x)b]^{\alpha+\beta}}, \quad (\text{E.0.7})$$

The integral becomes

$$\begin{aligned} I &= \frac{1}{B\left(n, \frac{1-2m}{2}\right)} \frac{1}{(2\pi)^D} \int_0^1 dx \int d^D k \frac{x^{n-1} (1-x)^{\frac{1-2m}{2}-2}}{[x(k^2 - 4kQ + 4Q^2) + (1-x)k^2]^{n+\frac{1-2m}{2}}} \\ &= \frac{1}{B\left(n, \frac{1-2m}{2}\right)} \frac{1}{(2\pi)^D} \int_0^1 dx \int d^D k \frac{x^{n-1} (1-x)^{\frac{1-2m}{2}-2}}{[(k - 2Qx)^2 + 4Q^2x(1-x)]^{n+\frac{1-2m}{2}}} \\ &= \frac{1}{B\left(n, \frac{1-2m}{2}\right)} \frac{1}{(2\pi)^D} \int_0^1 dx \int d^D k \frac{x^{n-1} (1-x)^{\frac{1-2m}{2}-2}}{[k^2 + 4Q^2x(1-x)]^{n+\frac{1-2m}{2}}}, \end{aligned} \quad (\text{E.0.8})$$

where in the last line we have shifted $k - 2Qx$ to k . Now using the formula [51]

$$\int \frac{d^D k}{(k^2 + L)^a} = \pi^{D/2} \frac{\Gamma\left(a - \frac{D}{2}\right)}{\Gamma(a)} L^{\frac{D}{2}-2}, \quad (\text{E.0.9})$$

the integral becomes

$$\begin{aligned} I &= \frac{1}{B\left(n, \frac{1-2m}{2}\right)} \frac{\pi^{D/2}}{(2\pi)^D} \int_0^1 dx x^{n-1} (1-x)^{\frac{1-2m}{2}-1} \{4Q^2x\}^{\frac{D}{2}-a} \\ &= \frac{1}{B\left(n, \frac{1-2m}{2}\right)} \frac{\pi^{D/2}}{(2\pi)^D} (4Q^2)^{\frac{D}{2}-a} \frac{\Gamma\left(a - \frac{D}{2}\right)}{\Gamma(a)} B\left(n + \frac{D}{2} - a, \frac{1-2m}{2} + \frac{D}{2} - a\right), \end{aligned} \quad (\text{E.0.10})$$

where $a = n + \frac{1-2m}{2}$ and in the last line we have used the definition of the Beta function

$$B(z_1, z_2) = \int dt t^{z_1-1} (1-t)^{z_2-1}. \quad (\text{E.0.11})$$

Now using $D = 3 - 2\epsilon$ and $a = n + \frac{1-2m}{2}$, we get

$$I = \frac{B\left(1 + m - \epsilon, \frac{3}{2} - n - \epsilon\right) \Gamma(-1 - m + n + \epsilon)}{B\left(n, \frac{1}{2} - m\right) \Gamma\left(\frac{1}{2} - m + n\right)} (4Q^2)^{\frac{D}{2} - (n + \frac{1-2m}{2})}. \quad (\text{E.0.12})$$

To get results of various values of n and m in a simplified formate, we redefine the integral as $[(4Q^2)^m (1 - 2\epsilon \ln 2 - \epsilon \ln Q^2)]^{-1} I = \text{loop}(n, m)$. Now using $n = 1$ and $m = -1, 0, 1, 2$

and expanding around ϵ , we get

$$\text{loop}(1, -1) = -\frac{1}{4\pi^2\epsilon} + \frac{\gamma_E - \ln\pi}{4\pi^2}, \quad (\text{E.0.13})$$

$$\text{loop}(1, 0) = \frac{1}{4\pi^2\epsilon} + \frac{4 - \gamma_E + \ln\pi}{4\pi^2}, \quad (\text{E.0.14})$$

$$\text{loop}(1, 1) = \frac{1}{12\pi^2\epsilon} + \frac{16 - 3\gamma_E + 3\ln\pi}{36\pi^2}, \quad (\text{E.0.15})$$

$$\text{loop}(1, 2) = \frac{1}{20\pi^2\epsilon} + \frac{92 - 15\gamma_E + 15\ln\pi}{300\pi^2}. \quad (\text{E.0.16})$$

These results were obtained using Mathematica. Now substituting these results back into the contracted Eqs. (E.0.4) and (E.0.5), we reproduce Eqs. (7.5.7) and (7.5.8). For reference, the FORM code is given as follows

```
#- off stats;
* checking Eq. 87 and 88 in 2208.05029
* They are Eq.7.5.7 and 7.5.8 in the thesis

s [k2-4kQ+4Q2],[k],n,m,D;
s EulerGamma,ln2,ep,Pi,lnPi,lnQ2;
d D;
v k,Q;
i i,j;
ct P;
cf loop;
.global

g int7 = 2*(3-2*ep-2)*Q(i)*Q(j)*P(i,j)/[k2-4kQ+4Q2]/[k]; * Eq.7.5.7
g int8 = 2*(Q.k - Q.Q)*Q(i)*Q(j)*P(i,j)/[k2-4kQ+4Q2]/[k]; * Eq.7.5.8

id P(i?,j?) = d_(i,j) - k(i)*k(j)/k.k;
id Q.k = (k.k + 4*Q.Q - [k2-4kQ+4Q2])/4; if (count([k2-4kQ+4Q2],1) >= 0) discard; *scaleless
id 1/[k2-4kQ+4Q2]^n? * k.k^m?/[k] = loop(n,-m) * (4*Q.Q)^m * (1-2*ep*ln2-ep*lnQ2);

id loop(1,1) = -1/4*1/(ep*Pi^2) + (EulerGamma - lnPi)/(4*Pi^2);
id loop(1,0) = 1/(4*ep*Pi^2) + (4 - EulerGamma + lnPi)/(4*Pi^2);
id loop(1,-1) = 1/(12*ep*Pi^2) + (16 - 3*EulerGamma + 3*lnPi)/(36*Pi^2);
id loop(1,-2) = 1/(20*ep*Pi^2) + (92 - 15*EulerGamma + 15*lnPi)/(300*Pi^2);
if (count(ep,1) > 0) discard;
.store

g check7 = Q.Q/3/Pi^2*(1/ep-lnQ2+EulerGamma-5+2*ln2+lnPi+2*(8/3-EulerGamma-2*ln2))-int7;
g check8 = Q.Q^2/(15*Pi^2)*(-1/ep+lnQ2-EulerGamma+3-2*ln2-lnPi-2*(46/15-EulerGamma-2*ln2))-int8;
print +s;
.end
```